Treatment of steam assisted gravity drainage praoduced water using polymeric membranes

by

Javad Hajinasiri

A thesis submitted in partial fulfillment of the requirements for the degree of

Master of Science

Department of Mechanical Engineering
University of Alberta

Abstract

Steam assisted gravity drainage (SAGD) method is the main oil extraction method in Alberta that produces a huge volume of waste water. This thesis is focused on investigating the viability of membrane processes, as emerging water treatment technologies, for treatment of SAGD produced water. Three different types of membranes including ultrafiltration (UF), nanofiltration (NF), and reverse osmosis (RO) were first used in a cross-flow filtering process with the intent to remove silica, salt, and dissolved organic matter (DOM) from warm lime softener (WLS) inlet water. All Experiments were conducted at the same initial permeate flux and feed flow rate to rationalize fouling behavior of membranes by their different hydrophilicity, zeta potential and roughness. The result showed that membranes with higher hydrophilicity and more negatively charged surfaces have lower tendency to fouling. Both RO and tight NF membranes showed higher total dissolved solid (TDS) and total organic carbon (TOC) rejections (<86%) in comparison with UF (<20% and <50% TDS and TOC rejections, respectively). NF with loose membrane removed <70% of salt and DOM. Applied transmembrane pressures to obtain 20 GFD initial water flux for RO, tight NF, loose NF and UF were 120, 80, 40 and 30 psig, respectively. Since in membrane processes the applied pressure is directly related to energy consumption, NF with tight membranes was found to be a promising candidate for treatment of WLS inlet water which removed as high amount of salt and DOM as RO but consumed less energy than RO. Hence, a tight NF membrane is suggested for further experimental investigations. In the second part, the performance of a tight NF membrane (NF90) for inorganic contaminants polishing and DOM removal from a model SAGD boiler feed water (BFW) was investigated thoroughly. A model BFW, prepared by diluting SAGD boiler blowdown (BBD) water obtained from a SAGD plant in northern Alberta. Experiments were conducted at a temperature of 50°C and at pH values of 10.5 (the typical BFW pH used in operating plants) and 8.5. Feed pH reduced to 8.5 to investigate the effect of

pH reduction, and subsequently precipitation of silica and DOM and deposition on the membrane surface on the flux decline. Decreasing the pH from raw water pH (10.5) to 8.5 decreased the water flux reasonably and increasing the pH back to 10.5 recovered the water flux. It is proposed in this study that a pH pulsation technique can be used to reduce the membrane fouling and recover the water flux. Throughout the study, fouled membranes, feed produced water and permeate were characterized to characterize the deposited materials on the membrane which were responsible for fouling. The presence of both organics (primarily carbon and oxygen) and inorganics (mainly silicon, calcium and iron) in the fouling deposits was confirmed by surface characterization techniques. Characterization of feed and permeate feed and permeate showed that the organic matter that passed through the membrane was mainly hydrophilic compounds. A suitably designed crossflow NF process is demonstrated be a superior alternative technique to current SAGD produced water treatment methods, especially in terms of producing higher quality water by consuming lower amount of chemicals and energy.

Keywords: Oil sands, SAGD, Membrane processes, Produced water treatment, Reverse osmosis, Nanofiltration, Ultrafiltration

Preface

In this study cross-flow filtration of SAGD produced water was conducted by applying UF, NF, and RO membranes to remove salt, silica and DOM. The highlights are (i) applying membrane processes for treatment of oil sands SAGD produced water for the first time, (ii) providing principles of membrane fouling by SAGD produced water, (iii) indicating outstanding role of pH as a pulsation technique to reduce membrane fouling and recover the water flux, (iv) Characterizing organic and inorganic materials primarily responsible for membrane fouling and performance decline, and (v) suggesting practical process schemes for SAGD produced water treatment.

Chapter 2 is a submitted paper to the *Desalination and Water Treatment* journal, and chapter 3 is a published paper in *Separation and Purification Technology* journal (141, 2015, 339353, doi:10.1016/j.seppur.2014.12.011). I am co-author in both papers.

Aknowledgement

I am using this opportunity to express my gratitude to everyone who supported me during doing my masters.

I would like to thank the postdoctrol fellow of our group Dr. Mohtda Sadrzadeh specifically for his perfect support and remarkable comments.

A special thanks to my supervisors Dr. Brian Fleck and Dr. Subir Bhattacharjee that provided me convenient situation during my research.

I also express my warm thanks to Stephanie Ostrander and her family who are just like family to me.

I would like to express the deepest appreciation to my family for their love, kindness and support.

Finally, I need to appreciate my coleagues' company and help, and also Natural Sciences and Engineering Research Council of Canada (NSERC), and also Suncor, Statoil, Kemira and Conoco philips companies' for support.

CONTENTS

List of Tables

List of Figures

NOMENCLATURE

Abbreviations

SAGD	Steam Gravity Drainage
BBD	Boiler Blow-Down
WLS	Warm Lime Softener
TOC	Total Organic Carbon
TDS	Total Dissolved Solid
IX	Ion Exchanger
OTSGs	Once Through Steam Generator
DOM	Dissolved Organic Matter
UF	Ultrafiltration
NF	Nanofiltration
RO	Reverse Osmosis
OSPW	Oil Sands Process Affected Water
TFC	Thin Film Composite Membrane
FEEMs	Fluorescence Excitation Emission Matrix spectroscopy
EDX	Energy Dispersive X-ray
ICP-OES	Inductively Coupled Plasma-Optical Emission Spectrometry
PA	Polyamide

PES	Polyethersulfone
PSf	Polysulfone
MWCO	Molecular Weight Cut-Off
PEG	Polyethylene Glycol
ATR-FTIR	Attenuated Total Reflectance-Fourier Transform Infrared
MCT	Mercury-Cadmium-Tellurium
CSS	Cyclic Steam Stimulation
BFW	Boiler Feed Water
FWKO	Free Water First Separated
ISF	Induced Static Flotation
WAC	Weak-Acid Cation exchanger
CCD	Charged Coupled Device
XPS	X-ray Photoelectron Spectroscopy
BE	Binding Energy
HPoA	Hydrophobic Acid
HPiA	Hydrophilic Acid
HPiB	Hydrophilic Base
HPoN	Hydrophobic Neutral
HPiN	Hydrophilic Neutral
HPoB	Hydrophobic Base
FESEM	Field Emission Scanning Electron Microscopy
CP	Concentration Polarization

TMOP	Trans-Membrane Osmotic Pressure
SDI	Silt Density Index
ED	Electrodialysis
MBR	Membrane Bioreacotr
MEUF	Micellar Enganced UF
SDI	Silt Density Index

Symbols

R	Selectivity
C	Concentration
A	Phenomenological coefficient
dX/dx	Driving force
D	Diffusion coefficient
J	Flux
L_p	Permeability coefficient
P	Pressure
R_m	Hydrodynamic resistance
π	Osmotic pressure

Subscripts

f	Feed
p	Permeate
m	Membrane
c	Cake

CHAPTER 1

INTRODUCTION

1.1 BACKGROUND AND OVERVIEW

Water covers about 75% of our planet's surface. Astronaut Edgar Mitchell illustrates our planet by this Sentence: "Suddenly, from behind the rim of the moon, there emerges a sparkling blue and white jewel, a light delicate sky-blue. It takes more than a moment to fully realize this is Earth". However there is an invisible problem in this blue jewel: lots of the water on the planet is polluted [3] which is mainly caused by disposed wastewater from various industries. Waste water is the water that is contaminated after usage and may also include surface water, storm water or ground water carrying industrial, residential or commercial wastes. The current rate of population increase, enhances demands on finite water resources which pushes the limits that our environment can sustain [4]. Hence water management is becoming crucial considering environmental aspects and the risk of depletion of fresh water for common usages. Another compelling reason to pay heed to water treatment is the strong relationship between water and energy, known as water-energy nexus, which implies water need for energy generation and energy need for water production or water treatment. Most of energy based companies (mainly oil and gas) need water to have production and survive. One of the most important industries which relies more than anything to water resources to produce oil, called oil sands, are located in Alberta, Canada. The main

focus in this study is to suggest a new technique for treatment of oil sands produced water to decrease energy consumption, operational cost and environmental damage.

Alberta's bitumen extraction is conducted either by open pit mining or in-situ thermal assisted techniques, based on the depth of the reservoir [5]. Almost 80% of Alberta's oil sands reservoirs exist at depths more than 200m which urges applying in-situ thermal assisted techniques. Hence, the future of oil sands industry lies in in-situ extractions techniques. However, in-situ processes rely on water much more than open-pit mining since in these processes steam plays a major role for bitumen extractions. As a matter of fact, water consumption for extraction of oil sands will most likely become a limiting factor for the growth of this industry. A water act came into effect since 1999 in Alberta which boasted the efforts to reduce fresh water use. In addition to the risk of depletion of surface water, there are concerns related to the environmental consequences of water disposal and groundwater contamination during deep well injection [6]. Under endless pressure to recycle as much water as possible, oil sands companies are continuously modifying their current water treatment processes and eagerly seeking novel technologies to avoid disadvantages of conventional techniques [7]. The most well-known in-situ process is SAGD which is currently the most widely practiced one for bitumen extraction from oil sands in Alberta, Canada due to its lower cost and higher efficiency.

In SAGD process, as shown in Figure 1.1, hot steam is injected underground into the horizontal wells that are drilled in oil sands reservoir to decrease the viscosity of bitumen, and make it flow by gravity. Heated oil and cooled steam are collected in production well that is drilled parallel to and beneath the steam well. Then the mixture gets pumped out to the ground where in steam chambers, steam condensates and bitumen flows down along the periphery of chambers and a mixture of bitumen, clay, and water is produced. At the next step by using oil skimmers, the water is deoiled. This water is treated by a train of WLS and ion exchange (IX) resins to

remove silica and divalent ions and acquire a reasonable quality to be re-used in steam generator.

A schematic view of a typical SAGD water treatment plant is shown in Figure 1.1. In the conventional process, organic diluents are added to the Bitumen/water mixture (produced fluid) to reduce the viscosity of bitumen. The diluted bitumen and the water are first separated using a series of gravity and flotation vessels to remove the bitumen, followed by gravity skim tanks and induced static flotation (ISF) to separate residual oil from the produced water. Walnut shell filters are also used to bring the free oil content in the produced water below 20 mg/L. The de-oiled produced water mixes with fresh water and recycled BBD water to make the inlet stream for WLS. This stream called WLS inlet water is at pH 9~10 and its silica, TOC and total dissolved solid (TDS) concentration is in the range of 50~100, 300~500 and 1500~2000 mg/L, respectively.

Softening is a process primarily to remove calcium and magnesium hardness by chemicals. However silica, alkalinity and other constituents are also removed during softening. In warm lime softening lime ($Ca(OH)_2$), soda ash (Na_2CO_3) and sodium hydroxide are added to water to convert soluble calcium and magnesium hardness to insoluble calcium carbonate and magnesium hydroxide by the following reactions [8, 9]:

1. Removal of carbonate hardness by lime:

$$Ca(HCO_3)_2 + Ca(OH)_2 \Rightarrow 2CaCO_3 \downarrow +2H_2O \tag{1.1}$$

$$Mg(HCO_3)_2 + Ca(OH)_2 \Rightarrow CaCO_3 \downarrow +MgCO_3 + 2H_2O \tag{1.2}$$

$$MgCO_3 + Ca(OH)_2 \Rightarrow CaCO_3 \downarrow +Mg(OH)_2 \downarrow \tag{1.3}$$

$$Ca(HCO_3)_2 + 2NaOH + Ca^{2+} \Rightarrow 2CaCO_3 \downarrow +2H_2O + 2Na^{+} \tag{1.4}$$

2. Removal of calcium non-carbonate hardness by soda ash:

$$CaSO_4 + Na_2CO_3 \Rightarrow CaCO_3 \downarrow + Na_2SO_4 \tag{1.5}$$

$$CaCl_2 + Na_2CO_3 \Rightarrow CaCO3 \downarrow + 2NaCl \tag{1.6}$$

3. Removal of magnesium non-carbonate hardness by lime and soda ash:

$$MgCl_2 + Ca(OH)_2 \Rightarrow Mg(OH)_2 \downarrow + CaCl_2 \tag{1.7}$$

$$CaCl_2 + Na_2CO_3 \Rightarrow CaCO_3 \downarrow + 2NaCl \tag{1.8}$$

$$MgSO_4 + Ca(OH)_2 \Rightarrow Mg(OH)_2 \downarrow + CaSO_4 \tag{1.9}$$

$$CaSO_4 + Na_2CO_3 \Rightarrow CaCO_3 \downarrow + Na_2SO_4 \tag{1.10}$$

During lime softening silica content is reduced significantly. This is due to the attachment of silica on the surface of the precipitated magnesium ions. At high pH values calcium-magnesium silicates are formed and precipitated.

About 90% of silica is leached out by warm lime and a filter is used to remove the residual sludge. In order to remove dissolved divalent ions like Ca^{2+} and Mg^{2+} a weak acid cation exchange is applied.

The weak acid cation exchanger is used for dealkalization of water by using WAC resins (e.g. carboxylic type acids) by the general formula of R-COOH. WAC resins remove all the alkalinity in hydroxyl, sulfate, carbonates, and bicarbonates as well as their relevant separate ions as follows [8, 10]:

1. Removal of carbonate hardness by WAC resin:

$$2RCOOH + Ca(HCO_3)_2 \Rightarrow (RCOO)_2Ca + 2CO_2 + 2H_2O \tag{1.11}$$

2. Removal of divalent ions by WAC resin:

$$2RCOOH + M^{2+} \Rightarrow (RCOO)_2Ca + 2H^+ \tag{1.12}$$

$$H^+ + HCO3^- \Rightarrow H_2O + CO_2 \tag{1.13}$$

$$2H^+ + CO_3^{2-} \Rightarrow H_2O + CO_2 \tag{1.14}$$

3. Removal of calcium and lead sulfate by WAC resin

$$RCOOH + NaOH \Rightarrow RCOONa + H_2O \tag{1.15}$$

$$2RCOONa + CaSO_4 \Rightarrow (RCOO)_2Ca + Na_2SO_4 \tag{1.16}$$

$$2RCOONa + PbSO_4 \Rightarrow (RCOO)_2Pb + Na_2SO_4 \tag{1.17}$$

The treated water by these three stages is almost free of divalent ions and contains small amount of silica (5~10 mg/L). This water is called BFW and used as feed in the steam generators. Since TDS of treated water is high, a special type of boilers known as once through steam generators (OTSGs) is used. A portion of the BBD is recycled back to the WLS and the rest is sent to disposal. Taking a closer look to Figure 1.2, it is found that current industrial water treatment configuration can not reduce the amount of DOM in WLS inlet water. TDS concentration even increased due to applying resins in cation exchanger. The high levels of DOM in this water causes numerous operational problems like fouling of pipelines and equipment and clogging of injection wells [1, 11, 12]. High TDS of water results in more blow-down volumes in OTSG and subsequently recycling more low quality water back to the process [1]. Hence, replacing the current scheme with a process which can separate almost all silica and divalent ions and reject more than 90% of DOM and TDS will considerably reduce the capital and operating costs due to the reduction of size and number of required

evaporators [7].

1.2 Emerging technologies for SAGD produced water treatmen

The potential technologies for oilfield produced water treatment are classified into five main groups [11, 13, 14]:

(i) Physical treatment such as adsorption, media filtration (sand, gravel, walnut shell), evaporation, distillation, air floatation and hydrocyclones

(ii) Chemical treatment such as precipitation, chemical oxidation (by chlorine, hydrogen peroxide, ozone and permanganate) and electrochemical process

(iii) Biological treatment such as activated sludge, anaerobic reactors, aerated lagoons and wetlands

(iv) Membrane filtration such as microfiltration (MF), UF, NF, RO and electrodialysis (ED) using both polymeric (mainly cellulose acetate, CA, PA, and polysulfone, PSf) and inorganic membranes (zeolite, ceramic and metal) Hybrid processes such as membrane bioreactor (MBR), micellar enhanced UF (MEUF), coagulation/MF, activated carbon/membrane, activated carbon/oxidation and oxidation/flocculation/membranes

Allen [5] accomplished a comprehensive study on the emerging technologies applied for oilfield produced water treatment. He introduced adsorption (by adsorbents such as activated carbon, zeolites, clays, resins and synthetic polymers) [15–19], oxidation (chemical, photocatalytic and sonochemical) [12, 19–28], biological treatment [22, 29–37] and membrane processes [37–43] as the state-of-the-art technologies in Canadas oil sands industry.

1.2.1 Adsorption

Adsorption process is used for removal of a broad range of pollutants in oilfield produced water, mainly DOM, oil and grease and heavy metals [5]. Low adsorption ca-

pacity for most of adsorbents and the environmental issues and costs associated with disposal, cleaning and regeneration of spent adsorbing media are the principle shortcomings of adsorption process [11].

1.2.2 Biological treatment

Biological treatment is a process which uses microbes to remove contaminants, particularly organic matter, microbes to remove organic material from waste water [44]. Since microorganisms are sensitive to the salinity of SAGD produced water and also toxic chemical, applying this method to treat the produced water in oil industry is challenging [5]. Although some methods like fixed growth and activated sludge are suggested to partially solve the problem, still the performance is not good because of the toxic environment of the water [45]. For oil sands produced water treatment, biological treatment is most probably feasible for removing naphthenic acids and ammonia [5].

Treatment wetlands can also be classified as biological treatment methods. In general, there are two types of wetlands. The first type is surface flow designs. This category of wetland is based on open flow of water through layers of sand, and special kinds of plants like reed [5]. The second type is subsurface wetland in which water flows through deeper layers of gravel, and roots of plants, where some biological and microbiological reactions happen. In this process water can flow through the layers either vertically or horizontally, and the needed area is smaller than the area needed for surface flow category [46]. In treatment wetlands, pollutants are removed either through physical processes like sedimentation, or chemical and biochemical processes like microbial degradation and photo-oxidation. Fouling of wetlands is a problem that should be considered, and pretreatment might be needed [5]. Cold weather also can affect the performance of water treatment by wetland since the cold can slow down the plants growth, decrease the activity rate of microorganisms, and cause in lack of

oxygen that can disturb removing some kind of compounds [47]. Meanwhile, more studies are needed to optimize the cost of constructing, and the size of wetlands since they need a vast area [5].

1.2.3 Chemical oxidation

In this process pollutant materials get degraded through some radical or ionic reactions by an oxidant molecule that can do both electron accepting and electron donating. Chlorine (Cl_2), ozone (O_3), hydrogen peroxide (H_2O_2), and permanganate (MnO_4^-). Produced radicals from ozonation or hydrogen peroxide are not usually enough to keep the required level of degradation in wastewater that is a complex environment, and it may be needed to add uv light, metal salt, electric current, ultrasound, or a combination of them. There are two combinations of the above elements called sonochemical and phtocatalytic that have had good performance [5].

In sonochemical oxidation, ultrasound is used to form and collapse some microbubbles in the wastewater. When microbubbles collapse, make some cavities. The temperature, and the pressure of the collapsed cavities is so high, that can cause the particles around it like organic molecules to break apart or degrade [48]. This method is used as a pre-treatment method, and has its own limitations like consuming too much energy, and difficulty of breaking big particles. It is also an expensive process compared to other processes [5].

Photocatalytic oxidation, benefits from producing radicals by exiting the valence electrons of a catalyst that usually is a semiconductor like titanium dioxide to oxidize pollutants. The process does not work very effectively in the high concentration of chloride. In addition the optimum pH for removing of TOC by this process is about 2 [49]. The other limitation of this process is that having dissolved salt in the water decreases the rate of producing radicals. Also presence of radical scavengers decreases the rate of reaction [5].

1.2.4 Membrane filtration

Nowadays membranes are used in a vast number of applications, and the number of Applications is still growing [50]. Oil industry has been fabricating and studying membranes for last 20 years because of their capability to remove oil, solid particles and other contaminants from water [5]. The advantages of applying membranes in comparison with other methods are their lower consumption of energy and operational cost. [51–53].

1.2.4.1 Governing equations

The main part of any membrane process is the membrane, and it can be defined as a barrier that is permeable to some components while it does not allow other components to pass. Because of this ability of membrane, it can separate unwanted components from the feed and purify it. Two parameters can determine how a membrane performs; selectivity and permeate flow. Selectivity refers to the ability of membrane to reject the undesired components, and pass the desired components. Selectivity also can be expressed as ability of keeping the solute on the feed side, and is calculated by the following equation:

$$R = \frac{c_f - c_p}{c_f} \tag{1.18}$$

Where c_{f} and c_{p} are concentration of solute in feed and permeate, respectively. The maximum of R is 100% which means all the solute has remained on the feed side of the membrane, and the minimum of R is 0 that means all the solute has passed through the membrane to the permeate side. The other parameter of membranes' performance is flux of desired material (water) through the membrane.

Components move through membranes by a driving force that can be physical like pressure or chemical like concentration. Usually transportation rate of components

across any membrane is a linear function of driving force. Flux (J) can be written as a function of driving fore by

$$J = -A\frac{dX}{dx} \tag{1.19}$$

Where J is the flux, A is a coefficient called phenomenological coefficient, and ($\mathrm{d}X/\mathrm{d}x$) is the driving force and can be defined as the slope of X's diagram (X can be pressure, temperature, or concentration) when the distance is increasing along x axis perpendicular to the surface of the membrane. When J is mass flux, X is concentration, A is defined as diffusion coefficient (D), and for J as the volume flux, X is pressure, A is called the hydrodynamic permeability coefficient of the membrane (L_P) and equation 1.19 turns into Darcy's law. In pressure driven membrane operations, the pure water flux through a membrane is directly proportional to the applied hydrostatic pressure as follows:

$$J = \frac{\triangle\, P}{\eta R_m} \tag{1.20}$$

Where R_m is the hydrodynamic resistance of the membrane and $1/\eta\ R_\mathrm{m}$ is the hydrodynamic impermeably coefficient over length ($L_\mathrm{P}/\mathrm{d}x$). The hydrodynamic resistance is a membrane constant and does not depend on the feed composition or the applied pressure. It can be measured by conducting a pure water flux experiments on the membranes. During the filtration of electrolyte solution using denser structure membranes, electrolyte concentration profile develops on the membrane surface due to the rejection of ions. Such boundary layer of higher concentration, called concentration polarization (CP) layer, generates a diffusive back flow of ions toward the bulk and develops a steady concentration profile at equilibrium. Hence, the driving force for permeate flux at the equilibrium condition decreases and is defined by the difference between the applied pressure ($\triangle$ P) and the trans-membrane osmotic pressure (TMOP,

$\triangle \pi$). Thus the permeate flux for salt rejecting membranes is described as:

$$J = \frac{\triangle P - \triangle \pi}{\eta R_m} \tag{1.21}$$

As the solutes in the polarized layer are suspended in liquid state, it is considered that there is no pressure drop across the polarized layer. The TMOP, is $\triangle \pi = \pi_{\mathrm{m}} - \pi_{\mathrm{p}}$, where π_{m} and π_{p} are osmotic pressure at membrane surface and permeate, respectively.

Equation 1.21 confirms that for salt rejecting membranes like tight NF and RO the transmembrane pressure must overcome the TMOP to force water through a dense membrane. Hence the applied pressure and subsequently energy consumption increase as the density of a membrane increases.

When silica particle and organic matter (any fouling material) present in the feed, they start depositing instantaneously on membrane surface, and their concentration increases on the membrane surface. In this case the permeate flux is represented by the following resistance-in-series model:

$$J = \frac{\triangle P - \triangle \pi}{\eta (R_m + R_c)} \tag{1.22}$$

This equation is the modified Darcy's equation. $\triangle \pi_{\mathrm{m}}$ in this equation is the enhanced TMOP because of fouling material, R_{c} is the total cake resistance including the hydrodynamic resistance of the packed bed and electroviscous resistance due to the presence of charged particles in electrolyte solution. This equation confirms that presence of foulants in the feed water has another deteriorating effect on the water flux. As the concentration of contaminants in feed water increases, denser and thicker cake layer will form on the membrane which increases R_{c} in equation 1.5 and decreases the flux. Meanwhile, presence of fouling material in the concentration polarization layer was proven to increase the TMOP which itself decreases the flux again [54].

1.2.4.2 Classification of membranes

Membranes can be categorized from different aspects. From the thickness aspect to thin and thick, form the structure aspect to homogeneous and heterogeneous, from the mechanism of material transfer to active and passive, from the type of membrane to natural and synthetic, and so on. The clearest way to classify membranes is to distinct membranes to biological and synthetic. Most of industrial membranes are synthesized membranes which are classified to symmetric and asymmetric membranes from the morphology aspects. The application of every membrane depends on its morphology since it determines the mechanism of separation in the membrane. Symmetric membranes have the same density across the thickness of the membrane, while asymmetric membranes have a denser layer at the top which is called skin layer. This skin layer improves both the selectivity and permeability of the membrane significantly. The top layer is the most resistant layer against mass transfer.

Composite membrane is a type of asymmetric membrane that has two different layers as top layer and support layer. In composite membranes, the type of top and support polymeric materials might be different and can be optimized independently. Most of the commercially available polymeric membranes applied for water treatment are thin film composite membranes (TFC) and comprise three layers: (i) a polyester support web (ii) a microporous polysulfone (PSf) or polyethersulfone (PES) inter layer and (iii) an ultrathin aromatic polyamide (PA) active layer. As indicated in Figure 1.3, the active layer is as thin as about 0.2 μm. The average roughness, hydrophilicity, zeta potential and density or molecular weight cut-off (MWCO) of this active PA layer governs the permeation properties of the membrane. The PA active layer is generally formed by interfacial in-situ polymerization of amines (e.g. m-phenylenediamine, MPD) and acyl chlorides (e.g. trimesoyl chloride, TMC) on a microporous support. Interfacial polymerization reaction can be controlled to synthesize thin film UF, NF and RO membranes. It must be noted that, the choice of the monomeric units deter-

mines the properties of the PAs. The commercially available PAs are produced by a limited number of monomers such as MPD and TMC. PAs are classified into three main categories of aliphatic, semiaromatic, and fully aromatic. Aromatic PAs, Figure 1.3, are considered to be high performance polymers due to their superior thermal and mechanical properties, which makes them suitable for membrane fabrication. All commercial TFC PA membranes applied in the present work has almost the same geometry and chemical structure as shown in Figure 1.3.

1.2.4.3 Liquid-based pressure-driven membrane process

The most well known and widely practiced membrane processes are liquid-based pressure-driven processes which are categorized as microfiltration (MF), UF, NF and Ro based on the porosity of their applied membranes. The pore size of membrane in these processes changes as follows:

MF > UF > NF > RO

The applied pressure (energy consumption) changes in exactly opposite trend, so that RO is the most energy intensive and MF is the less energy intensive.

(i) Microfiltration

The average pore size of MF membrane varies from 0.05 to 10 μm , so this process seems to be appropriate for separating particles from emulsions and suspensions. Osmotic pressure in microfiltration process is negligible due to the large size of particles, and the applied pressure is not higher than 2 bar. From the morphology aspects MF membranes can be divided into symmetric membranes with 10-150 μm thickness and asymmetric membranes with the skin layer thickness about 1 μm. The coefficient A in equation 1.19 for MF is a function of pore radius, dynamic viscosity, and the shape factor of pores. Ceramic MF membranes are also more common in this category due to their thermal and chemical stability.

MF has been commercialized for separation of particles larger than 0.1 μm in liquid

phase.

(ii) Ultrafiltration

The average pore size of a UF membrane is somewhere between 0.05 μm and 1 nm. Osmotic pressure in this process is very low that can be neglected. This process can be used to separate colloids and macromolecules from aqueous solutions. Applied pressure in UF process is between 1 to 10 bar, and the applied membranes are just asymmetric. The thickness of skin layer is in the range of 0.1-1.0 μm, and separation mechanism is molecular sieve. The hydrodynamic resistance of UF membranes is higher than MF membranes, due to their dense asymmetric structure. Similar to MF, the coefficient A in equation 1.19 depends on the structural and shape factors of the membranes.

In addition to the main task of separation, UF membranes can be used as the sub-layer NF and RO membranes.

(iii) Nanofiltration and reverse osmosis

NF and RO are used to separate solutes with low molecular weight such as glucose, lactose, salt, and micropollutants from water. Unlike MF and UF, in NF and RO, osmotic pressure is not negligible and can reach 1-25 bar. Like UF membranes, all the membranes in these two classes are asymmetric with the separating layer thickness 0.1 - 1.0 μm. Separation mechanism in these methods is based on difference in solubility and also diffusivity of the components in the membrane.

Since smaller solutes are getting separated by NF and RO than MF and UF, membranes in these classes are denser and their hydrodynamic resistance is much higher. Being more hydrodynamically resistant, NF and RO membranes need higher pressure in comparison with UF to get the same flux. The applied pressure in NF and RO should be able to compensate the high osmotic pressure. For NF and RO osmosis, A in equation 1.19 is called phenomenological coefficient, and is a function of solubility and the diffusivity of components in membrane.

The applied pressures for NF and RO are in the ranges of 10 - 20 bar and 20-100 bar respectively. Both of these ranges are obviously higher than the pressure range applied in UF. While in MF and UF, pore size is the most significant parameter in the separation properties of the membranes, in NF and RO membranes material of the membrane and its chemical properties play the major role. It means that the affinity of membranes' material should be high for the solvent (for example hydrophilic when the solvent is water) and low for the solute.

Although NF and RO membranes are similar from many aspects, the structural network of NF is more open. As a result retention of monovalent salts like Cl^- and Na^+ is lower for these membranes, however there is a high retention of divalent ions like Ca^{2+} and CO_2^{2-}, microsolutes or micropollutants, and also other components with low molecular weight like sugars and dyes. When high rejection of NaCl in highly desired, RO overcomes NF, whereas divalent ions and microsolutes must be retained, NF is preferred due to production of more product (high recovery) and less energy consumption as compared to RO.

1.2.4.4 Memebrane characterization methods

Membranes can be utilized for various applications based on their properties including hydrophilicity, MWCO, roughness, morphology or structure, and surface potential. For instance, for separation of DOM and salt from SAGD produced water more hydrophilic, denser, smoother membranes with more negatively charged surface are needed. Meanwhile, the membrane should be TFC membrane to increase both flux and rejection at the same time.

SAGD produced water mainly contains negatively charged silica and DOM. Hence, more negatively charged membranes are desired to increase the electrostatic repulsion between membrane and SAGD water constituent. In addition, our previous studies [1] revealed that DOM in SAGD water are hydrophobic matter. Hence in order to avoid

hydrophobic interactions between membrane and organic matter, more hydrophilic membranes are selected. Lowering the roughness of the membrane always decreases the chance of valley blocking and cake formation on the membrane surface. In order to have a higher quality water product, denser membranes tight NF and RO membranes are needed. For measuring each of these characteristic, a standard characterization instrument is used which are discussed in this section.

(i) Scanning Electron Microscopy (SEM)

Scanning electron microscopy method is a convenient method to provide images from structure of the membranes. The highest resolution that can be achieved is about 5 nm or 0.005 μm. In this method, the membrane is hit by a thin electron beam with the kinetic energy of 1-25 KV. The electrons that hit the membrane are called primary electrons, and have a high level of energy. The reflected electrons by the surface of the membrane have lower level of energy than primary electrons and are called secondary electrons. In reality the secondary electrons are not reflected by the membrane, but they are electrons that have been released by the atoms of membrane's surface, and build the SEM image of the membrane. Usually depending on the membranes material and the intensity of electron beam, the beam can leave a burning effect on the membrane. To avoid the burning effect, samples are coated by a conductive material like gold, chrome or graphite.

Scanning electron microscopy can provide very high quality images of cross section and surface of the membrane. Employing this method, pore size distribution and surface porosity can be studied. Surface SEM images of fouled membranes provides valuable information about the morphology of deposited materials on the membrane surface. When equipped with energy-dispersive X-ray spectroscopy (EDX) elemental analysis of fouling materials becomes possible.

(ii) Atomic Force Microscopy(AFM)

Atomic force microscopy is a method to find the roughness of membrane. In this

method surface scanning is prefromed by a probe that has a tip, which its diameter is smaller than 10 Å and applies a constant force while scanning. While the tip is scanning the surface, van der Waals-London interaction happens between the atoms at the end of the tip and the atoms at the surface of the membrane. The created forces can be detected by the probe. Scanning can be done on a line, or a profile of the surface, and since the tip is so small, scanning can be performed by applying very small forces. No pretreatment on the sample is needed for AFM scanning, and the scanning can be performed in air. AFM method is capable to spot location of the pores, and can give very useful information about the roughness of the scanned line on the sample.

(iii) Zeta potential measurement

Most of the solid surfaces have electrostatic charges, so they carry an electrical potential at the surface. In cases the liquid contains a certain concentration of ions like an electrolyte or an impure liquid, counterions of the solid surface that exist in the liquid are attracted to the surface. As a result concentration of counterions near the surface becomes higher, but it decreases by moving toward the bulk where it has bulk concentration. This layer of counterions is called double layer. Right next to the surface of the solid, a thin layer of ions exist that are attracted to the surface so strongly that can not be detached. This layer is usually called stern layer, and its thickness is about several angstroms. Measuring the electrical potential right at the interface of solid-liquid is difficult, however electrical potential can be measured at the shear plane (where velocity of the moving liquid on the surface is zero), and is called streaming potential (ζ). Electrical potential at the interface of solid and liquid can be approximated by streaming potential. [55].

Zeta potential is a very important property in membranes that can determine the energy of interaction between components and the membrane, so it is very critical in studying fouling behaviour of the membrane. Most of the commercially available membranes are negatively charged over a wide range of pH (the iso electric, IEP, for

most of them is higher than 4). The surface charge of these membranes is inherited from their functional groups. Commercial membranes are PAs which contain carboxylic (R-COO^-) and amine (R-$NH3^+$) ionizable functional groups. These groups are responsible for development of surface charge [50, 56–58]. The equilibrium dissociation reactions of these groups are as follows [56]:

$$R - COOH \leftrightarrows R - COO^- + H^+ \tag{1.23}$$

$$R - NH_3^+ \leftrightarrows R - NH_2 + H^+ \tag{1.24}$$

According to these reactions, the surface charge is dependent on degree of ionization, and obviously the pH of the solution [56]. At high pH values, H+ in reaction 1.23 reacts with OH- and reaction progress to right. Higher R-COO^- on the surface makes the membrane negatively charged. In contrast, at low pH values reaction 1.24 moves backward and the resulting membrane becomes positively charged. Hence, in order to have more negatively charged membranes, it is recommended to operate at higher pH values.

(vi) Contact angle measurement

Contact angle is a measurable property of a surface that shows hydrophobicity or hyrophilicity . Contact angle can be measured by dropping a liquid (usually water for measuring the hydrophilicity) on the surface. The droplet makes an angle with the surface at the edge of drop where three phases of liquid (water), solid (the surface), and gas (usually air) meet. Depending on the interfacial tension between the surface and water drop, the angle can vary. Bigger contact angles mean that the surface is more hydrophobic and smaller contact angles represent a more hydrophilic surface. Hydrophilic material have low interfacial tension with water, while the interfacial tension of hydrophobic material is high [59]. For water treatment applications when water must pass through the membrane, as in the present work, more hydrophilic membranes

(smaller contact angles) are desired.

1.3 Membranes for oil sands produced water treatment: Literature survey

Membrane processes have been broadly used for treatment of industrial produced water due to their advantages over traditional processes primarily lower operating costs and energy consumption. Most of earlier studies were focused on the use of looser membranes, MF and UF, oily wastewater treatment [60–69]. For removal of monovalent and divalent ions, silica and organic matter from produced water, as in the current study, tighter NF and RO membranes must be used. Although, NF and RO are widely applied in wastewater treatment, there are a few records in literature for their application in treatment of oilfield produced water. This is probably due to the high susceptibility of membranes to fouling by high TDS and TOC oilfield produced water. Meanwhile, oilfield produced waters are mostly at high temperature and pH and cannot be directly subjected to membranes. In some applications, these streams must be cooled or pH tuned solely to accommodate a membrane separation process, after which the processed fluid will be readjusted back to initial condition [67–69]. This temperature and pH adjustment causes waste of a considerable amount of energy and chemicals which is obviously tried to be avoided by industries. Applying hydrophilic membranes with outstanding antifouling properties, at their operating threshold with respect to pH and temperature, will certainly facilitate practice of membrane processes in the oilfield produced water treatment. According to our research in peer reviewed journals the following results are obtained:

1. Oil sands produced water treatment by NF and RO was already studied [38, 39, 43]. Peng et al. [39] and Kim et al. [38] worked on oil sands process affected water (OSPW) associated with the surface mining and extraction of bitumen. Many of earlier studies conclude that the DOM in mining OSPW consists primarily of naphthenic acid-like compounds [19, 70–72]. Mehrotra and Banerjee [43] applied RO for treatment of

produced water generated by an in situ oil sands process called steam flooding. The nature of in situ processes DOM is hypothesized to be different from the mining OSPW. Guha Thakurta et al. [64] demonstrated that DOM in SAGD produced water are more representative of humic acids than naphthenic acids. Every DOM has specific physicochemical properties, such as charge and molecular conformation, which controls the rate of fouling and subsequently performance of membrane process [73]. Meanwhile, the interaction of DOM functional groups with solution chemistry, e.g. monovalent and divalent concentrations, pH and presence of silica, induces different effects on properties of DOM macromolecules and thus the structure and hydraulic resistance of fouling layer [74–77]. Hence, performance of membrane processes changes vastly based on the type and concentration of organic matter and produced water chemistry.

2. Based on our search in literature, membrane processes have not been tested for SAGD produced water treatment.

3. pH is proven to be one of the most influential factors on DOM fouling through changing their surface charge [78–80]. Effect of pH on performance of NF and RO in oilfield produced water treatment was investigated by researchers [43, 67, 68, 81]. Dyke Bartels [67] showed that, DOM rejection increased by increasing pH up to a critical value, then remained constant. The amount of this critical value was different for different water sources. Mehrotra and Banerjee [43] observed exactly opposite behavior. When they adjusted produced water pH from 7-8 to 4, its colour turned deep black and the permeate TOC content decreased more than 90%. Mehrotra and Banerjee [43] attributed this to the precipitation of inorganic carbonates and bicarbonates on the membranes surface at lower pH and subsequently enhancing the permselective properties of membranes. Tao et al. [68] increased their feed pH from 7.8-8.0 to 10.6-11 to prevent oil precipitation on the membrane surface by reaching to beyond its solubility limit. Doran et al. [81] suggested an approach for increasing the boron removal by increasing the pH of the RO feed water to ionize the boron. Effect of

pH on TDS removal was not accounted in earlier studies

4. The only inorganic membrane used for desalination of oilfield produced water treatment was bentonite clay NF membrane. Liangxiong et al. [82] suggested the tested clay membrane was not suitable for purification of high TDS waters with just 10-35% rejection for Ca^{2+} and Mg^{2+} and 6-26% rejection for Na.

5. In most studies NF and RO resulted in similar TOC and TDS rejections [68, 81, 83, 84], however, Dyke and Bartels [67] and Mondal et al. [85] reported higher TOC rejection and Mehrotra and Banerjee [43] and Xu et al. [86] observed higher TDS rejection.

6. Nanofiltration (NF) and RO of oilfield produced water was already tested at higher temperature near to the operating threshold of applied polymeric membranes [67, 68, 81].

7. Indispensable role of silica in coupled silica-organic fouling, particularly by changing pH, was not taken into account.

1.4 Thesis Objectives

The main objectives of this thesis are

- To investigate the capability of commercial UF, NF, and RO membranes to remove salt and DOM from SAGD produced water, and choose the best membrane according to their performance (water quality and energy consumption).

- To test the performance of the selected membrane for salt and DOM removing and polishing calcium, magnesium, and silicon from SAGD BFW, and characterizing product water and fouled membrane to find the major responsible material for fouling.

- Outstanding role of feed pH on reduction of fouling and recovery of water flux.

In this work, effects of pore size, roughness, zeta potential, and hydrophilicity of the membranes on TDS and TOC rejection, and flux decline is studied by setting the same feed flow rate and initial permeate flux for all the membranes.

1.5 Organization of the thesis

In chapter 1 (Introduction) a general overview of in-situ oil extraction methods and conventional produced waste water treatment methods are given. Then emerging water treatment methods are discussed, and a summary of pressure-driven liquid-based membrane processes along with their governing equations is provided. After that common characterization methods in membrane field are introduced. At the end, a literature review on previous works on oil field produced water treatment and the objective of this study is presented.

In chapter 2, three different kinds of commercial membranes including one UF membrane (thin film UF from GE) and three NF membranes (NF270 and NF90 from Filmtec and ESNA from Hydranautics), two RO membranes (BW30 from Filmtec and ESPA from Hydranautics) are used to treat WLS inlet water through cross-flow filtration. NF270, ESNA and ESPA membranes were tested at the pH of raw feed, while UF, NF90 and BW30 were tested at dynamic pH (9-7-10) to investigate the effect of pH on their performance. It was shown that NF90 had a rejection of salt and DOM as high as RO by consuming less energy. Tests under dynamic pH showed the determinant role of pH in flux recovery and fouling reduction. The dominant mechanism of fouling was studied by characterizing fouled membranes, feed and permeates. According to the results NF90 showed a better performance (high water quality and reasonable energy efficiency) and is recommended for further study.

In chapter 3, due to better performance of NF90, further tests were conducted on it to study the performance of the membrane at different pH and the effect of dynamic pH at flux recovery and selectivity of the membrane. Although at both NF90 showed

the same rejection of TOC, silica and divalent cations, TDS rejection was higher at pH 8.5. On the other side decreasing pH left a negative effect on permeation flux. Surface characterization of membranes was accomplished after the tests to study the nature of deposited material on the membranes surface at different pH and the effect of pH pulsation of flux recovery.

In the last chapter, a summary and the main outcome of the thesis are provided . Some research works are also suggested as the continuation of this thesis to make the outcomes more practical for oil sands industry.

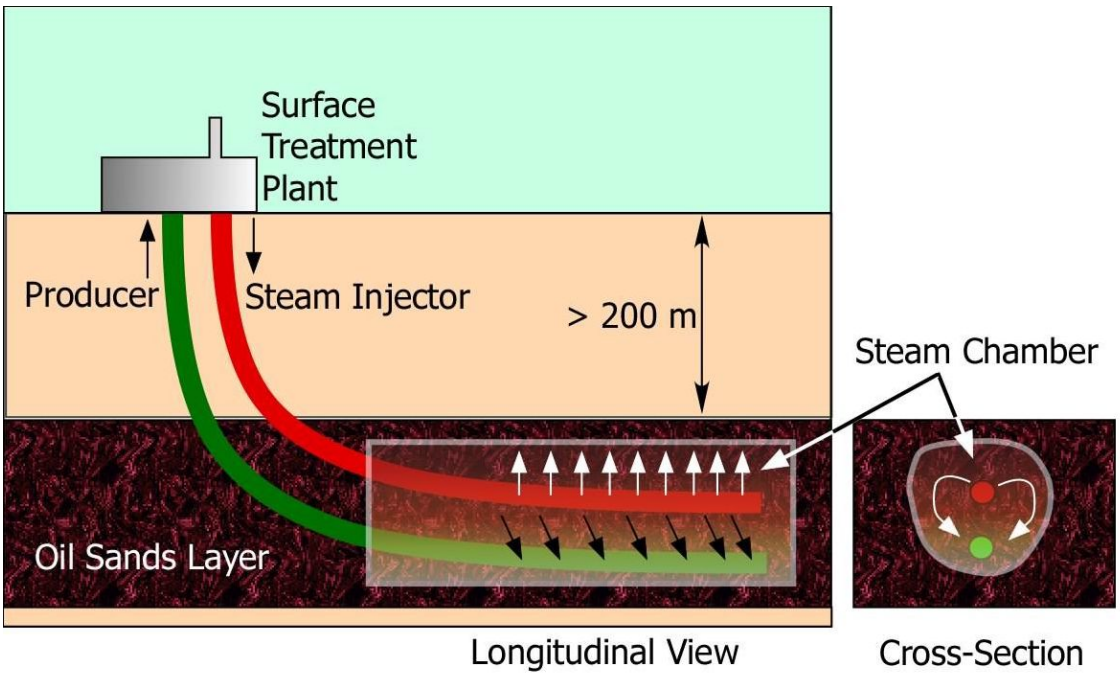

Figure 1.1: Schematic representation of the basic operating principle of a SAGD operation [2]

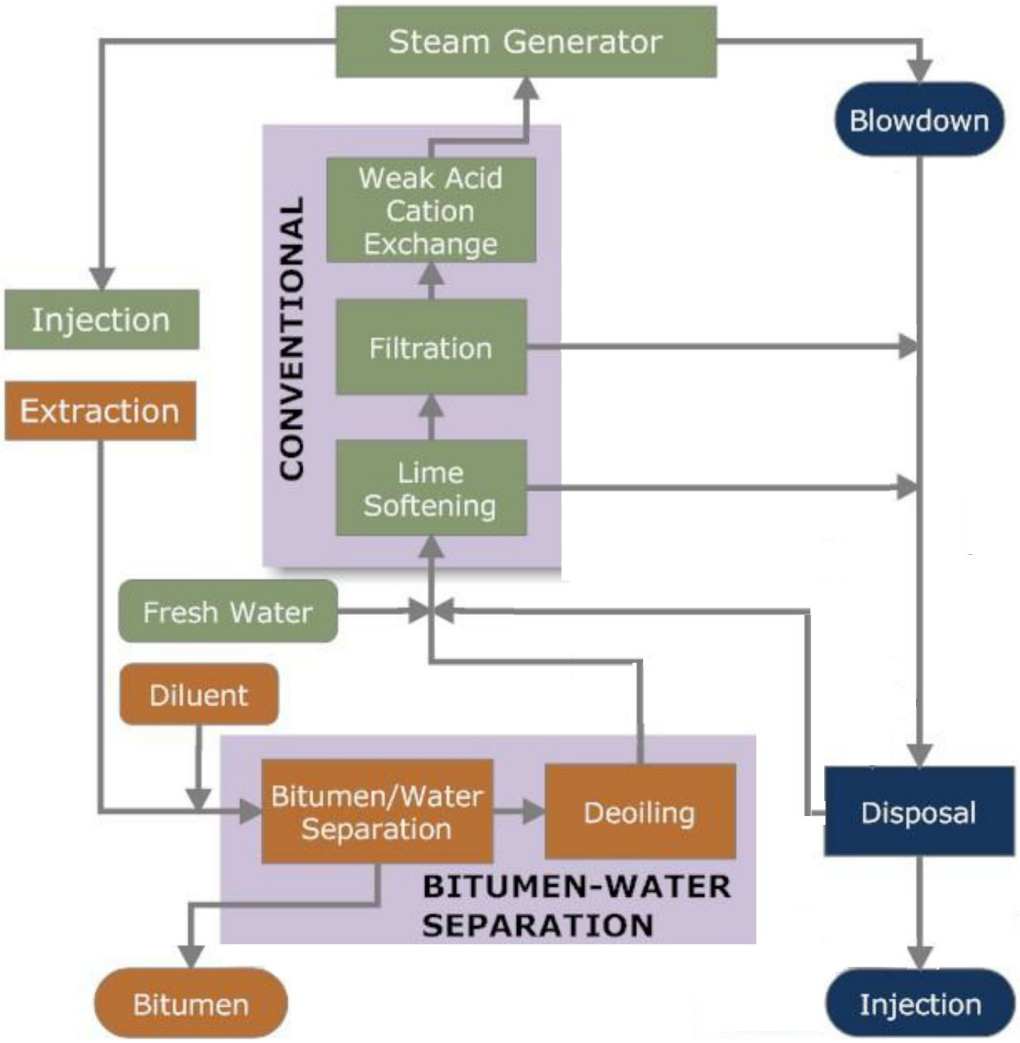

Figure 1.2: Main steps in SAGD surface treatment operation, indicating the steps of oil-water separation, and conventional de-oiled water treatment [2]

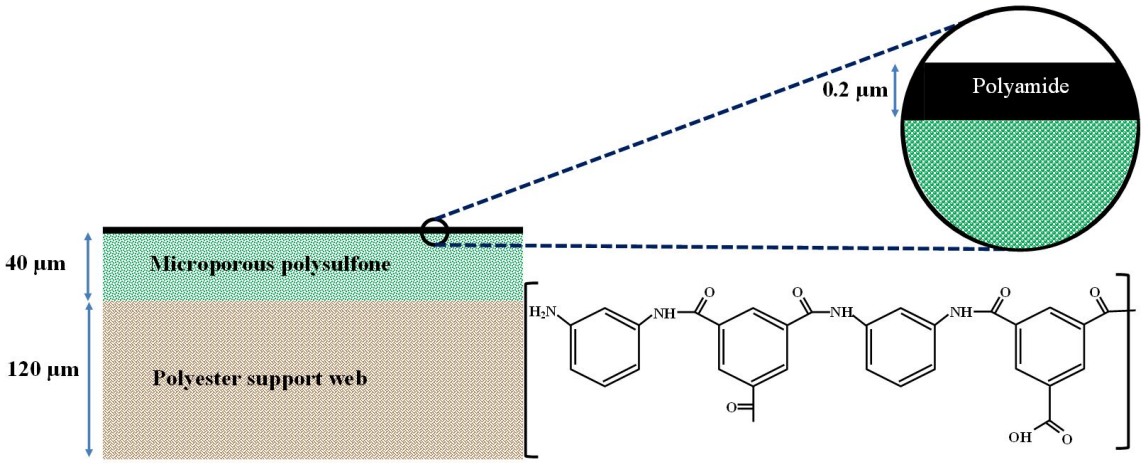

Figure 1.3: PA TFC membrane, different layers and chemical structure of active layer (taken form technical report of the Dow Chemical Company, Form No.609-02004-504)

CHAPTER 2

TREATMENT OF AN IN SITU OIL SANDS PRODUCED WATER BY POLYMERIC MEMBRANES

2.1 INTRODUCTION

SAGD is a thermally enhanced heavy oil recovery method which is widely practiced for bitumen extraction from oil sands in Alberta, Canada. In this process, steam is injected through a horizontal well into the bitumen-containing formation to decrease the viscosity of the bitumen and effect its extraction. An emulsion of steam condensate and heated bitumen flows down along the periphery of the steam chamber to the production well which is located below the injection well. This emulsion is then pumped to the surface where the bitumen and water are separated and the water is treated for reuse as boiler feed water.

In a typical SAGD surface treatment plant, the produced emulsion is first sent through a series of gravity separation vessels to remove the gases, and separate the bitumen and water. The produced water is then deoiled utilizing oil skimmers, as well as induced gas flotation devices. Finally, the water passes through an oil removal filter to remove traces of free oil and grease from the water. In the conventional SAGD-based in situ bitumen extraction surface treatment plant, the de-oiled produced water mixes with make-up water and recycled BBD water to make the inlet stream for a

WLS. This stream, called WLS inlet water, is at pH 9~10 and its silica, TOC and TDS concentration is in the range of 50~100, 300~500 and 1500~2000 mg/L, respectively. About 90% of silica is removed by warm lime softening and a filter is used to remove the residual particles. In order to further remove dissolved divalent ions like Ca^{2+} and Mg^{2+} a weak acid cation exchanger (IX) is applied. The treated water is used as feed in the steam generators. The steam generators, known as OTSGs, can tolerate relatively high amounts of TDS and TOC in the boiler feed. However, OTSGs typically produce only a low quality steam (75-80%), resulting in a large volume of BBD. A portion of the BBD is recycled back to the WLS and the rest is sent to disposal.

The economics of a SAGD process depends on the energy consumed for steam generation as well as for produced water deoiling and treatment and blowdown disposal [6]. BBD water management is becoming crucial to the in-situ oil sands industry which is continuously seeking novel technologies and improved water management strategies [7].

Current WLS-IX water treatment configuration cannot reduce the amount of DOM in WLS inlet water and the boiler feed water. TDS concentration even increases in the boiler feed due to applying resins in cation exchanger. The high levels of DOM and TDS in the OTSG feed water cause numerous operational problems like fouling of pipelines and equipment and clogging of injection wells [1, 87, 88]. To reduce the injection water volume, evaporators are sometimes used as a downstream BBD recovery process. Evaporators have also been used to desalinate produced water to make high-quality boiler feed water, but energy use is high. High TDS and DOM of boiler feed water results in more blowdown volumes and necessitates recycling more low quality BBD water back to the process [1]. In light of the above, it may be of interest to compare the WLS-IX scheme with an alternative membrane-based process which can separate almost all silica and divalent ions and reject more than 90% of DOM and TDS in a single step operation [7].

Among emerging technologies applied for oilfield produced water treatment [5], membrane separation processes have been found to be appropriate candidates due to their distinct advantages over traditional processes mainly lower operating expenses and lower energy consumption. Microfiltration and UF membranes were shown to be ineffective for separation of silica, DOM and salt from produced water [51, 52, 89]. However, tighter UF membranes were reported to remove up to ~60% of organic matter and silica depending on the characteristics of feed water constituents and operating condition (pH and ionic strength) and consume relatively low amounts of energy [51, 90, 91]. NF and RO are widely used for separation of organic matter, salt and silica from water and wastewater. However, there are few records in the peer-reviewed literature for their application in desalination and organic removal of oil sands produced water [38, 39, 43]. This is mainly due to their high susceptibility to fouling by high TDS and TOC of such water.

Fouling is the principal obstacle in developing a sustainable and energy efficient membrane process. It significantly reduces membrane performance and their lifetime and subsequently increases operation and maintenance costs [92]. Peng et al. [39] and Kim et al. [38] studied membrane fouling by OSPW associated with the surface extraction of bitumen which primarily contains naphthenic acid-like DOM [19,23,34,70,72]. Kawaguchi et al. [93] showed that naphthenic acids also predominated in all SAGD process water samples (>74% of the organic acids) while traces of fatty acids (originated from the groundwater, used as makeup water and became concentrated in the water treatment process) were also found. They indicated that the fingerprints of the DOM of the water samples from the SAGD operation varied as the process water treatment progressed. Petersen and Grade [94] divided organic species in the SAGD produced water samples into three primary groups: saturated aliphatics (n-alkane and cycloalkane), aromatics (benzenes and polyaromatic rings), and polar compounds (alcohols, ketones, phenols, etc.) , all indicative of presence of naphthenic acids as the

main DOM in SAGD produced water. However, Guha Thakurta et al. [1] demonstrated that DOM in SAGD produced water are significantly different form OSPW DOM and more representative of humic acids than naphthenic acids. It must be noted that every DOM has specific charge and molecular conformation which controls the rate of fouling and subsequently performance of membrane process [95]. Also, the interaction of DOM functional groups with ions and silica at various pH induces different properties on DOM and thus the structure and hydraulic resistance of fouling layer [75, 77, 92, 96–99]. Hence, performance of membrane processes changes vastly based on the type and concentration of DOM and water chemistry. Based on our search in literature, membranes have not been tested for SAGD produced water treatment.

The aim of this study is to investigate the performance of commercial UF, NF and RO membranes for desalination and DOM removal from industrial SAGD produced water. Effects of hydrophilicity, zeta potential, roughness and pore size of membranes on flux decline and TOC and TDS rejection were investigated by doing experiments at the same initial permeate flux and feed flow rate. It was found that more hydrophilic and negatively charged membranes with the lower average roughness were less prone to fouling, regardless of membrane pore size. RO membranes and denser NF membranes removed more than 86% of TOC and TDS. For these membranes TDS rejection remained constant or enhanced slightly as fouling progressed while TOC rejection increased over time due to the pore and valley blocking by DOM and silica. Loose NF membrane rejected more than 70% of TOC and TDS which makes their application reasonable if very high quality water is not demanded. The UF membrane removed less than 50% of salt, silica and DOM. This makes UF impractical as a single step technique for WLS inlet water treatment.

pH is proven to be the most influential factor on DOM fouling through changing both DOM and membrane surface charge [67, 68, 79–81, 99–101]. In the present work, decreasing feed pH from 9 to 7 increased TDS rejection for salt rejecting NF and RO

membranes but decreased that for UF membrane. TOC rejection slightly decreased for NF and RO by decreasing pH while it increased for UF membrane. Generally, effect of pH alteration on flux and rejection was found to be more influential for denser membranes with high salt rejecting properties. Impulsive change of pH is suggested as an important mitigation technique to reduce the membrane fouling and recover the water flux. FEEMs results showed that the majority of the DOM that remained in the RO and tight NF permeates were hydrophilic matter. For loose NF and UF membranes, all types of DOM found in the feed were also found in the permeate. EDX analysis of the fouled membranes indicated presence of silica, iron and calcium in the foulant material. Membrane process was realized to be a superior alternative technique to current SAGD produced water treatment methods, especially in terms of producing higher quality water by consuming less chemicals and energy.

2.2 Material and methods

2.2.1 Feed water

SAGD WLS inlet water is provided as feed water from a SAGD water treatment plant located in the Athabasca oil sands region of Alberta, Canada. Samples were collected in sealed containers and kept in a nitrogen blanket until they were opened for treatment. pH, conductivity and TOC of samples were first measured (Table2.1).

Concentration of the dissolved silica and other inorganic ions, as presented in Table2.1, are measured by ICP-OES. Chloride concentration was measured by automated colourimetry using SSMA 4500 CL-E method. TDS was measured through SM 2540-C protocol. The data presented in Table2.1 indicates that WLS inlet water contains high concentration of DOM, TDS, and dissolved silica.

Table 2.1: Properties of WLS inlet water

Elements	**Units**	**Feed water**
pH	–	9
Conductivity	μS/cm	1680
TDS	mg/L	1200
TOC	mg/L	420
Disolved Silicon(Si)	mg/L	89
Sodium (Na^+)	mg/L	350
Cloride (Cl^-)	mg/L	170
Calcium (Ca^{2+})	mg/L	1.9
Magnesium (Mg^{2+})	mg/L	0.59
Iron (total Fe)	mg/L	0.39
Boron (B)	mg/L	19

2.2.2 Membranes

Membrane filtration experiments were conducted using six types of polymeric membrane, (i) Three NF membranes (NF270 and NF90 from Filmtec and ESNA from Hydranautics), two RO membranes (BW30 from Filmtec and ESPA from Hydranautics) and one UF membrane (thin film UF from GE). All these membranes are thin film composite membranes consist of three layers: a thin film as an active layer, an intermediate microporous layer and a mesoporous polyester fabric support [85]. The very thin PA active layer determines the membrane separation properties and fouling behavior of DOM and inorganic materials.

The properties of applied membranes are collected from manufacturers' manual and literature and listed in Table2.2 [77, 85, 95, 102–144].

[102–108]

Table 2.2: Properties of applied polymeric membranes (Data are taken from membrane manufacture manual otherwise referred)

Membrane properties	**NF270 (Filmtec)**	**NF90 (Filmtec)**	**BW30FR (Filmtec)**	**UF TF (GE)**	**ESNA (Hydranautics)**	**ESPA (Hydranautics)**
Membrane type	NF PA Thin−Film composite	NF PA Thin−Film composite	RO PA Thin−Film composite	UF PA Thin−Film composite	NF PA Thin−Film composite	RO PA Thin−Film composite
Maximum operation pressure (Psi)	600	600	600	400	600	600
Maximum operation temperature (°C)	45	45	45	50	45	45
pH range, continuous operation	2−11	2−11	2−11	1−11	2−10	2−10
Salt rejection (%)	40−60	85−95	99.5	N/A	75−92	99.3
MWCO (D_a)	330±48 [102–108]	201±25 [102–104, 109–114]	116±30 [102, 111, 123]	3000	223±37 [107, 108, 115–117]	125±35 [111, 118]
Contact angle ($\theta°$)	34±5.5 [77, 85, 102, 106–108] [113, 119–123]	62±6.7 [77, 85, 102, 108, 109] [113, 119, 120, 123]	63±7.3 [85, 102, 108] [119, 121–123]	42±3.4 [113, 117, 124, 125]	60±6.2 [107, 115–117] [125–130]	56±6 [120, 127, 131–134]
Zeta potential (mV)	-12.1 at pH 4.5 [77, 85] -21.6 at pH 7 [103, 145] -24.0 at pH 9 [121]	5.1 at pH 4.5 [144] -24.9 at pH 7 [114] -27.3 at pH 9 [144]	-12.1 at pH 4.5 [85] -20.0 at pH 7 [121] -26.0 at pH 9 [121]	-21.8 at pH 7 [124] -28.8 at pH 8 [125]	0.0 at pH 4.5 -11.5 at pH 7 -11.0 at pH 9 [116, 117, 125] [129]	-11.1 at pH 4.5 -26.0 at pH 7 [131] -26.8 at pH 9 [131]
Isoelectric point (IEP, KCl 10^{-3}M)	3±0.20 [135, 136]	4.0	4.0	N/A	4.9±0.10 [135, 136]	4.0 [131]
Mean roughness (nm)	5±0.25 [95, 106, 111, 145] [121, 137–139]	65±2.2 [95, 109, 111] [137, 138]	65±3.4 [85, 111, 121] [137, 138, 140]	N/A	50±3.5 [130, 139, 141] [142, 145]	73±5.5 [118, 130–132] [143]

As can be seen, all membrane can withstand feed temperature and pH as high as 45 °C and 10, respectively. Main characteristics which govern permeation properties of membranes are membrane MWCO, surface charge and hydrophilicity and roughness. MWCO is described as the molecular weight for which 90% of the solute, usually polyethylene glycol (PEG) is retained by the membrane [146]. The higher the MWCO the larger the pore size of membrane. Membranes having higher MWCO, e.g. UF in Table 2.2, are more susceptible to fouling than denser membranes due to the higher permeation drag.

By retaining a constant permeation drag for all membranes by conducting experiments at constant initial permeation flux, fouling intensity can be compared to other surface properties like surface charge, hydrophilicity and roughness. The surface charge and hydrophilicity of a membrane are quantified by measuring the zeta potential and contact angle. More negatively charged and hydrophilic membranes are proven to be less prone to fouling by hydrophobic organic and negatively charged inorganic materials. Membrane surface roughness also plays a major role in fouling until the cake layer grows enough to make the initial surface roughness less significant. Rougher surfaces favor the entrapment of foulants in zones by the reverse flow due to the eddy occurring behind the peaks. Clogging of valleys on the surface of salt rejecting NF and RO membranes results in significant loss of permeate flux [147].

2.2.3 Cross flow membrane filtration setup

Schematic view of cross flow membrane filtration setup is shown in Figure 2.1 The setup consists of a stainless steel feed tank, membrane cell, a constant flow diaphragm pump of maximum capacity 6.8 LPM (1.8 GPM) from Hydra-Cell, a chiller/heater (Isotemp 3013, Fisher Scientific) to keep the feed temperature at 50 °C, a bypass valve and a back pressure regulator to control applied pressure and cross flow velocities (Swagelok). A digital weighing balance (Mettler Toledo) was used to measure the per-

meate flow rate and the data were directly collected into a computer using LabVIEW (National Instruments) data acquisition software.

2.2.4 Experimental methodology

Six experiments were conducted to find the effect of pH and membrane properties on water flux, TOC and TDS rejection and deposition of organic and inorganic matter on the membrane surface (Table 2.3).

Table 2.3: Variation of pH with time in conducted experiments

	Time		
Membrane	1−2	3−4	5−6
UF-TF (GE)	pH=9	pH=7	pH=10
NF90 (Filmtec)	pH=9	pH=7	pH=10
BW30 (Filmtec)	pH=9	pH=7	pH=10
NF270 (Filmtec)	pH=9	pH=9	pH=9
ESPA (Hydranautics)	pH=9	pH=9	pH=9
ESNA (Hydranautics)	pH=9	pH=9	pH=9

Constant pH (raw WLS inlet water pH=9) experiments were conducted on NF270, ESNA and ESPA and dynamic pH experiments (9-7-10) were carried out on UF-TF, NF90 and BW30 membranes. Membrane samples were stored in de-ionized water for 24 hr in order to remove preservatives. Before each experiment, membrane compaction was performed with de-ionized water at the pressure range of 800-1400 kPa, depending on the type of membrane.

2.2.5 Characterization techniques

2.2.5.1 Fluorescence excitation emission matrix spectroscopy (FEEMs)

The fluorescence excitation-emission matrix spectroscopy (FEEM) detects fingerprint of the soluble and insoluble organic matter. This detection was obtained over a wavelength range of 200 to 500 nm with 5 and 10 nm intervals for excitation and emission

wavelengths, respectively. The WLS inlet samples were diluted using DI water to a TOC level of around 15 mg/L to avoid inner filtration (quenching) effects on fluorescence analysis. For all experiments fluorescence analysis was performed on feed and permeate samples at pH 9.

2.2.5.2 Total organic carbon (TOC)

TOC detects the concentration of all organic carbon atoms covalently bonded in the organic molecules of sample of water. It is a parameter for monitoring the amount of DOM and evaluation the efficiency of treatment process. A typical analysis for TOC is calculated based on total carbon (TC) and inorganic carbon (IC) measurements (TC-IC=TOC). TOC in the present work was measured using a TOC analyzer (Shimadzu, model TOC-V; detection range 3-25,000 mg/L). All samples were filtered with 0.22 μm MF membranes (Cellulose Acetate, Millipore, USA) to remove the suspended solids before TOC analysis.

2.2.5.3 Inductively coupled plasma-optical emission spectroscopy (ICP-OES)

Emission spectroscopy using ICP is a rapid, sensitive and convenient method for the determination of metal ions in aqueous solutions. Concentration of dissolved silica and other inorganics presented in Table 2.2 was measured by ICP-AES instrument (Agilent 735 ICP-OES) using EPA 200.7 method. In this method the water sample is nebulized and the resulting aerosol is transported into inductively coupled argon plasma generated by radio frequency power. The high temperature (6000-10000 K) of the plasma leads to almost complete dissociation of molecules and efficient atomization and ionization in the sample. Emission spectra are produced when the excited atoms and ions return to lower energy states. The spectra are dispersed by high resolution echelle polychromator and the intensities of the lines are monitored by a charged coupled device (CCD). In OES, the power of the radiation emitted by a constituent

after excitation is directly proportional to its concentration.

2.2.5.4 Field emission scanning electron microscope- energy dispersive X-ray (FESEM-EDX)

Field emission scanning electron microscope (FESEM) provides images of sample surface to analyze surface morphology. Prior to the analysis, the membranes were coated with a thin film of chromium. Surface images of the membranes were obtained by using JEOL 6301F model of FESEM. All membranes were imaged at a magnification of 20,000 times. Field emission scanning electron microscope provides qualitative information on deposition of foulants on the membrane. Semi-quantitative elemental analysis was done via a PGT IMIX EDX system with 135 eV resolution.

2.2.5.5 Attenuated total reflectance-fourier transform infrared (ATR-FTIR) spectroscopy

ATR-FTIR spectroscopy provides information on the type of functional groups present to the depths less than 1 μ m. All membranes before and after WLS inlet filtration were examined using ATR-FTIR microscope (Thermo Nicolet Nexus 670 FTIR, USA). This instrument is equipped with a mercury-cadmium-tellurium (MCT) detector and has a resolution of 4 cm^{-1}. A total of 512 scans were averaged for each spectral measurement. The internal reflection element was a zinc selenide (ZnSe) ATR plate with an aperture angle of 45$\circ$. All membrane samples were scanned over the range of 600-4000 cm^{-1}.

2.3 Results and Discussion

Measuring the permeation flux of desired materials and removal of undesired matter is the most common way for evaluating the performance of membranes. Fouling tendency of the applied membranes and fouling potential of the treated water are

generally measured by finding the rate of water flux decline over time. Fouling deteriorates the performance of membranes by decreasing the permeation flux and the quality of membranes, and consequently shortens membrane life [73]. Membrane fouling is influenced by a great number of parameters including hydrodynamics (feed flow rate, permeation drag and feed channel dimension), solution chemistry (salt and divalent ion concentrations, presence of sparingly soluble solids and pH), and surface properties of membrane (hydrophilicity/ hydrophobicity, zeta potential, surface roughness and pore size). Regardless of feed water properties and membrane module hydrodynamics, membrane manufacturers are continuously seeking to develop more antifouling membranes with modifying their surface properties. In the present work, effects of hydrophilicity, surface charge and roughness of various types of polymeric membranes on the water flux and TOC and TDS rejection during UF, NF and RO of industrial SAGD produced water were investigated. Experiments were conducted at constant feed flow rate and permeation flux on a same industrial feed (WLS inlet water) to minimize the effect of feed chemistry and hydrodynamics. Despite the many modification and fouling preventive strategies, membrane fouling is inevitable. Online reduction of membrane fouling by physical techniques like vibration, ultrasound, vortex generation and flow and pressure pulsation have been widely studied [148–153] Another technique for mitigating fouling during operation is impulsive change of environmental conditions such as pH, ionic strength, light, temperature and electric and magnetic fields, especially in presence of stimuli responsive membranes [154]. In this study, effect of pH on water flux recovery and TOC and TDS rejection, during cross flow filtration of SAGD produced water was investigated. Since, the performance of membrane process is proven to be influenced by the characteristics of feed water and interaction of its constituents with the membrane under specific operating condition, feed, permeate and fouled membranes are characterized in detail.

2.3.1 Continuous operation at fixed pH

Water flux and TOC and TDS rejection of NF270, ESNA and ESPA membranes at 50 °C and a constant pH=9.0 is shown in Figure 2.2. It must be noted that the initial water flux of 20 GFD was obtained at different pressures of 40, 80 and 120 psi for NF270, ESNA and ESPA membranes, respectively. As can be observed in Figure 2.2, water flux declined due to the combined fouling of silica, organic matter and divalent ions present in the WLS inlet water. According to Table 2.1, the concentration of silica and divalent ions in the WLS inlet water (~90 mg/L) is almost 5 times lower than the concentration of organic matter (420 mg/L). Hence, DOM fouling is expected to be the principal mechanism in the present work. Initial adsorption of DOM on the membrane surface decreases permeate flux due to DOM gel formation, pore blocking, and induced hydrophobic properties.

Flux decline due to pore blocking and pore constriction was found to be more severe with membranes having a larger pore size (UF and loose NF membranes). For salt rejecting NF and RO membranes, plugging of hot spots by DOM was found to be critical for the sharp initial flux decline [121, 147, 155–157]. Hot spots are the valleys on the membrane surface with the minimum thickness and the maximum local water flux. Rapid clogging of these hot spots lead to substantial loss of permeate flux [147]. It is also proven that the hydrophobicity of hydrophilic membranes increases after fouling by particularly hydrophobic organic matter [121, 158, 159]. Increasing hydrophobicity generally leads to more susceptibility to fouling due to the hydrophobic interactions between the membrane surface and the hydrophobic materials [121].

In this study, the major organic matter in the WLS inlet water are hydrophobic acids (mainly humic type [1]) and all applied membranes are hydrophilic based on contact angle values in Table2.1. Hence, membranes' surface will definitely become hydrophobic after fouling.

The bar chart in Figure 2.2 shows that the initial flux decline for NF270 is lower

than two other membranes. At constant initial permeate flux, feed flow rate and feed solution chemistry (pH and ionic strength), rate of flux decline is strongly dependent on surface properties of membranes. According to data presented in Table 2.2, NF270 is a very smooth membrane with stronger hydrophilic properties than ESNA and ESPA membranes as indicated by their surface roughness and contact angle values. In addition, surface of NF270 membrane is more negatively charged than ESNA membrane. Earlier studies found that more negative zeta potential and hydrophilicity of the membrane surface leads to less fouling by organic matter due to the higher electrostatic repulsion and lower hydrophobic interaction between the foulant and the membrane surface [121, 155, 160]. ESNA membrane showed less initial decline than ESPA in spite of being less negatively charged. The rougher surface of ESPA membrane results in enhanced deposition of silica particles onto the membrane surface and, hence, more severe fouling [161, 162]. As a matter of fact the role of colloidal fouling becomes governing in combined organic/colloidal fouling of rougher membranes. Meanwhile, higher salt rejection of the ESPA membrane during fouling experiment resulted in a more severe osmotic pressure build-up near the membrane surface and hence a greater flux decline [54, 163].

It is worth noting that all these membranes were tested at same permeation flux (20 GFD) which is hypothesized to be around their limiting flux according to the moderate flux decline (7-10% after 6 hr experiment). Higher initial permeation flux could result in more severe flux decline. Tu et al. [121] observed 50% and 30% water flux decline after 6 hr filtration of humic acid and silica by NF270 membrane at initial permeate flux of 50 GFD. They attributed higher flux decline in NF270 membrane compared to BW30, despite having lower surface roughness and higher negative zeta potential and hydrophilicity, to the governing effect of initial permeation flux.

Membrane fouling in earlier studies is considered as two successive stages where foulant-membrane and foulant-foulant interactions are governing deposition of ma-

terial at first and second stages, respectively [144, 155]. Very low values of initial permeate flux decline, in NF270, ESPA and ESNA membranes, implies that foulant-membrane interaction is minimized either by favorable surface properties of applied membranes and hydrodynamics of experiments. In the case of good interaction between foulant and membrane, foulants (mainly DOM in the present work) adsorb on the membrane surface and decrease permeate flux sharply due to pore blocking, induced hydrophobic properties and lowered permeation drag [96, 121, 161, 164–167].

Figure 2.3 shows variation of TOC and TDS rejection with time using NF270, ESPA and ESNA membranes. As can be observed, for all of these membrane TOC rejection increased with time which is an evident of hydrophobic interaction in the second stage of fouling. According to literature, adsorption of organic matter on the membrane surface makes the membrane more hydrophobic [96, 121, 158, 166, 168]. This intensifies deposition of organic matter on each other due to hydrophobic foulant-foulant interaction. As a result, TOC rejection increases. For more hydrophilic NF270 membrane, rate of increase in TOC rejection is greater. This result can be explained by the findings of Cho et al. [159] and Tu et al. [121]. They both observed more severe induced hydrophobicity for the more hydrophilic membrane after fouling by organic matter.

TDS rejection remained constant for more salt rejecting membranes, ESPA and ESNA (>90% rejection), whereas decreased for looser NF270 membrane. According to literature, for salt rejecting membranes both flux and salt rejection decline as fouling progresses due to the cake enhanced concentration polarization [54, 169–171]. As foulants (silica and organic matter) deposit on the membrane surface, the salt concentration at the membrane surface significantly increases because back diffusion of salt away from the membrane surface is hindered by the foulant cake layer [163]. The increased salt concentration at the membrane surface increases the driving force for salt transport through the membrane. This results in a significant passage of salt

to the permeate steam and consequently decrease the TDS rejection. However, in this study, TDS rejection increased slightly for denser membranes which confirms the dominance of organic fouling in WLS inlet water filtration. Plugging of hot spots by organic matter resulted in formation of denser screening layer against transport of salt as demonstrated in literature [121, 147, 155–157].

For NF270 membrane, however, TDS rejection decreased which seems to be a paradox to less fouling potential of this membrane as discussed before. Lee et al. [163] showed that, there is not necessarily a direct relationship between rate of flux decline (fouling severity) and rejection decrease. They observed a much greater salt rejection drop for the NF membrane compared to the RO despite having similar flux decline trend. They attributed this to different mechanisms governing salt rejection by NF and RO. The predominant mechanism of salt rejection for RO membranes is size exclusion, while for NF membranes both size and charge (Donnan) exclusion are critical. Hence, salt concentration increase on the membrane surface due to cake formation has a more significant effect on reduction of membrane charge exclusion.

2.3.2 Membrane operation with varying pH

Dynamic pH experiments were conducted on UF, NF90 and BW30 membranes. The transmembrane pressure was adjusted on 30, 80 and 120 psig to acquire the same initial permeation flux of 20 GFD. pH of WLS inlet feed decreased from 9 (raw WLS inlet feed pH) to 7 after 120 min, then increased to 10 after 240 min. Variation of water flux with time and pH is shown in Figure 2.4. Decreasing pH from 9 to 7 declined water flux sharply for all membranes. Flux increased by increasing the pH from 7 to 10. Sharp decline was found to be more severe in the salt rejecting NF90 and BW30 membranes. Flux recovery became more evident for the denser BW30 membrane. The FESEM images, as will be shown later, demonstrated re-dissolving of fouled material on the NF and RO membranes by increasing pH, which resulted in reversible fouling

and flux recovery. By increasing the pH from 7 to 10, the flux increased to even more value than the initial flux at raw WLS inlet water pH. Decreasing the pH increases the rate of coprecipitation of organic matter and silica which causes a sharp decline especially for denser membranes [1, 171]. This is attributed to the quick change of foulant/foulant and foulant/membrane interactions by pH alteration.

The permeate flux under various pH values is affected by the properties of both membrane and solution. The surface charges of DOM were shown to become more negative with increasing pH and vice versa [79, 80, 92, 99–101]. The higher negative charge results in formation of more porous cake layer due to the inter-foulant repulsion, and consequently higher permeation flux. Silica and DOM are the major constituents in WLS inlet water. Surface charge of silica particles is negative charged at pH values more than their isoelectric point (pH>3), the magnitude of which increases with increasing pH and increasing salt concentration [172, 173]. In the case of DOM, protonation of functional groups (mainly COOH) at lower pH decreases the charge and ultimately electrostatic repulsion [79, 80, 92, 99–101]. Also, pH affects the macromolecular conformation of DOM, so that smaller configuration is formed at lower pH values [92, 96, 174]. This causes formation of a more compact fouling layer and subsequently, a flux decline. In addition to foulant/foulant interaction, foulant/membrane interaction strongly affects membrane performance at various pHs. Generally, the zeta potential of the membranes, particularly PA membranes containing carboxylic ($R\text{-}COO^-$) and amine ($R\text{-}NH_3^+$) ionizable functional groups, become more negative as pH increases [56, 160, 175, 176]. Altogether, both inter-particle and particle-membrane repulsions prevent the particles from depositing, and lead to formation of thinner fouling layer. Hence, higher permeation fluxes were observed at higher pH values [92, 96, 97, 109, 177–179].

At raw pH the minimum and maximum initial flux decline was observed for UF and NF90 membranes, respectively (bar chart in Figure 2.4). Based on the data pre-

sented in Table 2.2, the UF membrane is more hydrophilic and negatively charged than both BW30 and NF90 membranes. This resulted in less flux decline at a constant permeation flux. Taking a closer look into Table2.2, it is found that BW30 and NF90 membranes have almost the same surface properties (see roughness, contact angle and zeta potential values) and are predicted to show the same fouling behavior. A slightly higher fouling of NF90 membrane can be attributed to a minor pore blocking by DOM with molecular weight less than 250 Da. Our previous study showed that almost 40% of the DOM in the BBD have molecular weight less than 500 Da [1]. This increases the chance of pore blocking by DOM in membranes having MWCO in the range of 100-300 Da (see Table 2.2). At pH 7, exactly opposite behavior compared to pH 9 was observed. At lower pH, when coprecipitation of silica and organic matter happens, size of the deposited materials increase which makes pore blocking more severe in UF membrane. FESEM images of fouled membranes showed presence of particles with 100 nm diameter as will be discussed later.

Figure 2.5 shows the effect of step change in pH on TDS and TOC rejection during filtration by UF, NF90 and BW30 membranes. As can be seen, for tighter BW30 and NF90 membranes, higher TDS rejection was obtained at pH 7. 1000 ppm WLS inlet feed TDS was reduced to 60-63 ppm at pH 9, 30 ppm at pH 7 and around 96 ppm at pH 10 by both BW30 and NF90 membranes. Precipitation of silica nanoparticles and also coprecipitation of organic compounds by adsorption on the surface of the silica nanoparticles at lower pH resulted in formation of closely packed cake layer. The cake filtration increased the TDS rejection almost five unit. For UF membrane, pH reduction decreased the TDS rejection which was found to be irreversible by increasing the pH up to 10. This interesting result confirms irreversible pore blocking of loose UF membrane at lower pH values. By UF treatment, permeate TDS reduced to 580 ppm at pH 9, 690 ppm at pH 7 and 750 ppm at pH 10.

Effect of pH on TOC rejection was almost insignificant particularly for salt reject-

ing membranes. At pH 9, TOC rejection increased over time due to cake filtration, then decreased very slightly by decreasing the pH to 7. Cake filtration at lower pH was predicted to increase the TOC rejection similar to TDS rejection. However, the slight decrease might be due to the precipitation of very small MWCO hydrophilic DOM which could pass through both cake layer and the membrane. According to Figure 2.5, both NF90 and BW30 membranes were able to reject 90-93% of the DOM. This minor change in TOC rejection is attributed to the larger size of organic matter as compared to the dissolved solids, mainly Na^+ and Cl^- monovalent ions. DOM/membrane interaction at higher pH and DOM/cake layer interaction at lower pH had the same effect on the removal of DOM. In the case of UF membrane, deposition of precipitated DOM on the walls of membrane's pores, made the pores narrower which improved screening performance. It must be noted that, pore constriction of UF membrane could not screen salts due to their smaller size than DOM, and TDS rejection even decreased drastically owing to less electrostatic repulsion of fouled membrane.

2.3.3 Suitable membrane for WLS inlet filtration

In order to select a suitable membrane for WLS inlet filtration, the trade-off relationship between energy consumption and product quality was considered. It is always favorable to minimize energy consumption and improve the quality of water based on environmental standards and/or technical constraints. In pressure-driven membrane processes energy consumption is directly related to the applied trans-membrane pressure. Hence, UF and loose NF membranes are less energy intensive than tight NF and RO. The applied pressure for UF and NF270 membranes was 30 and 40 psig, respectively. Based on Figures 2.3 and 2.5, TOC and TDS rejections increased considerably from about 50% and 30% for UF to more than 70% for NF270 just by applying 10 psig more pressure. Therefore, when very high quality water is not required NF270 can be selected as an excellent energy efficient membrane.

ESNA and NF90 were found to give 20 GFD water flux at the same trans-membrane pressure of 80 psig. However, TOC and TDS rejection of NF90 was slightly better than ESNA (Figures 2.3 and 2.5). TDS rejections for NF90 and ESNA were 93% and 91%, respectively. The initial TOC rejection for NF90 membrane was also 4% higher than ESNA (90% compared to 86%). In fact, the water produced by NF90 membrane had the same quality as RO, BW30 and ESPA which operated at 120 psig. Hence, NF90 membrane is suggested as the best candidate since it provided reasonable product quality and is found to be more energy efficient than RO.

2.3.4 Rejection of organic matter

DOM is a heterogeneous mixture of aromatic and aliphatic organic compounds containing oxygen, nitrogen, and sulfur functional groups (e.g., carboxyl, amine and thiol) [180]. FEEMs is a reliable and inexpensive method which can provide valuable information about the nature of the dissolved organics. This method has been used in our prior investigations of SAGD water characterization [1]. The FEEMs techniques works based on excitation of electrons to a higher energy level by absorption of light energy, and then releasing energy as light as they drop to a lower energy level. Aromatic organic compounds, like humic acids, which absorb and re-emit light are called fluorophores. The excitation/emission (Ex/Em) wavelength ranges for peaks associated with pure organic compounds are obtained by researchers and can be used as scales to identify types of organic matter in a mixture. In our previous work FEEMs output is correlated to DOM classification by a resin-fractionation technique for this SAGD produced water stream [1].

Figure 2.6 shows the FEEMs results related to signatures of DOM in WLS inlet feed and permeates of applied polymeric membranes at pH 9. The fluorescence response for WLS inlet feed was observed over a wide range of wavelengths, with dominant peak at Ex/Em wavelength range of 220-350/350-450. This wide range of

wavelengths demonstrates that various types of organic compounds exist in WLS inlet feed. The fluorescence peaks of DOM are generally noticed due to the presence of high aromaticity as well as hydroxyl (mainly in carboxylic acid), and amine (mainly in PA polymer and/or amino acid organic matter) groups in the organic fluorophores. The fluorescence intensity of any uorophore can be reduced by the interfering effects of other molecules present in a mixture of uorophores.

According to Figure 2.6, WLS feed water contains wide range of organic matter including hydrophilic acid (HPiA), hydrophilic base (HPiB), hydrophilic neutral (HPiN), hydrophobic acid (HPoA), hydrophobic base (HPoB) and hydrophobic neutral (HPoN) based on the classified results of our previous studies. This variety still exist in the permeate stream of NF270 and UF membranes. This means that UF and looser NF membranes could not totally remove any organic matter and all types of organics passed through the membranes. In the case of RO and tight NF membranes, the main organic in the permeate stream were hydrophilic compounds (HPiN, HPiA and HPiB). This means that hydrophobic acidi organic matter in the WLS inlet water, like humic acid, was almost completely removed by these membranes. Since TOC rejection for NF and RO membranes increased with time (Figures 2.3 and 2.5) it is found that the hydrophilic matter traced by FEEMs was mainly passed through the membranes at the early stage of filtration. At the initial stage of filtration, the hydrophilic parts of DOM in WLS inlet water were in direct contact with the surface of hydrophilic membranes. This facilitated their transfer to the permeate side. Hydrophobic organics are suggested to be the main materials responsible for membrane fouling [96, 97, 101, 181]. FEEMs results confirms that hydrophobic signature of organic matter in the WLS inlet water were mostly deposited on the membrane surface and made the fouling more severe especially at the second stage of filtration when hydrophobic interaction of organic matter becomes important. Figure 2.6 demonstrates that tight NF and RO membranes are the favorable options for removing DOM from WLS inlet water.

2.3.5 Rejection of inorganics

ICP-OES analysis was performed on the permeates of UF, NF90 and BW30 membranes to find the rejection of inorganic constituents of WLS inlet water. The results are presented in Table 2.4.

Table 2.4: Inorgnaic rejection for UF, NF90 and BW30 membranes

Elements	**Unit**	**RDL**[a]	**Feed Water**	**UF Permeate**	**NF90 Permeate**	**BW30 Permeate**
Boron(B)	mg/L	0.2	19 [b]	17[b]	8.6[b]	5.8[b]
Calcium (Ca^{2+})	mg/L	0.3	1.9	0.42	<0.3	<0.3
Iron(total)	mg/L	0.06	0.39	<0.06	<0.06	<0.06
Magnesium (Mg^{2+})	mg/L	0.2	0.59	<0.2	<0.2	<0.2
Silica (disolved silicon)	mg/L	0.1	89	61	2.9	3.2
Sodium (Na^{+})	mg/L	0.5	350	290	26	20
Chloride (Cl^{-})	mg/L	1.0	170	120	5.3	3.8

[a] Reportable Detection Limit

[b] Detection limits raised due to dilution to bring analyte within the calibrated range

Total inorganic rejection for NF90 and BW30 is more than 90% which confirms our previous results on TDS rejection. NF90 and BW30 removed almost all divalent ions and iron in the feed. However, about 4% of silica passed through these membranes. Sodium and chloride rejection by NF90 and BW30 were found to be about 93 and 97%, respectively. NF90 and BW30 demonstrated almost the same performance in terms of total inorganic rejection. UF membrane rejected ~ 30%, 20% and 75% of silica, sodium and calcium. This shows that the UF membrane was inefficient for rejection of inorganic materials and cannot be applied for WLS inlet water treatment. The low levels of inorganic, scale-forming species in the NF and RO permeate, would greatly reduce the fouling propensity of the WLS inlet water if NF and RO were applied as a polishing step in the conventional SAGD process train. According to the data presented in Table 2.4, it can be concluded that NF90 is the most promising alternative

for removing inorganic material from WLS inlet water considering both membrane performance and energy consumption.

2.3.6 Results of surface analyses

Fouled membranes were characterized by FESEM-EDX and ATR-FTIR to find the elements deposited on the membrane surface. Furthermore, analysis of fouled membranes helps to find the fouling intensity at different pH values. Precipitation of more foulants on the membrane surface at lower pH and re-dissolving of deposits by increasing the pH can be simply observed by FESEM images.

2.3.6.1 Field emission scanning electron microscope- energy dispersive X-ray (FESEM-EDX)

The morphology of deposited materials on the membrane surface has been qualitatively detected by FESEM analysis. Figure 2.7 shows the FESEM image of fouled membranes with magnification of 5,000. As can be seen, more organic and inorganic materials were deposited on the membranes which experienced lower pH values, e.g. UF membrane. In the case of NF90 and BW30, increasing pH back to 10, re-dissolved foulants. For these membranes surface of membranes is not fully covered by the foulants and morphology of the virgin membrane is noticeable. This confirms the substantial effect of pH on flux recovery in salt rejecting NF and RO membranes.

NF270, ESNA and ESPA membranes are indicated to be fouled similarly. However, the morphologies of fouled materials are different in these membranes. It must be noted that these 20× 20 μ m FESEM images are not representative of the whole effective membrane surface area (140 cm^2). For instance, NF270 membrane is mostly covered by a black material which is assumed to be mainly pure organic matter. In the case of ESNA and ESPA a mixture of organic and inorganic materials are deposited on the membrane which is identifiable by the spongy structure of cake layer. Since

the same feed is filtered in all experiments and subsequently, the same materials are deposited on all membranes, it was found that fouling layer was not homogenously covered throughout the membrane surface. Hence, the morphology of deposited fouling layer is different form one point to another point. However, FESEM images give a pretty good idea about the intensity of fouling using different types of membranes.

The morphologies of the adsorbed materials on the membrane surface are more noticeable in Figure 2.8 by higher magnification images. As can be seen, deposited mass on the membrane are mainly in the form of particles which was detected by EDX analysis to be silica particles. Crystal shapes on the membrane surface are found to be iron and calcium crystals. Sponge shapes contain sulfur, organic matter and silica. Silica in the sponge shapes confirms coprecipitation of silica and organic matter on the membranes especially at lower pH values. The size of particles is about 100 nm. This result demonstrates adsorption of organic matter on the surface of silica particles, therefore enhanced diameter of these particles.

2.3.6.2 ATR-FTIR result

All samples were scanned from 500 to 4000 cm^{-1} wavelength and the FTIR peaks of virgin and fouled membranes are shown in Figure 2.9. This figure shows that the peak heights related to the fouled membrane are reduced after filtration. Membranes prepared by Filmtec (NF270, NF90 and BW30) and GE (UF) clearly show different peaks from Hydranautics ones (ESNA and ESPA). This shows that the type of PA thin film in these membranes is different. All these membranes show ATR-FTIR spectra peaks at range of 600 to 1500 cm^{-1} that indicate the presence of the polysulfone interlayer. Peaks at 1650 and 1541 cm^{-1} indicate amide I and amide II for all membrane. All Filmtec membranes are made from m-phenylene diamine, a primary amine. Though WLS inlet filtration leads to a decrease in PA and polysulfone associated peak heights no new peaks are detected. The absence of peaks representing organic foulants is most

likely due to the fact that the peaks associated with polysulfone and PA swamp any small peaks that represent adsorbed organic species.

2.4 Conclusion

WLS inlet water from SAGD process was treated with cross-flow UF, NF and RO processes. All experiments were conducted at constant feed temperature (50 °C) and various pH values. It was found that more hydrophilic membranes with more negative surface charge and less roughness were less prone to fouling regardless of their pore size. RO and tight NF removed more than 86% of TDS and TOC. TOC rejection increased significantly over time due to clogging of hot spots by DOM and silica. UF was found out to be not suitable for SAGD produced water treatment due to its low performance in rejecting silica and DOM. However, NF with loose membranes was found to be a reasonable choice when very high purification of water is not necessary. This membrane removed more than 70% of TDS and TOC. NF with tight NF membranes (NF90 and ESNA) was found to be a promising method because of producing high water quality comparable to RO and consuming less energy than RO. Flux, TOC rejection and TDS rejection were found to be strongly affected by changing the pH. Acidification of WLS inlet water during operation (pH change from 9-7), decreased the flux suddenly and increased TDS rejection for tight NF and RO membranes. However, TOC rejection decreased slightly by decreasing the feed pH. UF membrane showed exactly opposite behavior due to the different fouling mechanism governing the transport of salt and DOM in loose membranes. Increasing pH from 7.0 to 10.0 increased water flux about 40% immediately which demonstrated the critical role of pH on fouling reduction. Re-dissolving of fouling deposits by increasing pH was observed by doing surface characterization of fouled membranes using FESEM-EDX. ATR-FTIR and FESEM-EDX techniques provided valuable information about the constituents in WLS inlet water, which were deposited on the membrane. EDX indicated presence of

silica, iron and calcium in fouling deposits. FEEMs showed that the major organics that passed through the membrane were hydrophilic compounds.

This study shows the feasibility of performing membrane processes at a high pH on WLS inlet water. The results can be interpreted to provide a possible process configuration for SAGD PW treatment. NF processe can be seen as an alternative to the current WLS-IX process configuration, completely replacing the conventional treatment process, and providing reliable removal of TDS, silica, divalent ions and TOC from the produced water.

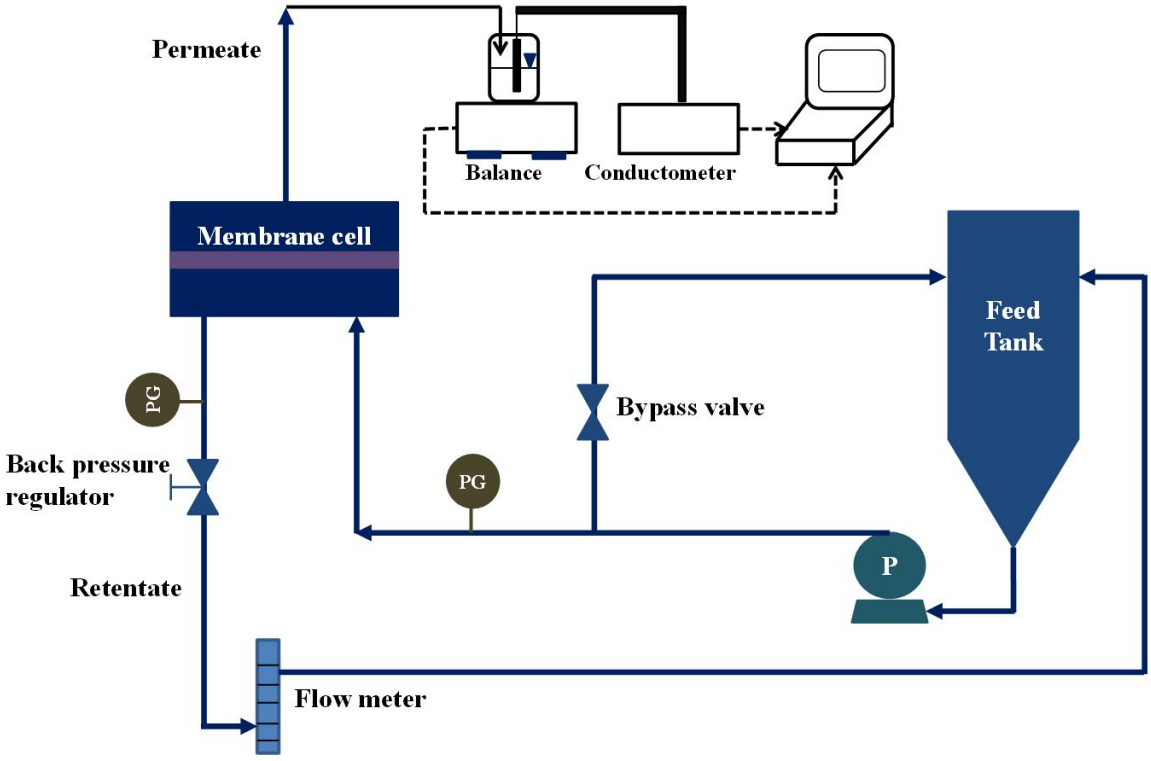

Figure 2.1: Schematic view of cross flow filtration setup

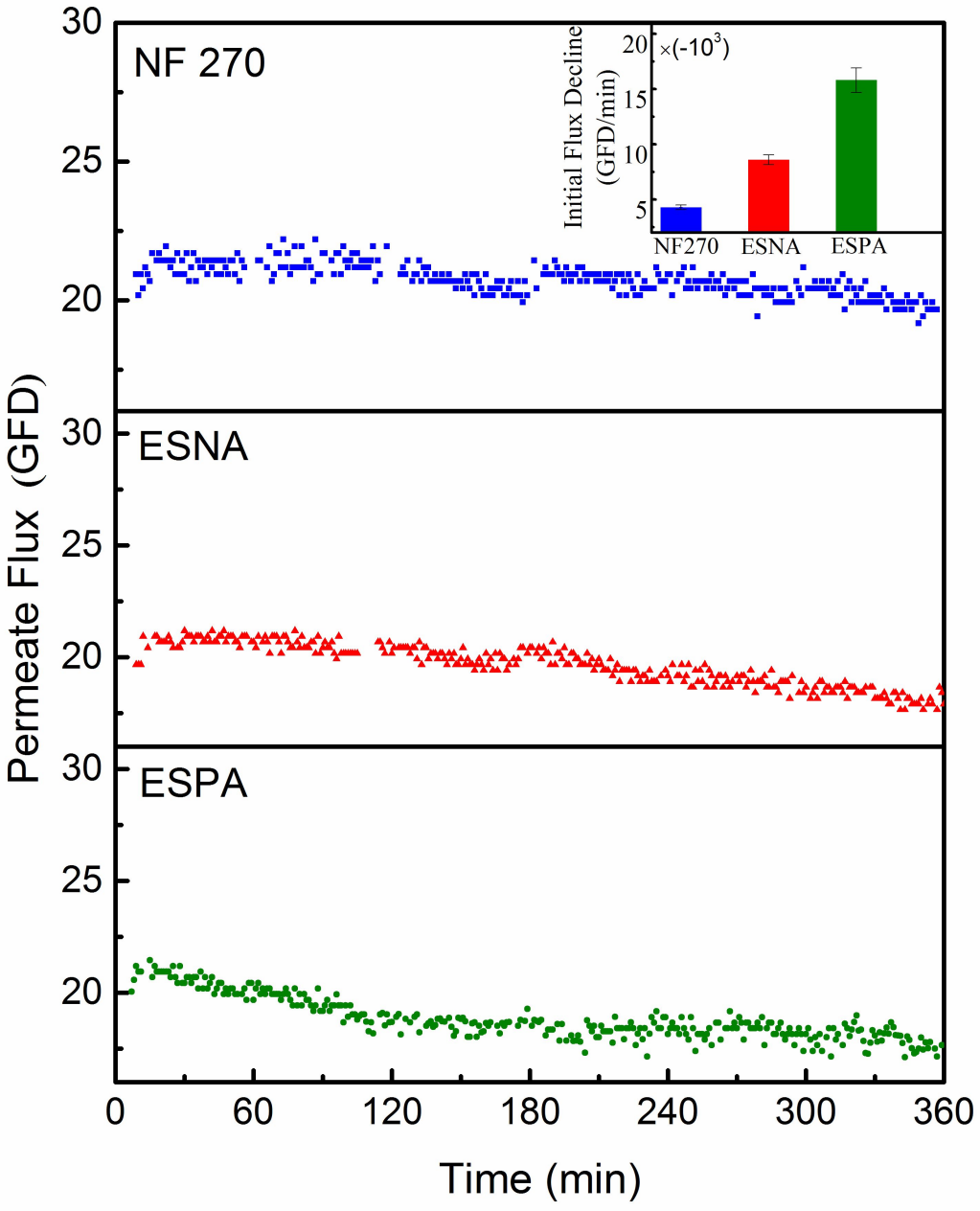

Figure 2.2: Water flux decline during cross flow filtration of WLS inlet water by NF270, ESNA

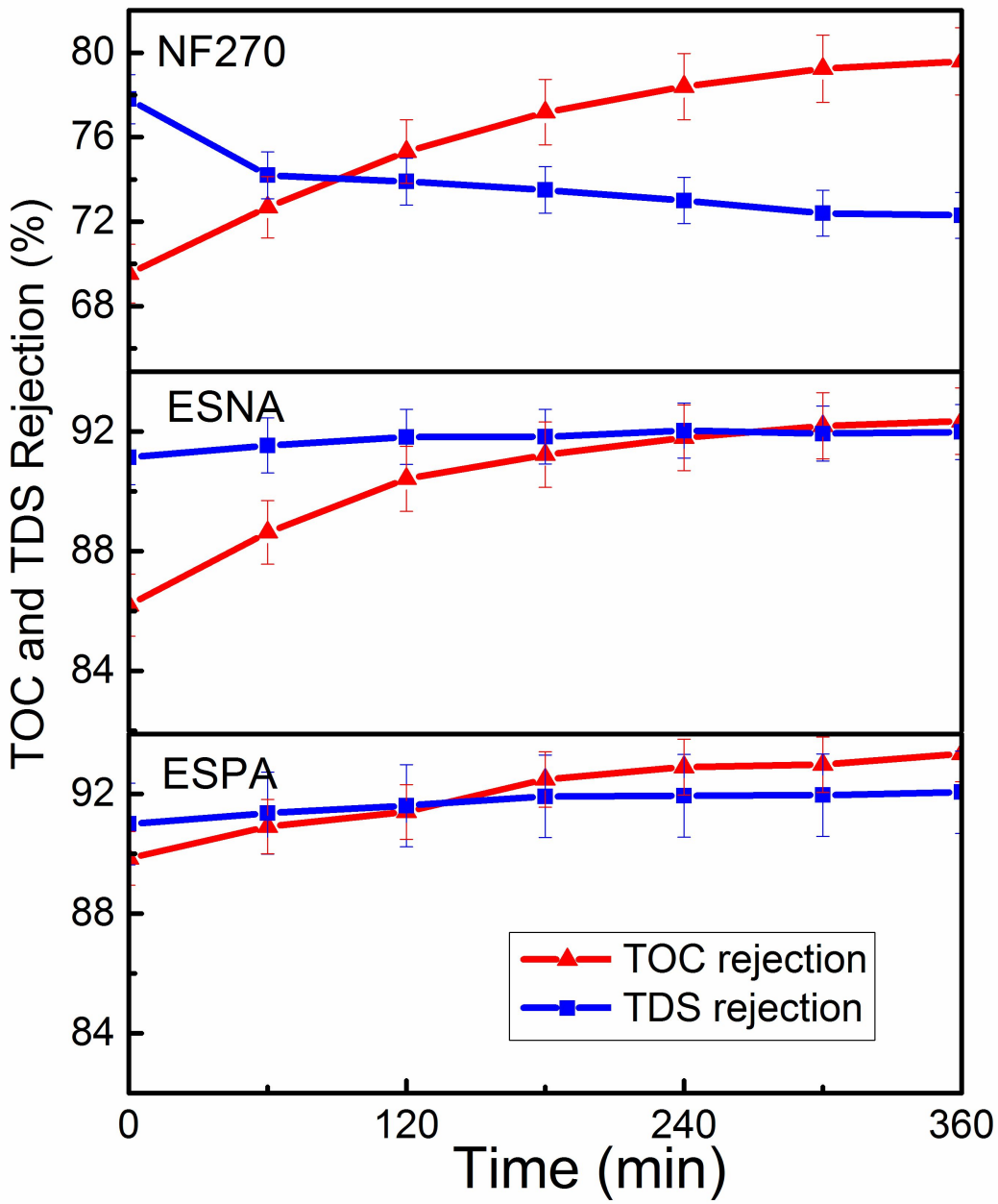

Figure 2.3: TOC and TDS rejection during cross flow filtration of WLS inlet water by NF270, ESNA and ESPA membranes at constant pH=9

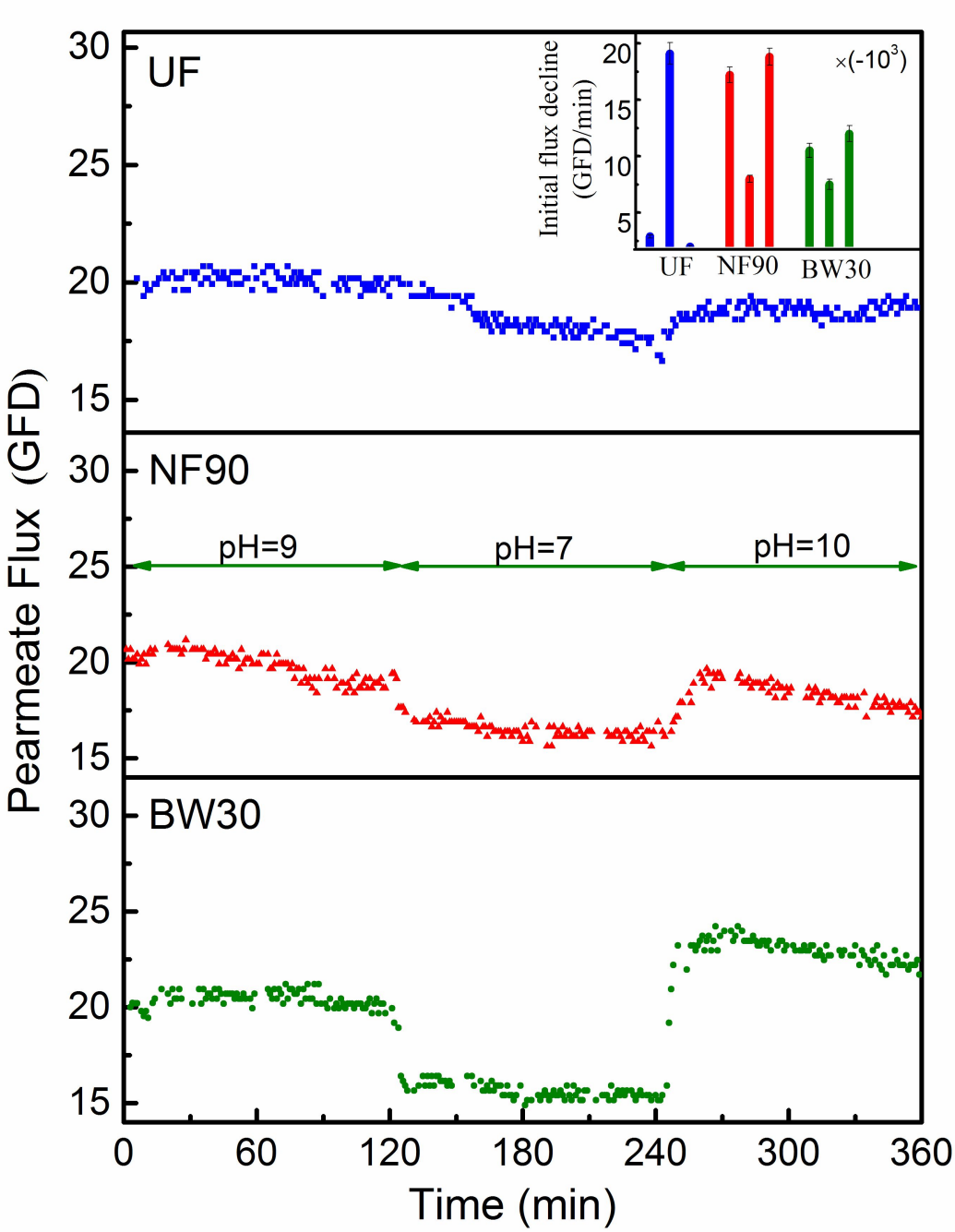

Figure 2.4: Water flux decline during cross flow filtration of WLS inlet water by UF, NF90 and BW30 membranes at various pH values (9-7-10)

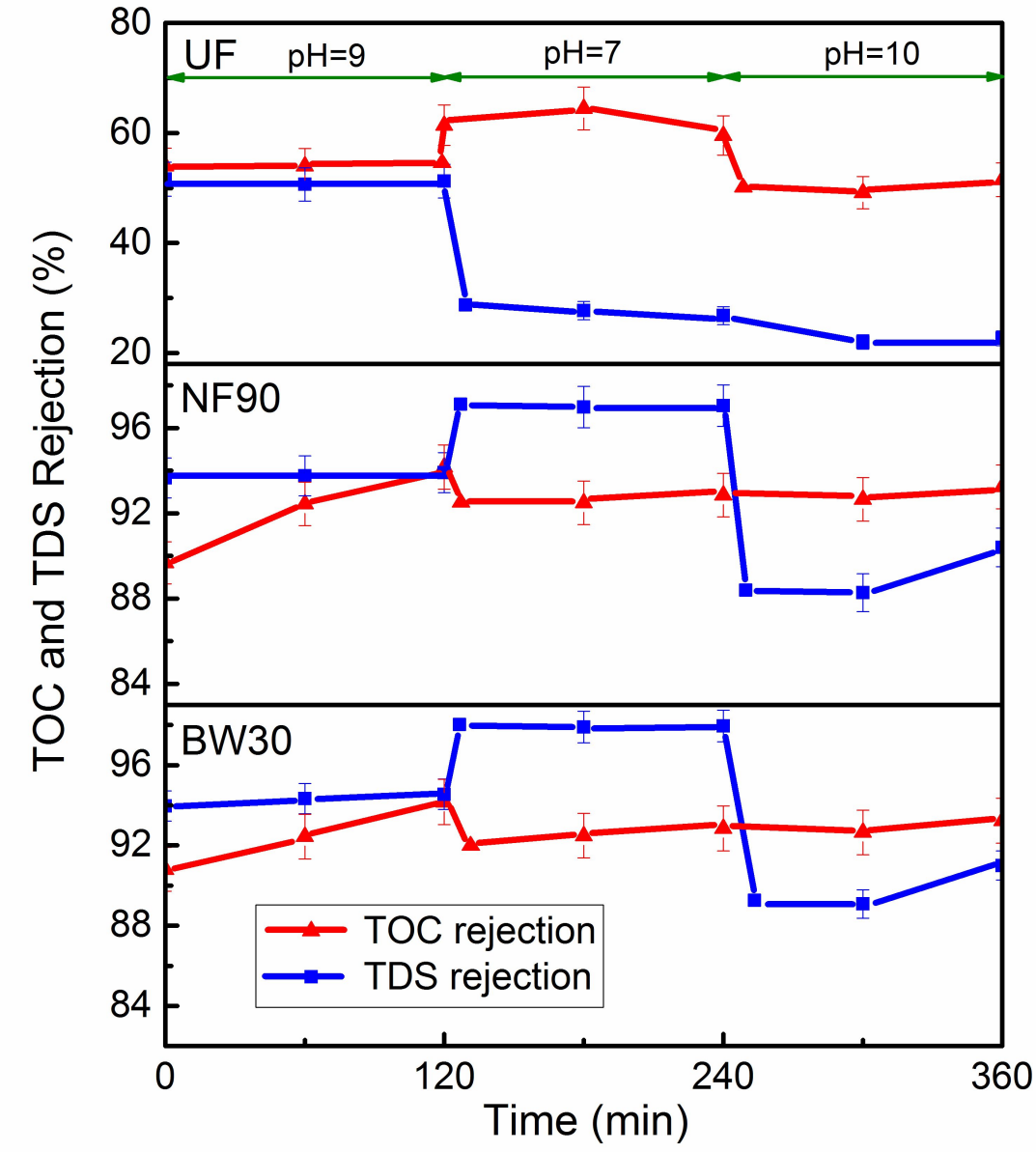

Figure 2.5: TOC and TDS rejection during cross flow filtration of WLS inlet water by UF, NF90 and BW30 membranes at various pH values (9-7-10)

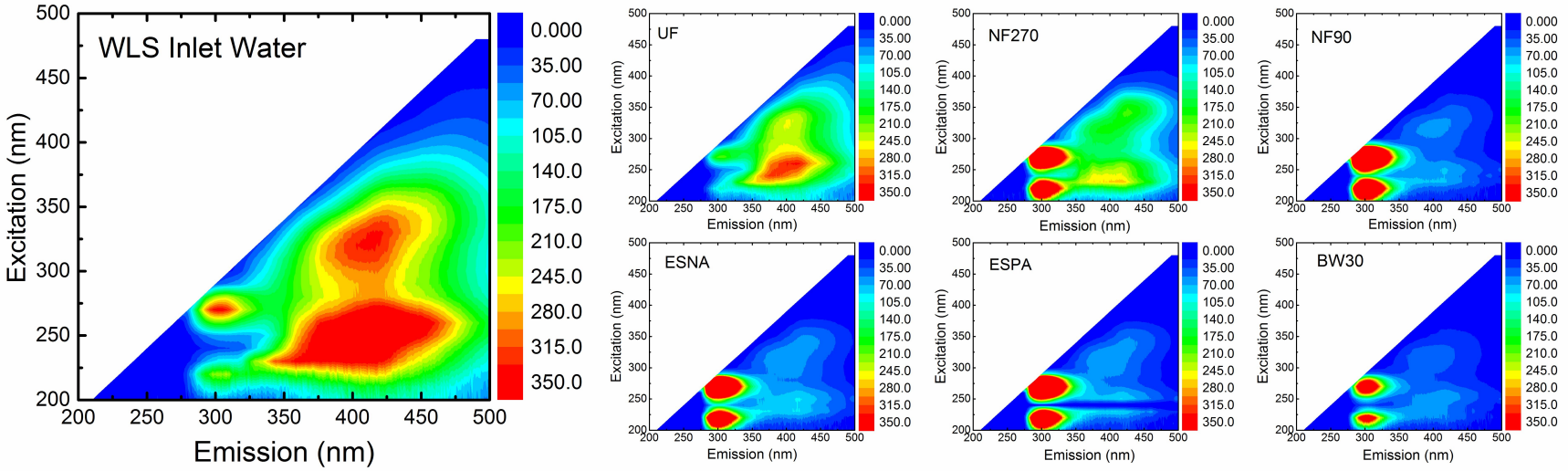

Figure 2.6: Excitation-emission matrices (EEMs) of WLS inlet water and permeates at pH=9. Excitation at 5 nm intervals from 200 to 500 nm and emission data collected at an interval of 10 nm. All permeate samples and WLS inlet feed were diluted using DI water to a TOC level of 15 5 mg/L to avoid inner filtration (quenching) effects on fluorescence analysis. Dilution time was 10:1 for UF permeate, 5:1 for NF270 permeate, 2:1 for NF90, ESNA, ESPA, BW30 permeates and 20:1 for WLS inlet water. The color scale representing the fluorescence intensity is logarithmic in all parts of these images.

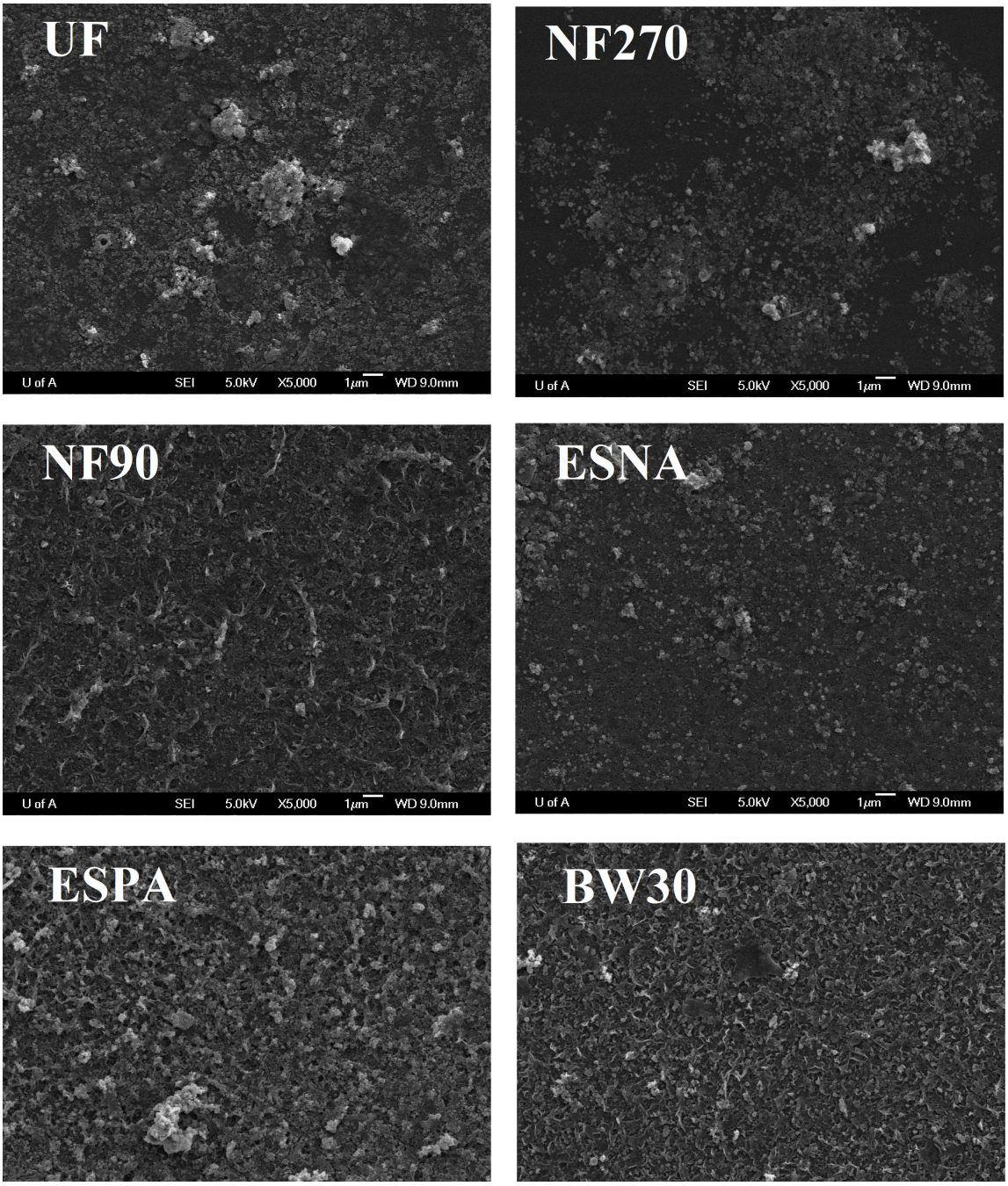

Figure 2.7: FESEM image of fouled membranes by WLS inlet water at 5 k manification

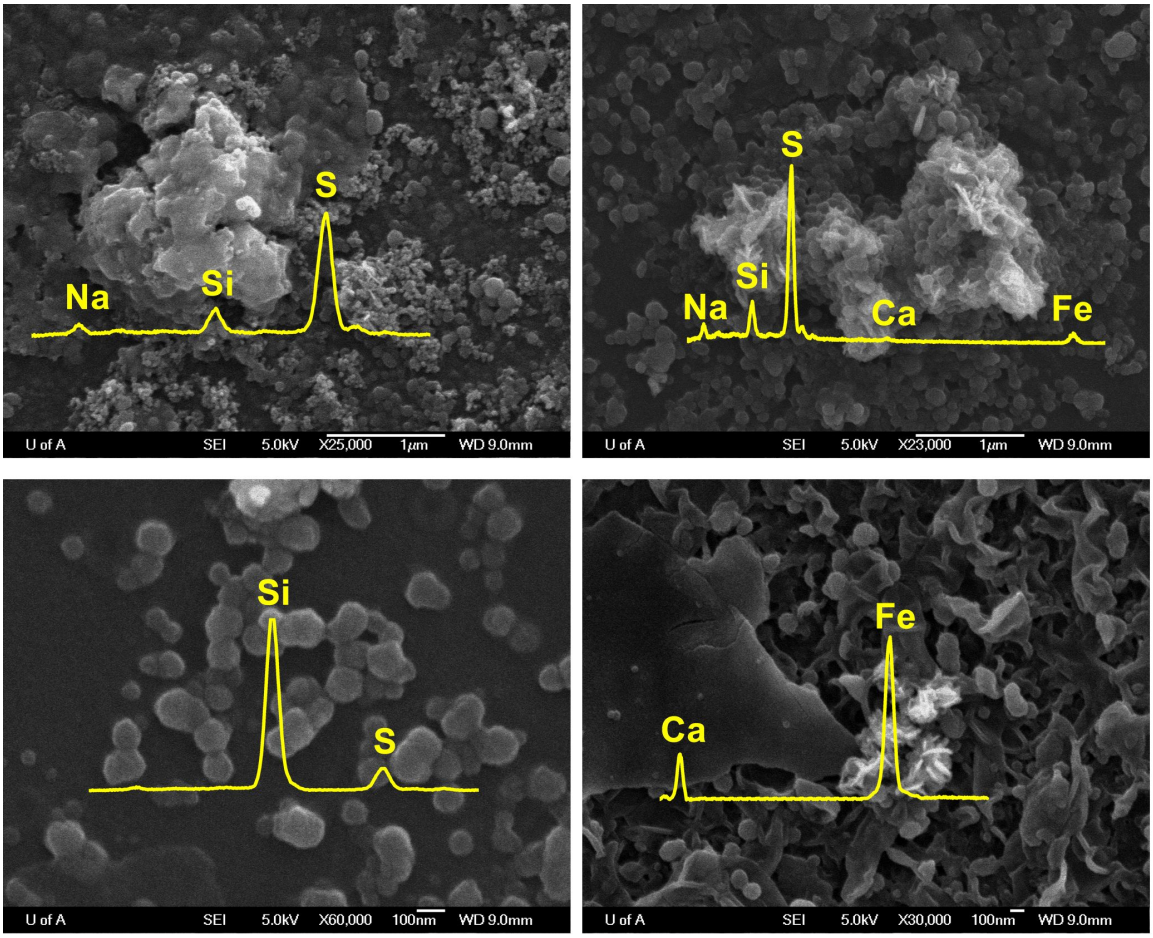

Figure 2.8: Different morphologies of foulants observed by FESEM with corresponding EDX results

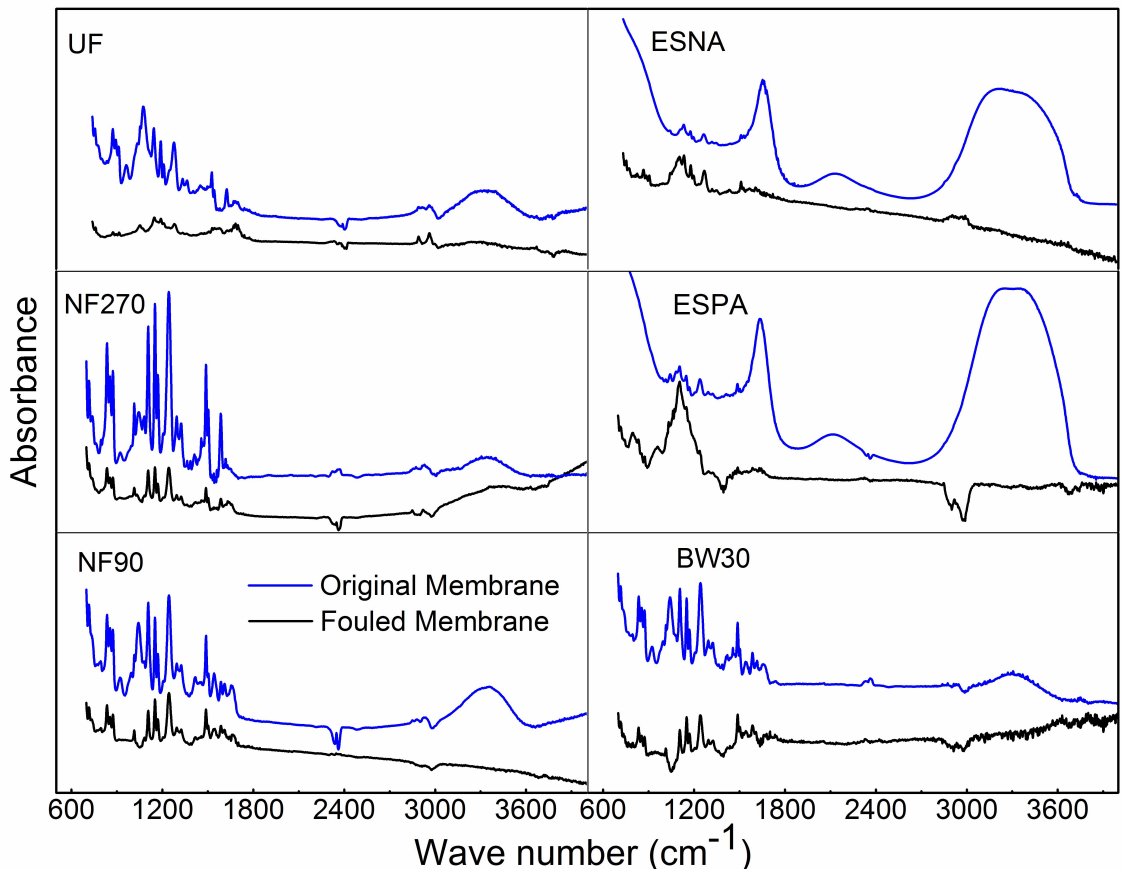

Figure 2.9: ATR-FTIR spectra of applied membranes before and after WLS inlet filtration

Chapter 3

Nanofiltration of oil sands boiler feed water: effect of pH on water flux and organic and dissolved solid rejection

3.1 INTRODUCTION

Thermally enhanced oil recovery methods such as SAGD and cyclic steam stimulation (CSS) are widely practiced for bitumen extraction from oil sands in Alberta, Canada. In this process, steam is injected underground, which condenses to heat up the bitumen, thereby reducing its viscosity. The bitumen and condensed water are pumped out to the surface where the bitumen and water are separated and the water is treated for reuse as BFW.

A typical conventional SAGD water treatment plant is shown in Figure 3.1. In the conventional diluted SAGD process, organic diluents are added to the produced fluids to reduce the viscosity of bitumen. The diluted bitumen and the produced water are first separated using a series of gravity and flotation vessels, namely, the free water knock out (FWKO) vessel to remove the bitumen, followed by gravity skim tanks and ISF to separate residual oil from the produced water, and walnut shell filters to bring the free oil content in the produced water below 20 mg/L. The produced water is then treated in a WLS to remove silica, following which, the suspended solids are removed

in after-filters, and the residual multivalent cations likes Ca^{2+} and Mg^{2+} are removed using weak−acid cation exchanger (WAC). The treated water is then used as BFW in OTSGs. A portion of the blowdown from the OTSGs is typically recycled to the WLS or the BFW tank; the remainder is sent to disposal. It is important to note that the entire water treatment process train operates at a water temperature of between 80 °C and 90 °C, a challenging temperature for polymeric membranes.

No treatment is provided for TDS removal or for the removal of DOM in the conventional process. OTSGs are therefore used in conventional SAGD applications as they are able to operate with BFW containing higher levels of TDS and Ca/Mg/Si than conventional drum boilers. To compensate for the use of lower quality BFW, steam quality in SAGD OTSGs has historically been limited to 80% to provide sufficient water volume to cool the inner surface of the tubes in the radiant section, and to prevent super−saturation and formation of inorganic scales. OTSGs BFW specifications vary somewhat between in situ operators, based on the manufacturers recommendations and by specific operating experience in the field. Typical SAGD BFW specifications are summarized in Table 3.1. It should be noted that an alternative process configuration using evaporators for desalination in conjunction with drum boilers has been employed in some SAGD installation [7].

Table 3.1: Typical SAGD OTSG BFW Specifications

Parameter	**Units**	**Specification**
Dissolved and/or Particulate Hardness	mg/L as $CaCO_3$	<0.5
pH	− − −	9.8−10.5
Silica	mg/L as SiO_2	<75
Free Oxygen	μg/L as O_2	<7
Conductiviy	mS	<12
Bitumen in Water (hexane extraction)	mg/L	<0.5
Turbidity	NTU	<7.5
Iron	μg/L as Fe	<250

Deviations from these BFW specifications have resulted in heat exchanger fouling

and boiler tube failures in the field [1,87,88], and significant research efforts are underway to understand the mechanisms of fouling. Analysis of deposits from failed tubes has found high levels of organic carbon in addition to Ca/Mg/Si. It is not clear whether the high levels of carbon are due to deposition and coking of free and emulsified oil, or whether they are due to temperature−related precipitation of dissolved organic material. In order to prevent tube failures, and to allow operation at higher steam qualities, NF was investigated as a polishing technology to further reduce the concentrations of Ca, Mg, and Si in the BFW, and to remove dissolved organic matter.

Membrane separation processes have been widely applied in produced water treatment due to their distinct advantages over traditional processes, primarily lower operating expenses and energy consumption. Numerous previous investigators have considered the use of loose membranes, MF and UF, for oil removal from oily produced water [51, 60–62, 182, 183]. For separation of silica, dissolved organic matter (DOM) and salt from produced water, tighter NF and RO membranes are required. Although, NF and RO are widely applied in water and wastewater treatment, there are a few records in peer−reviewed literature for their application in desalination and organic removal of oilfield produced water.

A brief overview of published efforts on oilfield produced water treatment using NF and RO membranes is summarized in Table 3.2.

Table 3.2: Overview of earlier studies on oilfield produced water using NF and RO membranes

Reference	Produced water type	Membrane type	Membrane salt rejection	Feed characteristics						Major findings
				pH	Temp. ($^{\circ}C$)	TDS[1] mg/L	TOC[2] mg/L	Silica mg/L	Ca^{2+} Mg^{2+} mg/L	
Kim et al. [38]	OSPW	NF& RO[7] (PA TFC)	NF 96-98%[8] RO 99-99.5%	8−9	22±1°C	2477	48.3	N/A	73	The average efficiency of salt removal was about 87.3% for RO membranes and 68.9% for NF membranes.
Peng et al. [39]	OSPW[3]	NF[4] (PA[5] TFC[6])	95%	7.3−8.5	20°C	1549−490 μS/cm	46−85	N/A	30−80	The applied NF membranes rejected more than 95% of TOC (mainly naphthenic acid) and divalent ions.
Mehrotra& Banerjee [43]	Oilsands in situ produced water	RO (PA TFC)	N−A	7.3	24°C	1770	270	N/A	70	Up to 98% and 78% of TDS and TOC were removed. Decreasing feed pH to 4, increased TOC rejection from 78% to 98%.
Dyke & Bartels [67]	Offshore produced water	NF (Polymeric ζ)	N/A	6.5	40°C	58000	176	19	1400	31 to 90% organic matter rejection and 6 to 11% inorganic rejection were observed. Rejection of organic matter increased 60% by increasing pH from 6.6 to 8.2.
Tao et al. [68]	Oilfield brine	RO (Polymeric[8])	N/A	7.8−8	40°C	6862	170	250	80	TDS rejection of 95% and TOC rejection of 96% observed. pH of feed increased to 10.6-11 to avoid oil precipitation on membrane.
Doran et al. [81]	Oilfield produced water	RO (Polymeric[8])	N/A	8.2−10.8	35°C	6000	120	10	1−5	TOC and TDS reduced by 98%. As the pH increased to 10.8 a larger faction of the boron become ionized and rejected.
Cakmakce et al. [83]	Oilfield produced water	NF & RO (PA TFC)	NF90%[8] RO 98-99.5%	7.1−7.8	25°C	7000−30000	780−1680	N/A	N/A	Different pretreatment alternatives to RO and NF were investigated and TDS and organic matter removal up to 98% obtained.
Murray-Gulde et al. [84]	Oilfield produced water	RO (PA TFC)	99%	7.7	Room temp.	6554	77	N/A	65	95% and 77% of TDS and TOC were rejected, respectively.
Mondal et al. [85]	Oilfield produced water	NF&RO (PA TFC)	NF 80−96% RO99.4	8.4−8.7	Room temp.	722−2090	69−136	7.4−14.4	1.7−12.3	RO membrane rejected 67% and 47% and NF membranes removed 28-34% and 15-47% of TOC and TDS, respectively.
Xu et al. [86]	Gasfield produced water	NF&RO (PA TFC)	NF 90−96% RO98−99.5%	8.5±0.2	22.5°	5520±718	1.8±0.2	2.7±0.6	40±5	Up to 98% of salt and 82% of organic matter rejected by NF and RO membranes. 28-34% and 15-47% of TOC and TDS, respectively.

[1]Total Dissolved Solids

[2]Total Organic Carbon

[3]Oil sands process affected water

[4]Nanofiltration

[5]Polyamide

[6]Thin Film Composite

[7]Reverse Osmosis

[8]Type of the polymer is unknown

Although several studies have been published on the use of NF and RO for treatment of OSPW associated with the surface mining and extraction of bitumen [38, 39], no published studies were found on the use of NF membrane processes for SAGD produced water treatment. Produced water from in situ oil sands operations is higher in dissolved organic carbon than OSPW [38, 39, 43], and the nature of the dissolved organics have been shown to be different [1], suggesting that organic fouling may be more severe in SAGD applications.

Every DOM has specific physicochemical properties, such as charge and molecular conformation, which controls the rate of fouling and subsequently performance of membrane process [95]. Meanwhile, the interaction of DOM functional groups with solution chemistry, e.g. monovalent and divalent concentrations, pH and presence of silica, induces different effects on properties of DOM macromolecules and thus the structure and hydraulic resistance of fouling layer [77, 92, 96, 97]. Many of earlier studies indicated that the DOM in mining OSPW consists primarily of naphthenic acid−like compounds [19, 23, 25, 71]. However, DOM in SAGD produced water was demonstrated to be more representative of humic acids than naphthenic acids [1] which is predicted to result in significant change in membrane performance.

The performance of membranes is proven to be significantly affected by the feed pH through changing DOM surface charge [79, 80, 99–101]. Dyke and Bartels [67] showed that, DOM rejection may increase or remain constant by increasing the pH, depending on the type of utilized produced water. In some waters they observed DOM reduction by decreasing the pH from their original value. However, Mehrotra and Banerjee [43] showed that by decreasing the feed pH from 8 to 4, the permeate TOC content decreased more than 90%. They attributed this to the precipitation of inorganic carbonates and bicarbonates on the membranes surface at lower pH and subsequently enhancing the permselective properties of membranes. Tao et al. [68] increased their feed pH form 8.0 to 11 to prevent oil precipitation on the membrane surface by reach-

ing to beyond its solubility limit. Doran et al. [81] suggested an approach for increasing the boron removal by increasing the pH of the RO feed water to ionize the boron. These findings suggest that the effect of pH on membrane fouling (flux decline) and rejection of organic and inorganic materials is entirely related to the characteristics of treated water.

A closer look to Table 3.2 reveals interesting differences for TOC and TDS rejection values. In some studies NF and RO resulted in similar TOC and TDS rejections [68, 81, 83], while higher TOC rejection than TDS or vice versa, were also observed [43, 67, 84–86]. This is attributed to different molecular weights and physicochemical properties of organic matter as well as different types and concentrations of monovalent and divalent ions in various produced waters.

In the present work, the performance of a commercial NF membrane for Ca/Mg/Si polishing and DOM removal from a model SAGD BFW was tested. A tight NF membrane was chosen in preference to a loose NF and a RO membrane as it offered significantly higher removal of organic matter and salt than loose NF as well as less energy consumption than RO. Crossflow NF experiments were conducted using a model BFW, prepared by diluting SAGD BBD water obtained from an operating conventional SAGD plant in northern Alberta. Tests were performed at a temperature of 50 °C and at pH values of 10.5 and 8.5. pH 10.5 corresponds to the typical BFW pH used in operating plants. pH 8.5 was tested to investigate the effect of pH reduction on membrane performance; pH reduction from 10.5 to 8.5 has been shown to increase UF membrane fouling when treating SAGD blowdown streams [171]. Based on a parametric study, it is proposed here that a pH pulsation technique can be used to reduce the membrane fouling and recover the water flux. A suitably designed crossflow NF process is demonstrated be a superior alternative technique to current SAGD produced water treatment methods, especially in terms of producing higher quality water by consuming lower amount of chemicals and energy.

3.2 Materials and methods

3.2.1 Water sample and reagents

A model SAGD BFW was prepared by dilution of BBD water from a SAGD water treatment plant located in the Athabasca oil sands region of Alberta, Canada. The samples were collected hot, shipped in sealed containers, and kept in a nitrogen blanket until they were opened for treatment [171]. BBD water was diluted five−fold to acquire the properties of BFW (Table 3.3). Concentrations of dissolved silica and other inorganics were measured by inductively coupled plasma−optical emission spectrometry (ICP−OES). 1 M HCl and NaOH (Sigma Aldrich) were used to adjust the model BFW pH.

Table 3.3: Properties of BBD water diluted to model BFW

Parameters	**BBD water**	**Model BFW**
pH	12.0	10.5
TOC (mg/L)	2450	500
TDS (mg/L)	10500	1800
Conductivity(mS/cm)	17.8	3.5
Na^{+}(mg/L)	4280	880
Cl^{-}(mg/L)	2700	510
Mg^{2+}(mg/L)	0.37	0.18
Ca^{2+}(mg/L)	3.30	0.66
Iron, total FE(mg/L)	2.12	0.48
SiO_2, Disolved(mg/L)	92	21

3.2.2 Membrane

NF was performed with a FilmTec NF90 membrane, which is a thin film composite membrane comprises three layers: (i) a polyester support web (ii) a microporous PSf inter layer and (iii) an ultrathin aromatic PA active layer. The average roughness of NF90 membrane is in the range of 60−70 nm [109, 184, 185] and its zeta potential from streaming potential measurement is −18 mV within the pH range of 7 to 10 in

10 mM NaCl solution [109]. The average hydraulic resistance (Rm), real rejection (Rr) and observed rejection (Ro) of the membrane are $4.0 \pm 0.1 \times 10^{-13} m^{-1}$, 97% and 90± 1%, respectively [186]. A loose NF (NF270) and a RO (BW30) membrane with observed rejection of ~ 50 and ~ 99.5, respectively, were also supplied from FilmTec and tested to provide sufficient evidence about the advantages of NF90 for treatment of BFW. Based on manufacturer data, maximum operating pressure and temperature and tolerable pH range for all membranes are 4135 kP, 45 °C and 3−10, respectively. In the present work, the feed water temperature and the pH were deliberately adjusted at 50 °C and 10.5, which are outside the manufacturers normal recommended operating envelope, to perform filtration under the harsh conditions expected for the full−scale industrial application. Hence, the experimental results are valid for the short−term use of polymeric membranes for treatment of BFW. Other researchers have also demonstrated successful NF and RO treatment of oilfield produced waters at polymeric membrane threshold temperatures [67, 68, 81].

3.2.3 Crossflow membrane filtration setup

The schematic view of the crossflow membrane filtration setup is shown in Figure 3.2. The maximum allowed operating pressure of the setup is 6895 kPa which is provided by a diaphragm pump (Hydra−Cell) of maximum flow 6.8 LPM. The effective filtration and flow channel area are 140 cm^2 and 1.62 cm^2, respectively. In all experiments crossflow rate was set at 1 LPM which gives a 0.1 m/s crossflow velocity and a laminar Reynolds number of 344. The model BFW was supplied from a 19 L atmospheric pressure tank. A bypass valve and a back pressure regulator (Swagelok) were used to adjust the feed flow rate and the trans−membrane pressures. The feed temperature was increased to 50 °C by a recirculating chiller (Isotemp 3013, Fisher Scientific). A weighing balance (Mettler Toledo EL4001) was used to measure the permeate flow rate. The conductivity of the feed water was obtained by an Accumet Research

(AR60) conductivity meter. The pH and conductivity of the permeate were measured by a Mettler Toledo (SevenMulti S47) pH and conductivity meter. All measurements were directly collected into a computer using LabVIEW (National Instruments) data acquisition software [186].

3.2.4 Experimental methodology

Four experiments were conducted using NF90 membrane to find the effect of pH on water flux, TOC and TDS rejection and deposition of organic and inorganic matter on the membrane surface (Table 3.4).

Table 3.4: Variation of pH with time in conducted experiments

	Experiment time(hr)					
	1	**2**	**3**	**4**	**5**	**6**
Run						
1	10.5	10.5	10.5	10.5	10.5	10.5
2	8.5	8.5	8.5	8.5	8.5	8.5
3	8.5	8.5	8.5	8.5	10.5	10.5
4	10.5	10.5	8.5	8.5	10.5	10.5

Two extra experiments were also conducted similar to run 1 (Table 3.4) using NF270 loose NF and BW30 RO membranes to compare their performances with NF90. During each 6 hr experiment, temperature, feed flow rate and permeate flux were maintained at 50 °C, 1.6×10^{-5} m^3/s and 1.8×10^{-5} $/m^2s$, respectively. The trans-membrane pressure was adjusted on 350, 550 and 825 kPa for NF270, NF90 and BW30, respectively, to acquire constant initial permeate flux of 1.8×10^{-5} m^3/m^2s. All membrane samples were soaked in de−ionized water for 24 hr prior to use. Before each experiment the membranes were compacted with de−ionized water at 1400 kPa until the permeate flux stabilized.

3.2.5 Characterization techniques

3.2.5.1 Total organic carbon (TOC) analysis

TOC is the amount of carbon bound in organic compounds present in the water and is used as an indicator of DOM in the present work. It was measured using a combustion−type TOC analyzer (Shimadzu, model TOC−V; detection range 325,000 mg/L). Since organics in the SAGD produced water are mainly water soluble [1], the unfiltered model BFW was analyzed by the TOC analyzer.

3.2.5.2 Inductively coupled plasma-optical emission spectroscopy (ICP-OES)

Emission spectroscopy using ICP is a rapid, sensitive and convenient method for the determination of metal ions in aqueous solutions. The concentrations of dissolved silica and other inorganics presented in Table 3.3 were measured by an ICP−OES instrument (Agilent 735 ICP−OES) using EPA method 200.7. In this method the water sample is nebulized and the resulting aerosol is transported into inductively coupled argon plasma generated by radio frequency power. The high temperature (6000−10000 K) of the plasma leads to almost complete dissociation of molecules and efficient atomization and ionization in the sample. Emission spectra are produced when the excited atoms and ions return to lower energy states. The spectra are dispersed by a high resolution echelle polychromator and the intensities of the lines are monitored by a CCD. In OES, the power of the radiation emitted by a constituent after excitation is directly proportional to its concentration.

3.2.5.3 Fluorescence excitation emission matrix spectroscopy (FEEMs)

Fluorescence excitation emission matrix (FEEM) spectroscopy has been shown in previous studies to be a useful tool for the classification of various dissolved organic fractions in present in SAGD produced water [1]. A wavelength range of 200 to 500

nm with 5 and 10 nm intervals for excitation and emission wavelengths, respectively was used in this research. The FEEM of de−ionized water was subtracted from the FEEM of the samples to remove most of the Raman peaks. The model BFW samples were diluted using DI water to a TOC level of around 12 mg/L to avoid inner ltration (quenching) effects on the fluorescence analysis. The pH values of feed and permeate were similar in all experiments which removes the pH induced effects on fluorescence for comparing feed and permeate FEEM results. For membrane feed samples adjusted to pH=8.5, the permeate pH was increased to 10.5 prior to FEEM analysis to find the effect of pH on FEEM results.

3.2.5.4 Attenuated total reflectance-Fourier transform infrared (ATR-FTIR) spectroscopy

ATR−FTIR spectroscopy provides information on the type of functional groups present to the depths less than 1 μ m. NF90 membranes before and after WLS inlet filtration were examined using ATR−FTIR microscope (Thermo Nicolet Nexus 670 FTIR, USA). This instrument is equipped with a mercurycadmiumtellurium (MCT) detector and has a resolution of 4cm^{-1}. A total of 512 scans were averaged for each spectral measurement. The internal reflection element was a zinc selenide (ZnSe) ATR plate with an aperture angle of 45. All membrane samples were scanned over the range of 600 – 4000 cm^{-1}.

3.2.5.5 Field emission scanning electron microscope- energy dispersive X-ray (FESEM-EDX)

The membranes were sputter coated with a thin film of chromium. Surface images of the membranes were obtained using JEOL 6301F FESEM. All membranes were imaged at a magnification of 20,000 times. FESEM provides qualitative information on the deposition of foulants on the membrane. Semi−quantitative elemental analysis

was done via a PGT IMIX EDX system with 135 eV resolution.

3.2.5.6 X-ray photoelectron spectroscopy (XPS)

XPS is a surface sensitive technique widely used for analyzing elemental composition (except for H and He). Chemical binding information for the top 1−10 nm of the surface can be provided by XPS. Original and used membranes analyzed using a Kratos AXIS ULTRA spectrometer equipped with a monochromatic Al Ka X−ray source. In the present work the source was run at a power of 210 W (14 mA, 15 kV) and a hybrid lens with a spot size of 700 μm $\times$ 400 μm. Survey spectra were collected with a pass energy of 160 eV, step size of 0.4 eV, and sweep time of 100 s in the range of 01100 eV. High resolution spectra (collected with pass energy of 20 eV, step size of 0.1 eV, and sweep time of 200 s) were measured in the appropriate binding energy (BE) ranges as determined from the survey scan for the Na 1s, Ca 2p, Fe 2p, Si 2p, O 1s, N 1s, C 1s, S 2p and Cl 2p core lines. The number of scans varied from 10 to 25 to obtain good signal/noise ratios. High resolution spectra were analyzed with the aid of the CasaXPS software.

3.3 Results and Discussion

When salt and DOM need to be removed from water, as in the present work, NF and RO are applied. NF and RO are pressure−driven processes where the transmembrane pressure must overcome the osmotic pressure of the feed water to force water through a dense membrane. Generating this pressure requires certain amount of energy which is directly related to the density of the membrane. Generally, for denser membranes rejection will be increased but so will the required pressure and thus the energy demand [187]. Hence, the type of the applied membrane for a specific application is typically identified by a trade−off relationship between energy consumption and product quality. Lower energy consumption is always favored and the product quality is

identified by environmental standards (for water disposal) and technical constraints (for water recycle and reuse).

In this section, energy requirement and product quality of a tight NF membrane (NF90), a loose NF membrane (NF270), and a RO membrane (BW30) are compared to select the winner and conduct further experiments on that. Flux (normalized with respect to initial flux) and TOC and TDS rejection of these membranes at 50 °C and pH of 10.5 are shown in Figure 3.3. All experiments were conducted at a constant feed flow rate (1.6×10^{-5} m^3/s) and permeation flux (1.8×10^{-5} m^3/m^2s) on a same model BFW to minimize the effect of feed chemistry and hydrodynamics. As can be observed, flux decline was similar for NF90 and BW30 membranes (~10%) after 6 hr run. NF90 and BW30 membranes have almost the same surface properties (roughness, contact angle and zeta potential values [51, 85, 188]) and are expected to show the same fouling behavior, thus flux decline. A slight improvement in NF270 flux decline is attributed to its very smooth surface and stronger hydrophilic properties than NF90 and BW30 as indicated by their surface roughness and contact angle values [51]. According to Figure 3.3, NF90 and BW30 rejected more than 98% of DOM which is the major responsible material for fouling of SAGD equipment [1, 87, 88]. The maximum TDS rejections obtained by NF90 and BW30 were 96% and 98%, respectively. NF270 rejected a maximum of 72% of salt and silica and 80% of DOM. Flux and rejection results demonstrated that the tight NF can produce a very high quality product which is comparable with the RO one. Compared with BW30, NF90 was also found to be less energy intensive, thus associated with lower operating cost. The applied trans−membrane pressure for NF270, NF90 and BW30 membranes were 350, 550 and 825 kPa, respectively. This shows that NF90 is more energy efficient than BW30 while providing almost the same water quality. Hence, a single stage NF with NF90 membrane is suggested for further experimental investigations. In what follows, permeation properties of NF90 membrane at various pH as well as characterization of

feed, permeate and fouling deposits on the membrane are presented.

3.3.1 Water flux and TDS and TOC rejections of NF90 membrane

The performance of a membrane process is generally monitored by measuring the permeation of the desired material (water) and the removal of unwanted material (salt and DOM). The rate of water flux decline over time gives an indication of the fouling tendency of the membrane and the fouling potential of the wastewater. Fouling deteriorates membrane performance by decreasing the water flux and its quality and ultimately shortens membrane life [95]. Hence, vast efforts have been devoted to reduce membrane fouling before operation (e.g. improving membrane properties and pretreatment of feed water), during operation (e.g. optimization of operating condition and pulsation techniques) and after operation (physical and chemical cleaning). In the present work, the effect of pH on water flux recovery and TOC and TDS rejection during crossflow NF of SAGD produced water was investigated.

3.3.1.1 Continuous operation at fixed pH

Flux and TOC and TDS rejection of the NF membrane at 50°C and a constant pH of 10.5 are shown in Figure 3.4. The normalized flux declined due to the combined fouling of silica, organic matter and divalent ions present in the model BFW (Table 3.3). However, according to the data presented in Table 3.3, the concentration of silica and divalent ions in the model BFW (~20 mg/L) is very low as compared to the concentration of organic matter (500 mg/L). Hence, DOM fouling is expected to be the dominant fouling mechanism in the present work. A rapid initial flux decline (seen after the first 6 hr of filtration), followed by a slower flux decrease is evidence of DOM fouling [121, 160, 164]. This behavior can be explained by considering the mechanism governing organic fouling. Initial adsorption of organic foulants on the membrane surface decreases permeate flux sharply due to DOM gel formation (plugging of

hot spots), pore blocking and constriction as well as induced hydrophobic properties. Slower flux decline, in the next fouling stage, is attributed to the compaction and thickening of the fouling layer, which induces an additional resistance as well as a reduction of permeation drag as permeation flux decreases [161, 164, 165, 167].

A study by Nghiem and Hawkes [144] showed that a sharp flux decline due to pore blocking and pore constriction would be more severe with membranes having a larger pore size. For salt rejecting NF and RO membranes, plugging of hot spots by organic matter has been found to be the key reason for the rapid initial flux decline [121,147,155–157]. Hot spots are the valleys on the membrane surface with the lowest thickness and highest water flux. Rapid clogging of valleys results in significant loss of permeate flux [147]. The membrane used in the present study (NF90), with the average roughness of 60−70 nm [109, 184, 185] and MWCO of 150−250 Da [103, 110], is certainly susceptible to valley blocking by particles larger than 60 nm as well as pore blocking by DOM with molecular weight less than 250 Da. As will be discussed later in this paper, FESEM images found the presence of particles with 100 nm diameter on the fouled membrane. Furthermore, our previous study showed that approximately 40% of the organic fraction in the BBD had molecular weight less than 500 Da [1] which increases the possibility of pore blocking by DOM.

Increasing hydrophobicity of membrane generally leads to more vulnerability to fouling due to hydrophobic interactions between the membrane surface and the hydrophobic foulants [121].The variation of the hydrophilic/hydrophobic properties of a membrane during filtration depends on the hydrophilic/hydrophobic properties of both the virgin (unfouled) membrane and the feed water constituents [114, 121]. Violleau et al. [158] observed that their initially hydrophilic PA membrane became more hydrophobic after the sorption of organic foulants. Cho et al. [159] showed that organic fouling decreased the hydrophobicity of hydrophobic membranes whereas increased the hydrophobicity of hydrophilic membranes, regardless of type of organic foulants.

Tu et al. [121] indicated that membranes fouled by humic acid, sodium alginate, colloidal silica and CaSO4 all became more hydrophobic than virgin membranes. The induced hydrophobicity was more severe in the more hydrophilic membrane. Yuan and Zydney [166] observed an increase in the hydrophobicity of hydrophilic polyethersulfone membranes (contact angle ~44°) fouled by two types of humic acids; more hydrophobic soil−based Aldrich and less hydrophobic aquatic Suwannee River. They reported more induced hydrophobicity by a soil−based NOM than an aquatic one. In this study, the major organic components in the model BFW are hydrophobic acids (mainly humic type ~40% [1]) and the active layer of the NF90 membrane is made of moderately hydrophilic PA (contact angle ~60° [104]). According to the literature, the specific UV absorbance at 254 nm (SUVA254, defined as the UV absorbance divided by the concentration of dissolved organic carbon) is a good criterion to classify organic materials as humic or non−humic type [189, 190]. SUVA254 values greater than 4 L $mg^{-1}m^{-1}$, as in the model BFW, indicate the presence of primarily humic type organics with high aromacity and hydrophobicity [1]. Hence, hydrophobicisation of the NF90 membrane surface after fouling becomes inevitable.

It must be noted that the flux decline observed in Figure 3.4 might be intensified (10% flux decline within 6 hr) by the interaction between organic matter and salt. Taking a closer look at Table 3.3, it is found that the ionic strength of the model BFW is relatively high with a Na^+ concentration of 880 ppm. As a general rule, organic fouling becomes more severe as the ionic strength of the feed water increases [92, 96, 109]. Higher ionic strength leads to a significant reduction of membrane and organic macromolecules surface charges due to double layer compression and charge screening. This causes a decrease in electrostatic repulsion between the membrane surface and DOM. Therefore, the deposition rate of DOM onto the membrane surface increases, which results in a thicker deposit layer. Furthermore, organic macromolecules become coiled due to reduced interchain electrostatic repulsion at high ionic strength, which leads

to the formation of a closely packed fouling layer. The resulting fouling layer provides a higher hydraulic resistance to water flow; this leads to a severe permeate flux decline [92].

Figure 3.4 shows that the NF90 membrane rejected 80% of the TDS during the initial stage of filtration, which is less than the real rejection of the membrane (90-95%). TDS rejection increased over time and reached the real rejection value after 6 hr of flow. Lee et al. [191] demonstrated that for the cake enhance concentration polarization (CECP) governed fouling mechanisms, like colloidal fouling, salt rejection decreases with time. However, the enhancement of TDS rejection with time in the present work again confirms the dominance of organic fouling in SAGD produced water filtration. Plugging of hot spots by organic matter resulted in a decrease in water flux as demonstrated in the literature [121, 147, 155–157]. TOC rejection was consistently ~98% during the experiment. This is attributed to the larger size of DOM compared to the dissolved solids, mainly Na^+ and Cl^- monovalent ions, in the water. As a matter of fact, the NF90 membrane was able to reject 98% of the organic matter at a feed pH of 10.5, regardless of the fouling progress on the membrane surface. DOM/membrane interaction during the initial stage of filtration and DOM/DOM interaction on the fouled membrane had the same effect on the removal of organic matter. It can be predicted that the portion of DOM which passed through the membrane was small hydrophilic organic compounds. This hypothesis can be tested by conducting FEEMs analysis on permeate and feed samples, as will be presented later.

By decreasing the feed pH, water flux and TDS rejection behavior with time changed significantly. As can be observed in Figure 3.5, water flux decreased to 93% of the initial flux after 2 hr, then remained constant. TDS and TOC rejections remained constant for the whole range of experiment at 98%. According to our earlier study, acidification of feed water causes precipitation of silica nanoparticles and also coprecipitation of organic compounds by adsorption on the surface of the silica nanoparticles [171].

This is due to the decrease in electrostatic repulsion of these foulants after protonation at lower pH values. Detailed explanation of electrostatic double layer interactions between the solutes is presented in the next section. Deposition of both silica particles and organic compounds on the membrane surface results in the formation of a cake layer with a high resistance to permeate flow, and subsequently low water flux. It must be noted that the vertical axis in Figure 3.5 is the ratio of water flux to the initial flux. This dimensionless value is helpful to find the rate of flux decline irrespective to the exact flux values. Rapid formation of a cake layer on top of the membrane at lower feed pH switches the membrane−foulant interaction phenomenon to foulant−foulant interaction in less than 2 hr. Consequently the steady state condition is reached in a shorter time. The cake filtration increased the TDS rejection from 95% (at pH=10.5 after 6 hr run) to 98% (at pH=8.5) which was constant during the experiment.

Comparing filtration results at pH 8.5 and 10.5, it was found that the lower pH value led to more stable results (in terms of water flux and rejection). However, coprecipitation of silica and organic matter on the membrane surface at lower pH is predicted to decrease the permeate water flux. In order to determine the effect of pH on water flux and flux recovery, fouling behavior was studied in a dynamic pH experiment. As will be discussed later, an instantaneous change in water flux by a sudden change in feed water pH helps to understand the key role of pH for SAGD NF treatment.

3.3.1.2 Membrane operation with varying pH

Figures 3.6 and 7 show the effect of a step change in feed pH during constant operation on flux and rejection. As shown in Figure 3.6, increasing the pH from 8.5 to 10.5 increased the flux by 20%, but decreased the TDS rejection. Figure 3.7 shows that pH reduction from 10.5 to 8.5 decreased the flux suddenly and increased the TDS rejection to 98%. Returning the pH back to 10.5 quickly returned the flux and rejection to previous trend. For all pH values, more than 98% of the organic matter was rejected by

NF. TOC reduced from 500 ppm to less than 10 ppm in all experiments. Dynamic pH experiments confirmed that a steadier water flux and higher TDS rejection occurred at lower pH. However, the overall water flux was higher at higher pH values. Instantaneous change of flux and TDS rejection by injecting acid or alkaline into the feed solution demonstrates the significant role of pH on fouling, especially in presence of both silica and organic matter. The reason behind this behavior is believed to be the rapid change in foulant/foulant and foulant/membrane interactions by changing the pH.

The permeate flux under various pH values is affected not only by the characteristics of the membrane but also by the properties of the solution. The effect of feed pH on the size and zeta potential of organic matter has been broadly reported in the literature [79, 80, 92, 99–101]. These investigations found that no obvious variation existed in the average size of organic matter under various pH values, however their surface charges were shown to become more positive with decreasing pH. The higher negative charge at higher pH values causes the cake layer to become more open due to the inter−foulant repulsion, and this increases the permeation flux. In the present work, DOM is the major constituents responsible for fouling. Protonation of DOM functional groups (mainly carboxylic acid) at lower pH reduces the charge and subsequently electrostatic repulsion of organic matter [79, 80, 92, 99–101]. In addition, macromolecular conformation of organic matter varies with pH, so that smaller configuration is created at lower pH values [96, 97]. This causes the formation of a denser fouling layer and subsequently, a flux decline.

In addition to inter−particle repulsion, there is also particle−membrane repulsion due to a larger negative charge on the membrane surface at higher pH [56, 175]. Elimelech and Childress [56, 160] conducted a comprehensive work on the effect of pH on zeta potential for thin film PA membranes at NaCl, Na_2SO_4, CaCl2 solutions of various concentrations. In all cases, the zeta potential of the membranes became more

negative as pH increased. PA membranes contain carboxylic ($R-COO^-$) and amine ($R-NH_3^+$) ionizable functional groups which are responsible for development of surface charge [56, 57].

The inter−particle repulsion as well as particle-membrane repulsion prevent the particles from depositing, and lead to the reduction of the thickness of cake layer. These phenomena can explain the higher permeation fluxes observed at higher pH values [92, 96, 109].

3.3.2 Rejection of organics

FEEMs has been used in prior investigations of SAGD waters to characterize the nature of the dissolved organics [1]. The FEEM signatures of DOM in the model BFW and the permeate at two pH values, 8.5 and 10.5, are shown in Figures 3.8 and 3.9. The fluorescence response for the feed occurs over a wide range of wavelengths, with a dominant peak at an excitation/emission (Ex/Em) wavelength range of 210−350/325−450 nm. This wide range of wavelengths demonstrates that a wide variety of organic compounds exists in the model BFW. The Ex/Em wavelength ranges for peaks associated with these organic compounds are presented in Table3.5.

Table 3.5: Fluorescence peak intensities of fluorophores in SAGD BFW (data related to signature of organic acid fractions was taken from Thakurta et al. [1])

DOM fractions	**Ex/Em range**
Model BFW	200−375/300−500
Hydrophobic acid (HPoA)	310−340/400−500
Hydrophobic neutral (HPoN)	225−250/325−380
Hydrophobic base (HPoB)	260−290/280−320
Hydrophilic acid (HPiA)	320−375/375−500
Hydrophilic neutral (HPiN)	210−225 and 250−275/280−320
Hydrophilic base (HPiB)	210−225/275−310 and 325−400

The fluorescence emission intensity peaks of DOM are generally observed due to the presence of high aromaticity, hydroxyl, and amine groups in the organic fluo-

rophores. The fluorescence intensity of any fluorophore can also be reduced by the interfering effects of other molecules present in a system containing a mixture of fluorophores. In the present work, in presence of high concentration of HPoA, HPiA, HPiB and HPoN, the fluorescence intensity of HPiN and HPoB fractions are quenched in the feed fluorescence EEM, especially at pH=10.5.

The FEEMs contour maps for the membrane permeates show that some signatures have been totally removed after NF. As can be seen, the major organic compounds in the permeate were hydrophilic compounds (HPiN, HPiA and HPiB). Lower molecular weight hydrophilic DOM could easily pass through the membrane, especially at the initial stage of filtration (see time 30 min in Figures 3.4 to 3.7). It is worth noting that all the FEEMs were obtained for identical TOC of 9−12 mg/L. Hence, the fluorescence intensity in the feed compared to the permeate was not a simple concentration effect.

It must be noted that the NF90 membrane rejected 98% of organic matter in the model BFW; from 500 mg/L to around 10 mg/L. Since hydrophilic matter makes up almost 45% of model BFW [1], more than 95% of these organic compounds were also rejected and deposited on the membrane surface. This observation suggests that all types of organic compounds in the model BFW were responsible for the fouling of the NF membranes.

3.3.3 Rejection of inorganics

Rejection of inorganic materials from model BFW was measured by ICP−OES analysis and the results are presented in Table 3.6.

Greater than 99% rejection was seen for divalent ions such as Fe^{2+}, Ca^{2+} and Mg^{2+}. 98% rejection was observed for the dissolved silica. These low levels of inorganic, scale−forming species in the NF permeate, would greatly reduce the fouling propensity of the BFW if NF was applied as a polishing step in the conventional SAGD process

Table 3.6: Inorganic rejection by NF90 membrane obtained by ICP−OES

Elements	**RDL**$^{\zeta}$	**Model BFW**	**NF90 permeate**	**Rejection (%)**
Na^{+}(mg/L)	0.5	880	53	94
Cl^{-}(mg/L)	1.0	510	15	97
Mg^{2+}(mg/L)	0.02	0.18	<0.02	> 99
Ca^{2+}(mg/L)	0.03	0.66	<0.03	> 99
Iron, total FE(mg/L)	0.03	0.48	<0.03	> 99
SiO_2, Disolved(mg/L)	0.1	21	0.4	98

$^{\zeta}$ Reportable Detection Limit

train.

3.3.4 Fouling characterization

Virgin and fouled membranes were analyzed by ATR−FTIR, FESEM−EDX and XPS to identify the elements deposited on the membrane surface and to quantify the amount of foulant.

3.3.4.1 ATR-FTIR results

All samples were scanned from 650 to 4000 cm^{-1}. Over the wave number range 20004000 cm^{-1} little change in the spectra of the base membrane was observed after filtration. Thus Figure 3.10 gives results only for wave numbers between 650 and 2000 cm^{-1}. This figure indicates that the peak heights associated with the base membrane are reduced after filtration. The ATR−FTIR spectra contain peaks at 694, 1151, 1487, 1503 and 1584 cm^{-1} that indicate the presence of the PSf interlayer. Peaks at 1650 and 1541 cm^{-1} indicate amide I and amide II for the NF90 membrane. NF90 is made from m−phenylene diamine, a primary amine. Though filtration leads to a decrease in PA and PSf associated peak heights, no new peaks are detected. The absence of peaks representing organic foulants is most likely due to the fact that the peaks associated with PSf and PA are much larger than the small peaks that represent adsorbed organic species.

3.3.4.2 FESEM-EDX results

Figure 3.11 shows FESEM images of the NF90 membranes before and after filtration. After NF, a coating of rejected solutes on the membrane surface was formed. Larger amounts of foulant were observed when the pH of the feed water was decreased to 8.5, as shown in Figure 3.11c,d. It is hypothesized that decreasing the pH caused precipitation of silica particles and coprecipitation of organic compounds, which are adsorbed on the surface of the silica nanoparticles. EDX elemental analysis indicated the presence of silica and iron in the foulant material for all used membranes. The sulfur and oxygen peaks in Figure 3.11 are likely related to the NF90 PSf microporous interlayer as seen in the ATR−FTIR spectra (Figure 3.10). The iron peak became larger and the sulfur peak became shorter as the pH decreased from 10.5 (Figure 3.11c) to 8.5 (Figure 3.11b). This result shows that more solutes precipitated on the membrane surface at lower pH. The most interesting result was obtained when the pH of the feed solution increased from 8.5 to 10.5 during filtration. As can be observed both silica and iron peaks shortened considerably which indicates re−dissolving of these materials at higher feed pH. This observation suggests that fouling is partially reversible by increasing the pH.

Taking a closer look to Figure 3.11, it was found that deposited foulants on the membrane surface were in three forms: beads, small crystals and large crystals. These three types of deposited solutes and their relevant EDX analysis are shown in Figure 3.12. According to this figure it can be concluded that silica/iron complexes are present in all forms and are homogenously distributed on the membrane surface. Needle−like crystals are believed to be mineral aegirine crystals (a sodium iron silicate complex has the chemical formula $NaFeSi_2O_6$ in which the iron is present as Fe^{3+}). Beads are assumed to be mainly silica particles capped with organic matter and inorganic precipitates (mainly metal oxides like Fe_2O_3). EDX results of beads, small crystals and large crystals suggest that sulfur and oxygen also exist in the foulant material.

3.3.4.3 XPS results

XPS spectra for original and used membranes are shown in Figure 3.13. The original membrane shows peaks corresponding to elements present in the PA thin film: C 1s, N 1s and O 1s. Filtration of model BFW led to a change in the peak heights for C, N and O. The C and O peaks increased in height while the peak for N decreased. Inorganic deposition (Fe, Si, Ca) was also observed on the used membranes. Further peaks corresponding to Na and O appeared as NaKLL and OKLL, representing Auger emission.

Table 3.7 gives elemental compositions for the original and used membranes. The NF90 membrane is a fully aromatic PA composite membrane [192].

Table 3.7: XPS surface elemental analysis (atomic%)

Membrane	**C**	**O**	**N**	**C:O:N ratio**	**S**	**Na**	**Ca**	**Fe**	**Si**	**Cl**
Original membrane	74.25	12.97	11.78	6.30:1.10:1.00	0.36	0.29	0.00	0.00	0.00	0.35
NF at pH=8.5	70.09	20.36	2.83	24.76:7.19:1.00	1.22	2.13	0.53	1.18	1.96	0.10
NF at pH= 10.5	68.27	18.57	7.76	8.79:2.39:1.00	0.30	1.97	0.49	0.80	1.62	0.22
NF at pH= 8.5-10.5	65.09	23.20	4.26	15.27:5.44:1.00	0.88	1.26	0.51	1.70	1.87	0.13

The theoretical O/N ratio is expected to be 1.0 when the PA layer is fully cross−linked. Table 3.7 indicates that the applied NF90 membrane in this study has an O/N ratio of 1.1 which is similar to that of a pure PA. A slight excess of oxygen with respect to the corresponding theoretical ratio for PA indicates a low content of impurities on the surface of this membrane. The surface of the NF90 membrane contains S, Na and Cl (<0.5%) in addition to the elements characteristic of the PA. This indicates that solvents and washing agents were not completely eliminated during the process of manufacturing the membrane [193].

Filtration led to a change in the C:O:N ratio. The amount of C increased significantly, indicating adsorption of organic foulants. Table 3.7 indicates that the greatest increases in the ratios of C/N and O/N occurred for filtration at pH=8.5. Higher amounts of inorganic matter were deposited on the membrane surface at pH=8.5.

High resolution XPS spectra give more information about the organic and inorganic components and bonds on the membrane surface. Based on Figure 3.14, it can be concluded that:

1. Na on the original membrane is NaCl remained after washing by manufacturer. However Na added after filtration is possibly related to either remnants of the feed water that have evaporated and left NaCl behind or Na_2O precipitates.

2. Ca, Fe and Si on the membrane surface correspond to oxides of these elements.

3. The position of the BE for SiO_2 is 101 eV. This BE is around 103 eV for pure SiO_2. The BE obtained in the present work could be related to a sodium iron silicate complex, e.g. $NaFeSi_2O-6$ called mineral aegirine.

4. Sulfate on the original membrane is related to sulfuric acid which is usually used for post−treatment of membranes. Kulkarni et al. [194] indicated that sulfuric acid may be used to hydrophilize PA thin film composite membranes. By carefully controlling the hydrophilization conditions, the permeate flux may be increased and fouling decreased without loss in the rejection behavior of the membrane. Used membranes showed sulfide spectra instead of sulfate which may correspond to metal and salt sulfides like FeS and Na2S.

The multi−region spectra of C 1s, O 1s, and N 1s for both membranes are shown in Figure 3.15. According to this figure, all spectra related to membrane chemical bonds were weakened. Aromatic/aliphatic bonds in the used membrane increased as compared to the original membrane (Figure 3.15 a, d). This may show the high aromacity of the organics in the model BFW. Carboxylic bonds also intensified in used membranes (Figure 3.15 b, e). A small peak related to Si−OH was observed in O

1s spectrum. Figures 3.15 c and f show the presence of amino acids in the deposited matter on the membrane surface.

3.4 Conclusion

Model SAGD BFW was treated with a crossflow NF process. First, a tight NF membrane was selected in preference to a loose NF and a RO membrane based on its superior rejection properties and energy efficiency. Then, experiments were conducted on this membrane at constant feed temperature (50 °C) and two pH values (10.5 and 8.5). The NF membrane rejected up to 98% of salt, DOM and silica, and >99% of divalent ions. TOC rejection was ~98% regardless of the pH. At higher pH (10.5), the initial TDS rejection was about 80% and increased up to 96% after a 6 hr run. However, at lower pH (8.5), TDS rejection was steady at 98% during the entire experiment. The higher TDS rejection at pH 8.5 was attributed to the formation of a cake−layer formed from the co−precipitation of silica and organic matter on the membrane. A step−change in pH from 8.5 to 10.5 increased the water flux by almost 20% immediately. Surface characterization of the fouled membranes using ATR−FTIR, FESEM−EDX and XPS analyses provided valuable information about the constituents in the model BFW, which were deposited on the membrane. EDX indicated the presence of silica and iron in fouling deposits. XPS showed the presence of inorganics (mainly metal oxides) and organics (having carboxylic and amino acid functional groups) on the membrane surface. FEEMs showed that hydrophilic compounds made up the major fraction of the organics that passed through the membrane. This study shows the feasibility of performing NF at a high pH as a polishing step in the conventional SAGD water treatment process train for the production of a higher−quality BFW. The results can be interpreted to provide two possible process configurations for SAGD produced water treatment and BBD recycle. First, the NF process can be seen as an alternative to the current WLS−WAC process configuration, completely replac-

ing the conventional treatment process, and providing reliable removal of TDS, silica, divalent ions and TOC from the produced water. Although more studies are needed to clearly indicate whether such a process will be economically viable, and what is the maximum recovery achievable from such a plant, the process seems to be technically feasible. Second, the BBD and makeup water can be combined and treated through a separate NF system, yielding a stream containing low silica, TDS, DOM, and divalent ions that can be mixed with a conventionally (WLS−WAC) treated BFW. This prevents the risks associated with mixing the BBD and makeup water with the entire produced water stream before the WLS in the current conventional process configuration, but rather conditioning the recycle and makeup streams from the produced water in a segregated manner.

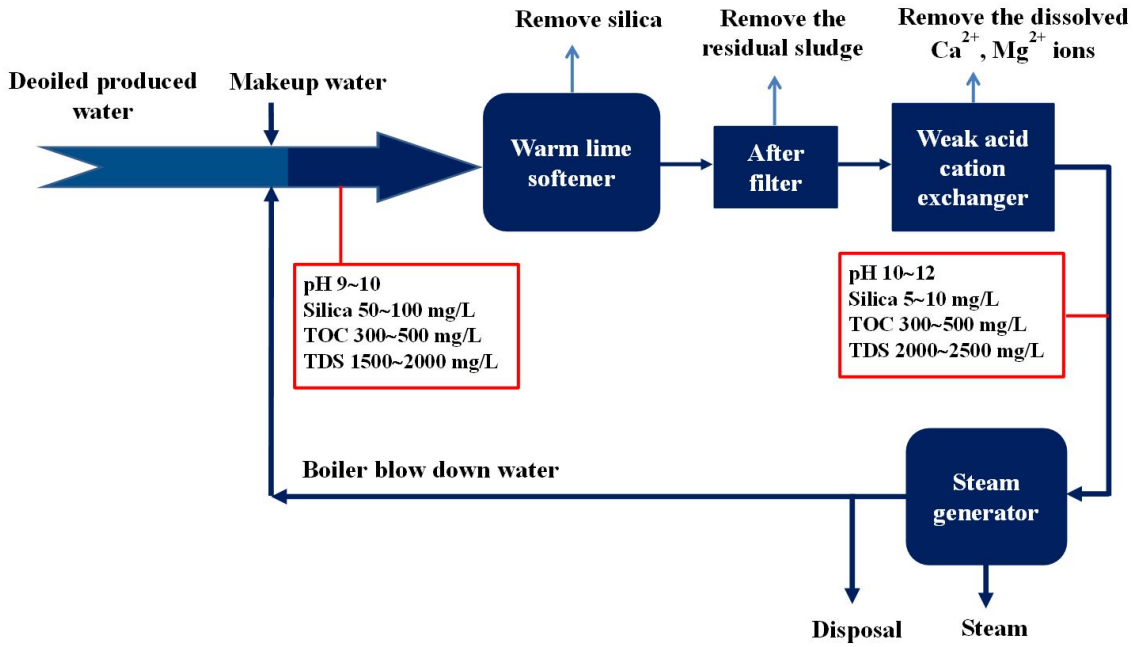

Figure 3.1: Process flow diagram of a typical SAGD-based in situ bitumen extraction water treatment plant

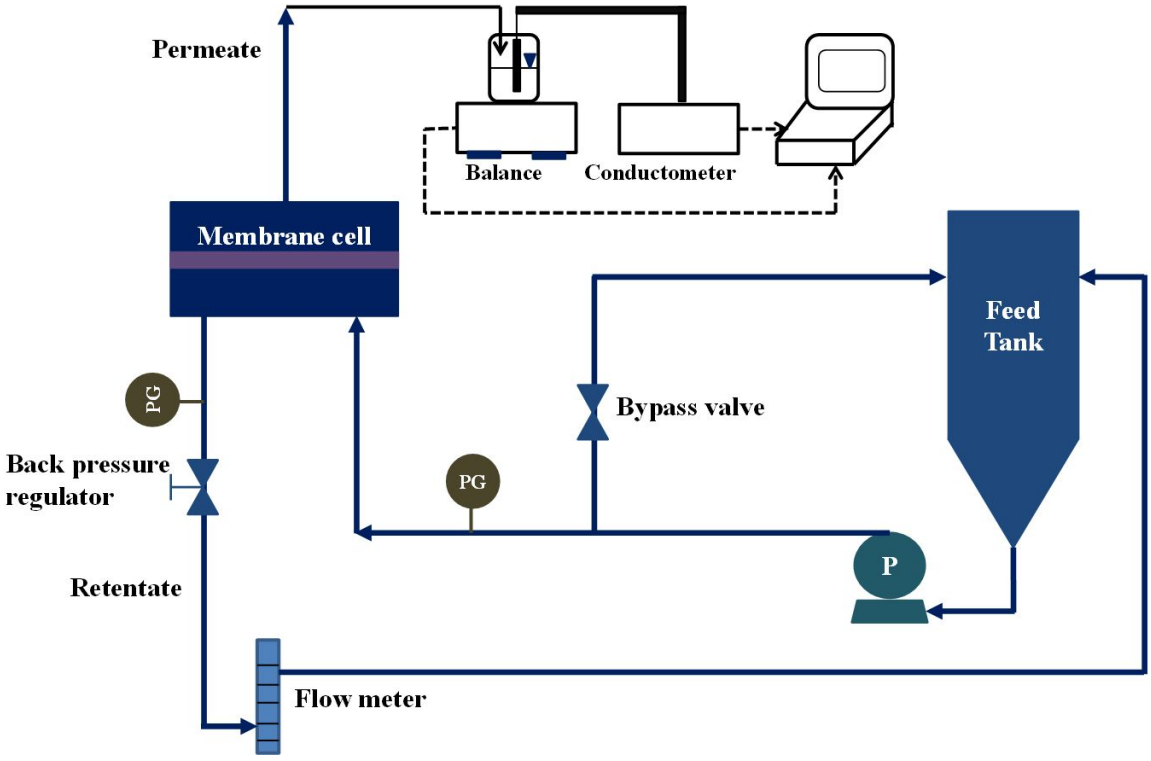

Figure 3.2: Schematic view of crossflow filtration setup

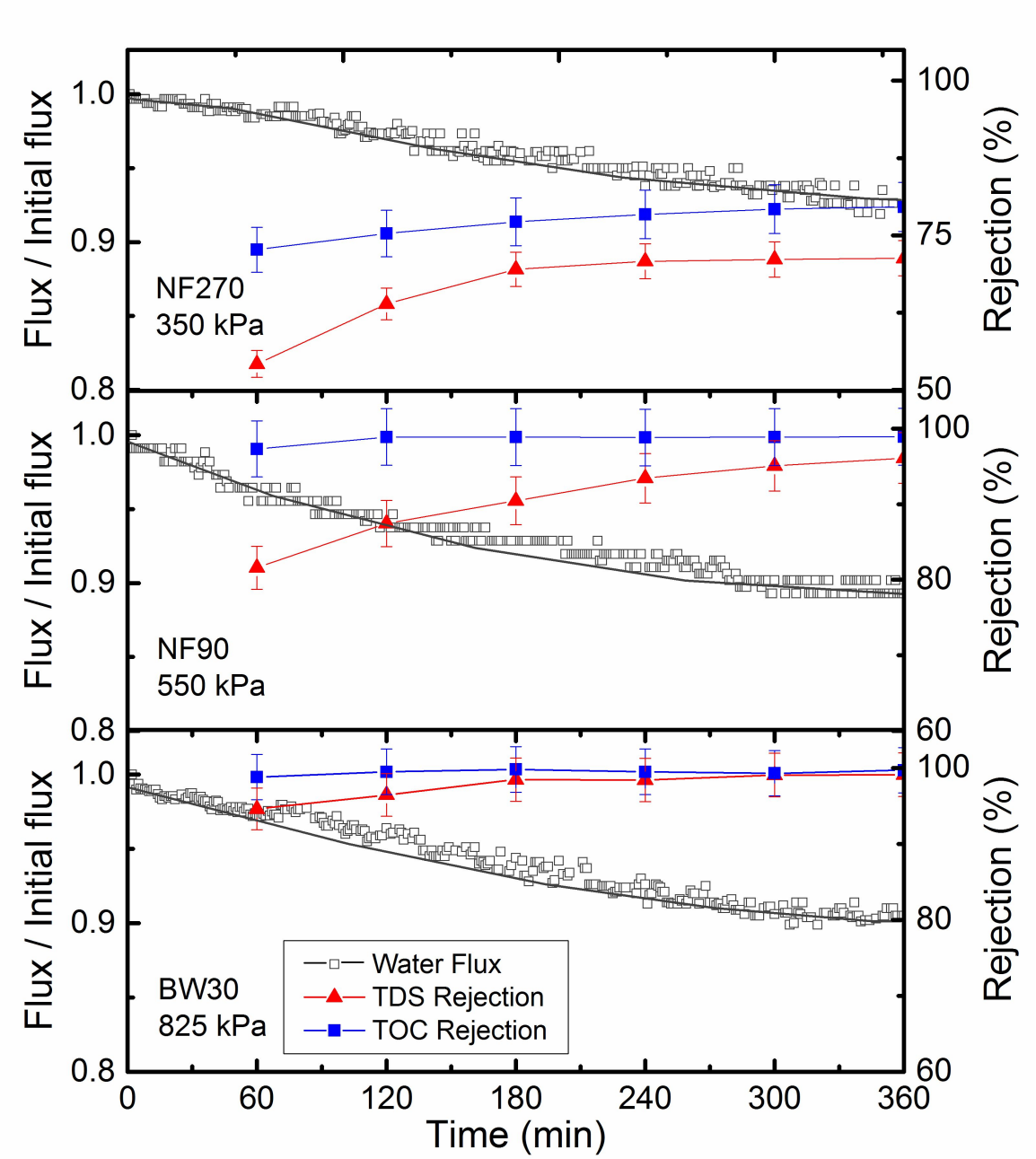

Figure 3.3: Water flux and rejection for model BFW filtration using loose NF (NF270), tight NF (NF90) and RO (BW30) membranes at pH=10.5

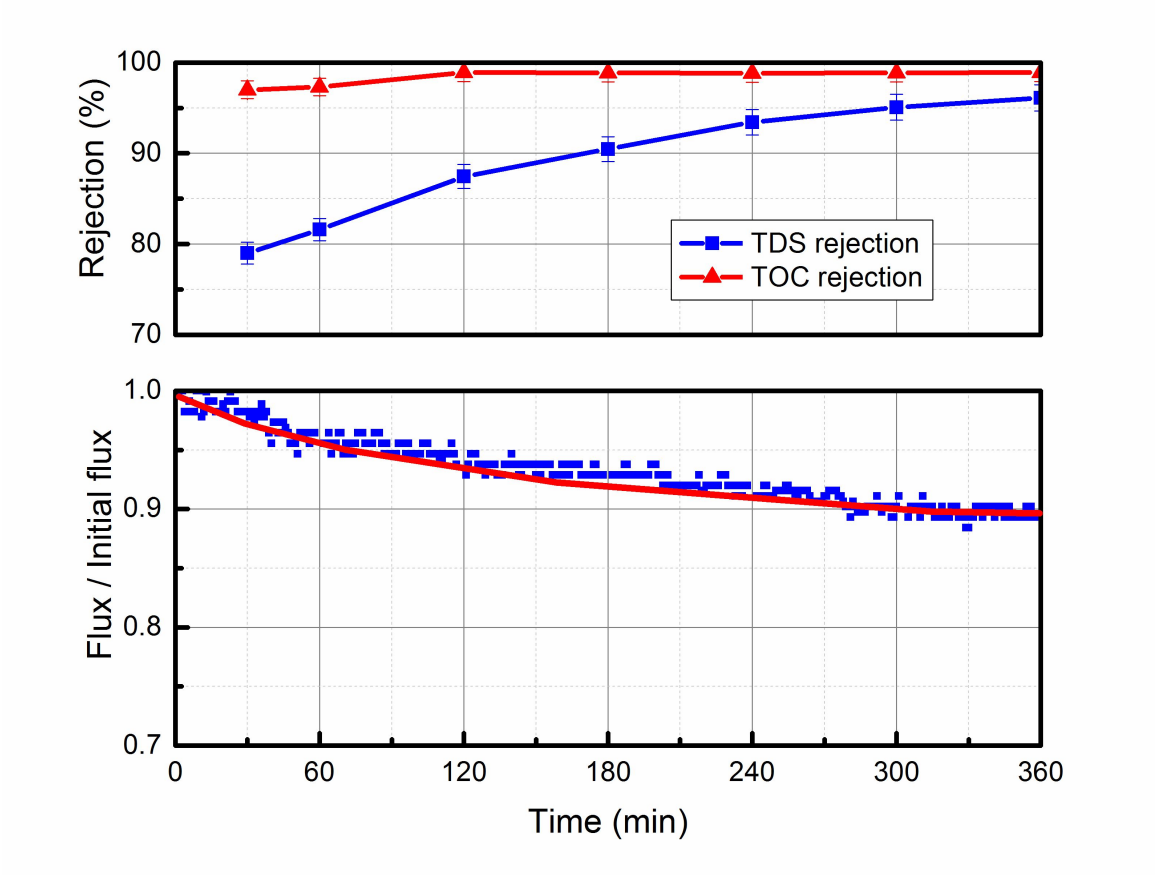

Figure 3.4: Water flux and rejection for model BFW filtration using NF90 membrane at pH=10.5

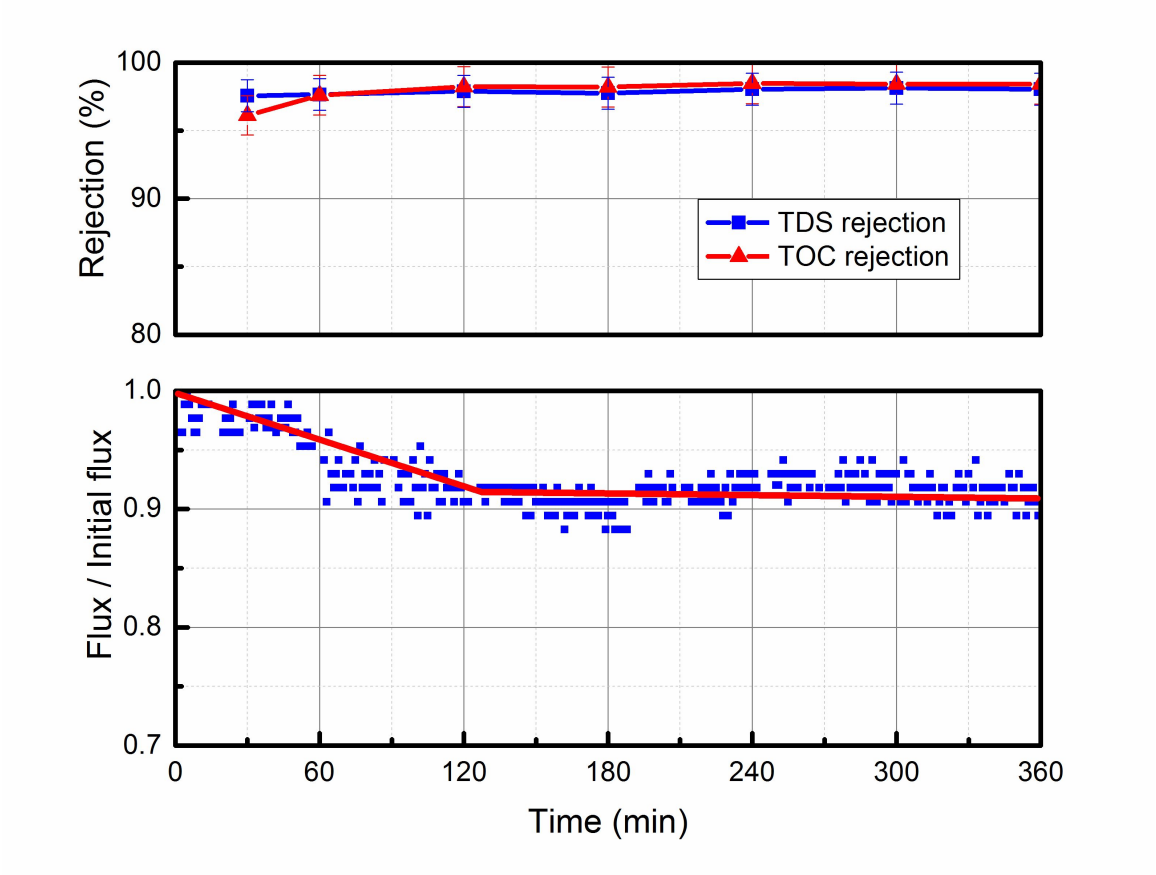

Figure 3.5: Water flux and rejection for model BFW filtration using NF90 membrane at pH=8.5

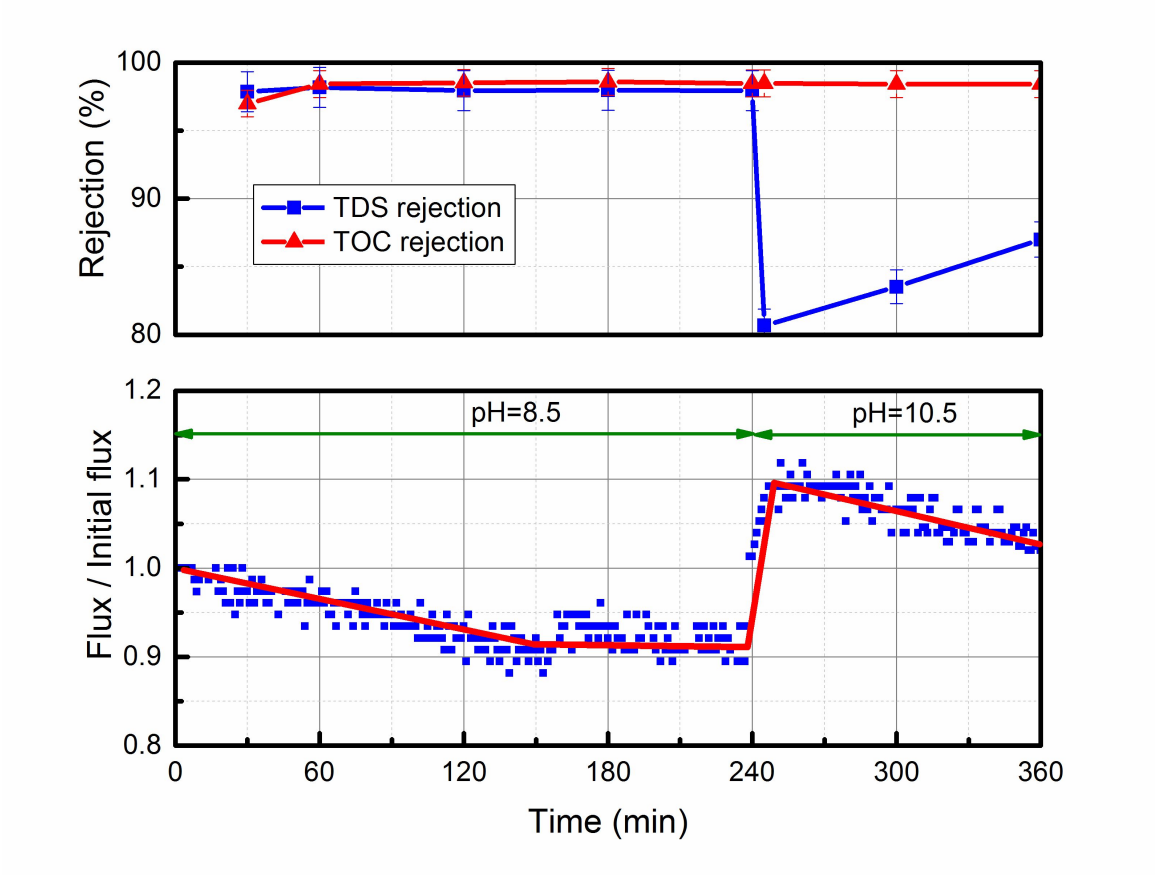

Figure 3.6: Water flux and rejection for model BFW filtration using NF90 membrane at pH=10.5-8.5

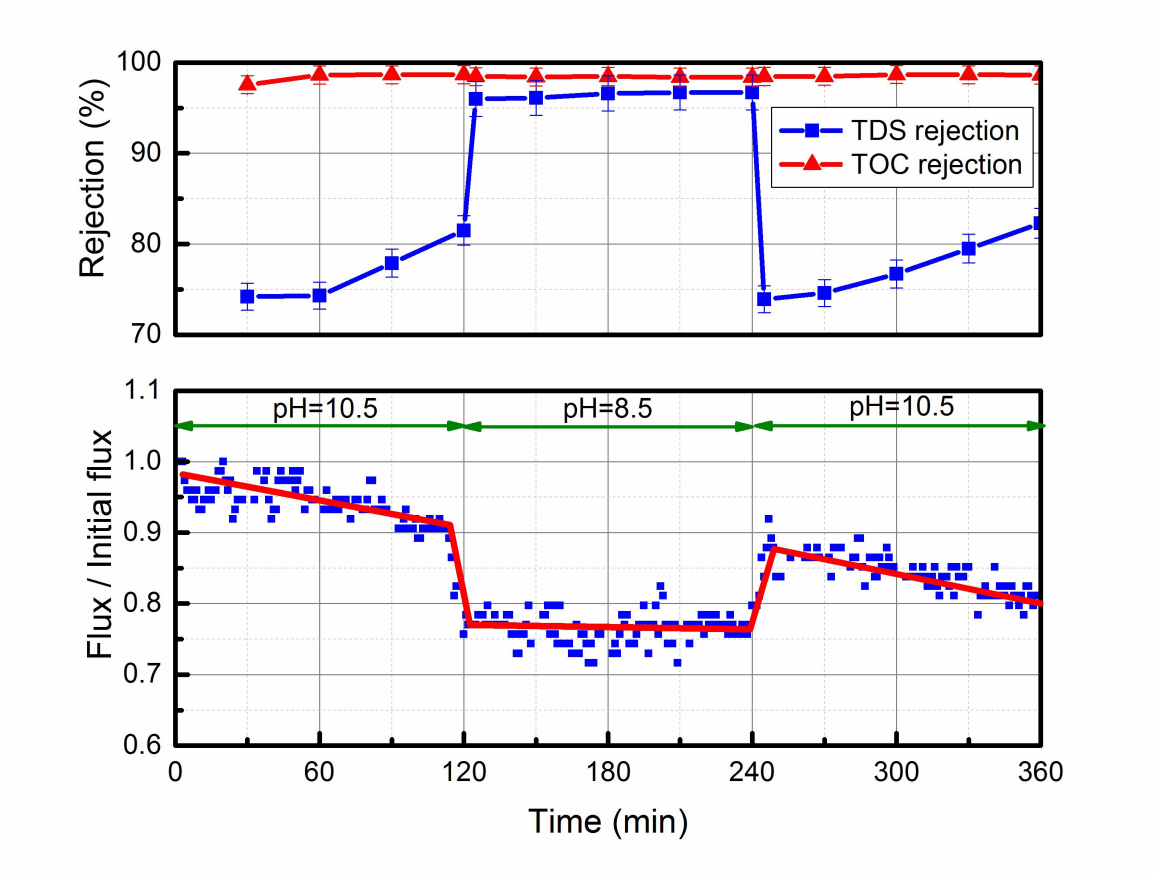

Figure 3.7: Water flux and rejection for model BFW filtration using NF90 membrane at pH=10.5-8.5-10.5

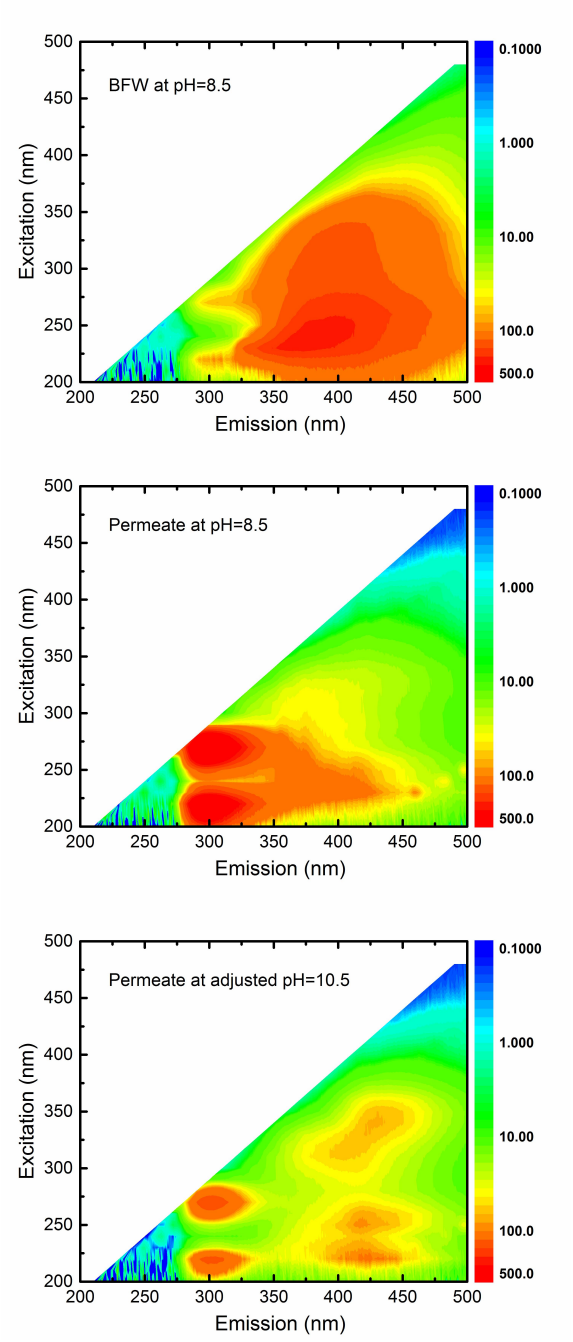

Figure 3.8: FEEMs of model BFW at pH=8.5, permeate at pH=8.5 and permeate at pH increased to 10.5. Excitation at 5 nm intervals from 200 to 500 nm and emission data collected at an interval of 10 nm. Permeate has the effective TOC of 9 and the feed was diluted to the TOC of 12 mg/L. The color scale representing the fluorescence intensity is logarithmic in all parts of the gure with the range varying from 0.1 (blue) to 500 (red)

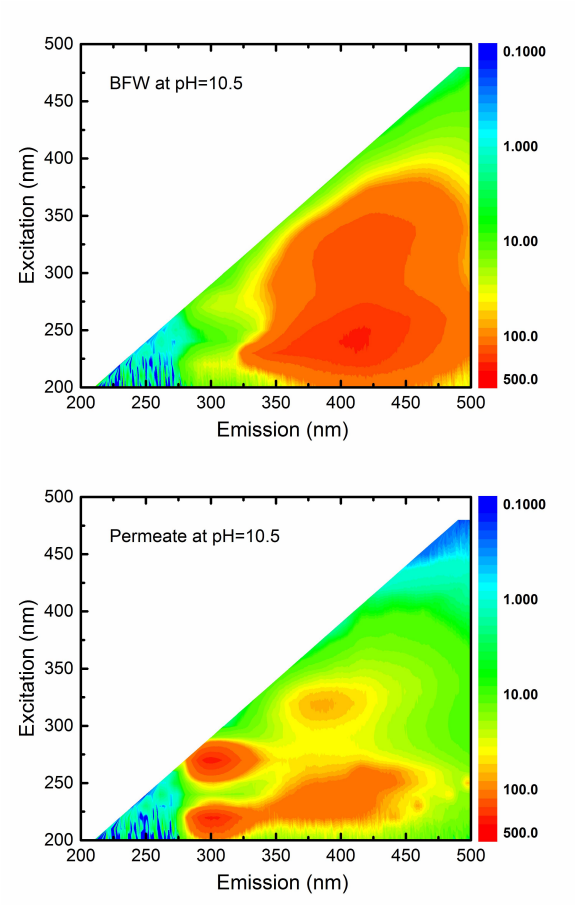

Figure 3.9: FEEMs of model BFW and permeate at pH=8.5. Excitation at 5 nm intervals from 200 to 500 nm and emission data collected at an interval of 10 nm. Permeate has the effective TOC of 9 and the feed was diluted to the TOC of 12 mg/L. The color scale representing the fluorescence intensity is logarithmic in all parts of the gure with the range varying from 0.1 (blue) to 500 (red)

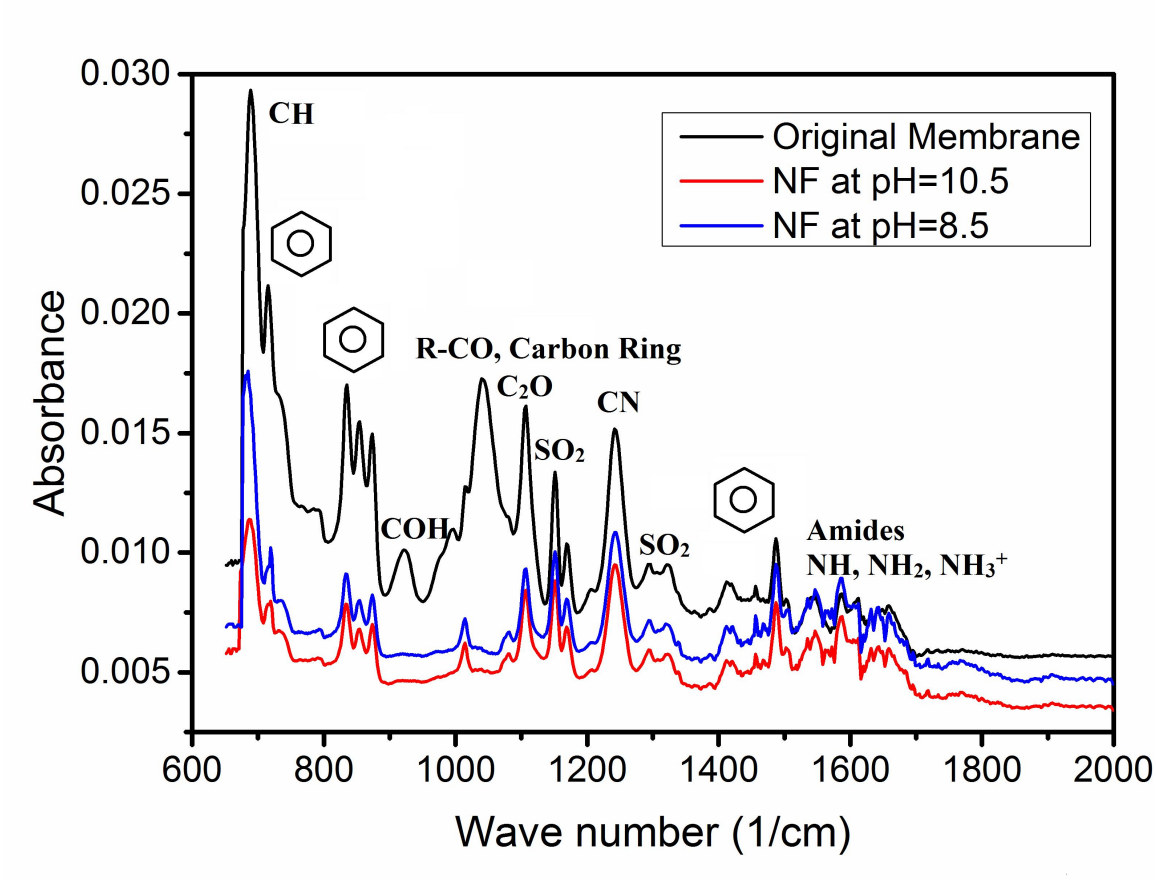

Figure 3.10: ATR-FTIR spectra of NF90 membrane before and after filtration

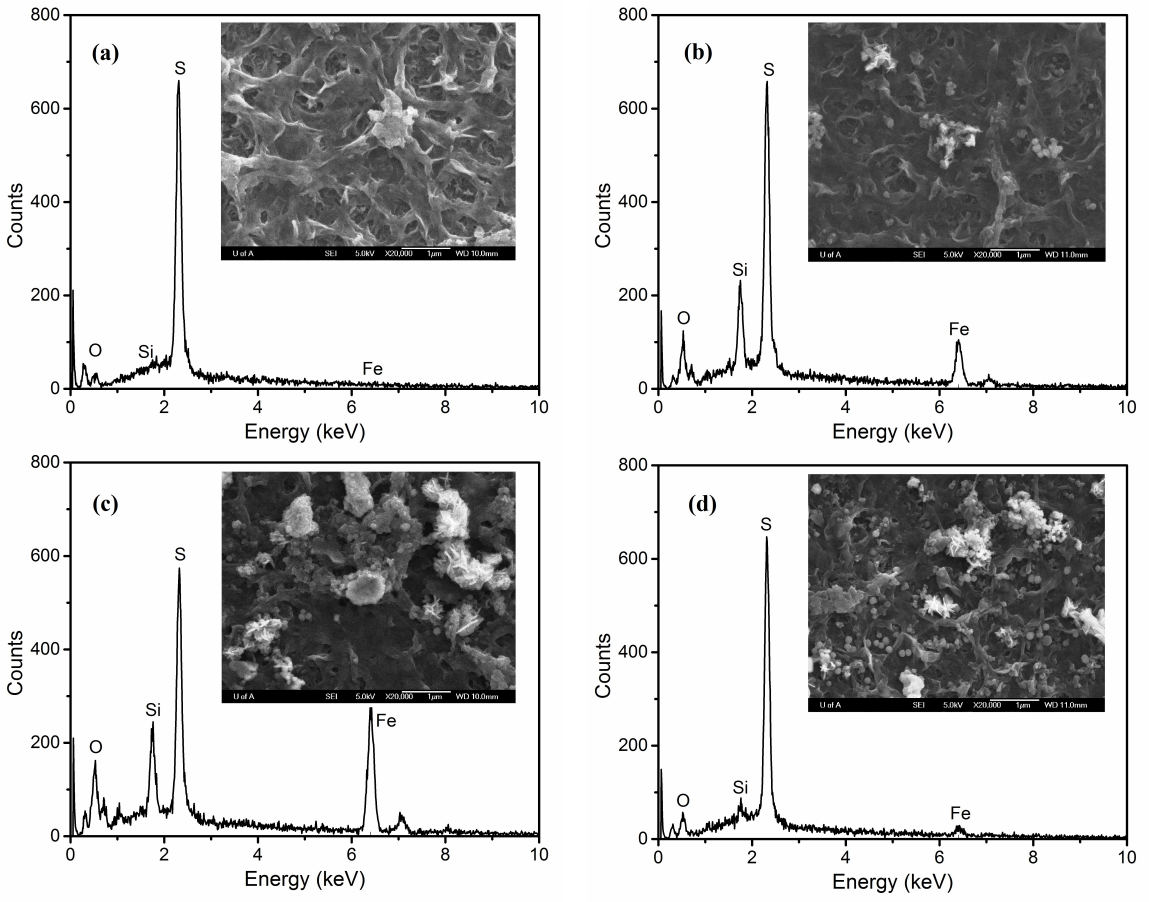

Figure 3.11: FESEM-EDX of (a) original membrane, (b) used membrane at pH=10.5, (c) used membrane at pH=8.5 and (c) used membrane at pH=8.5 then 10.5

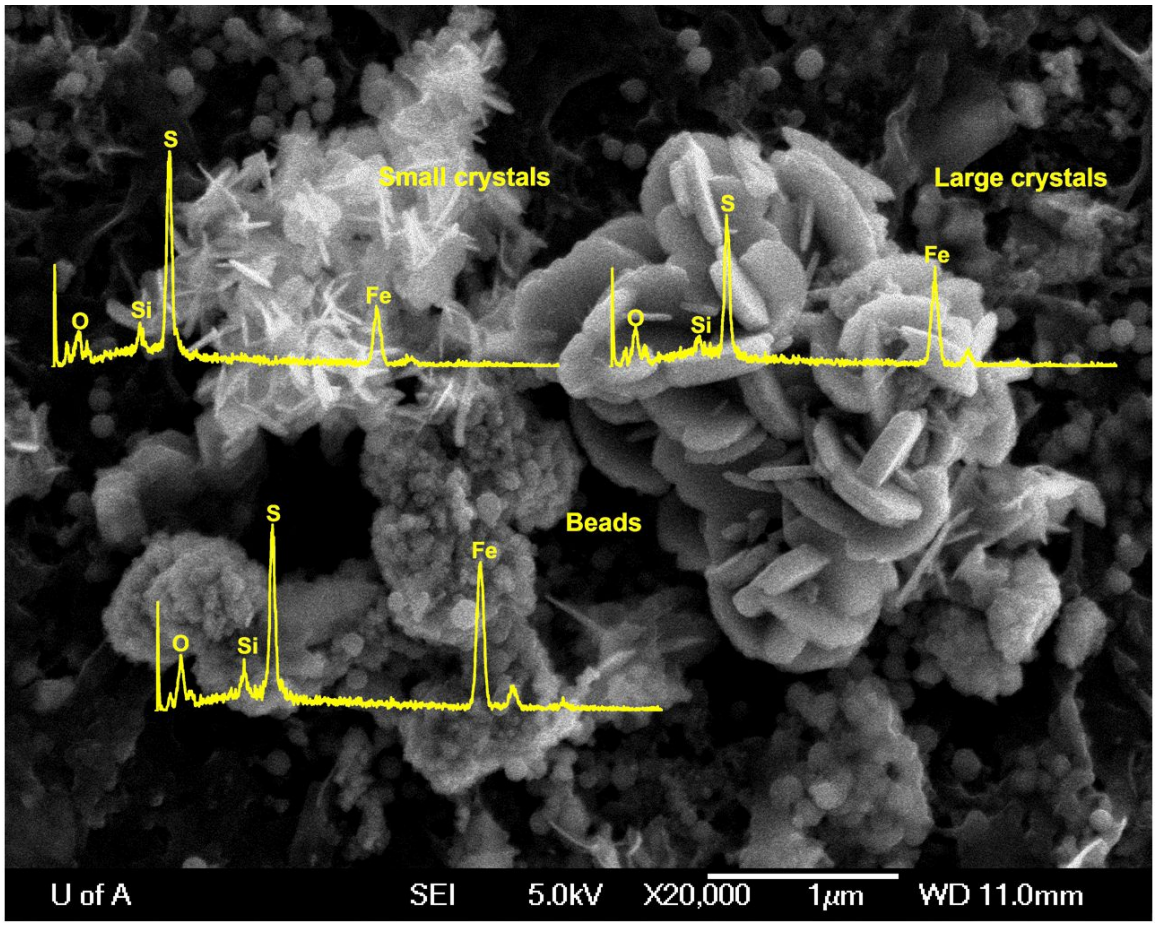

Figure 3.12: FESEM-EDX of beads, small crystals and large crystals deposited on the membrane surface fouled at pH=8.5

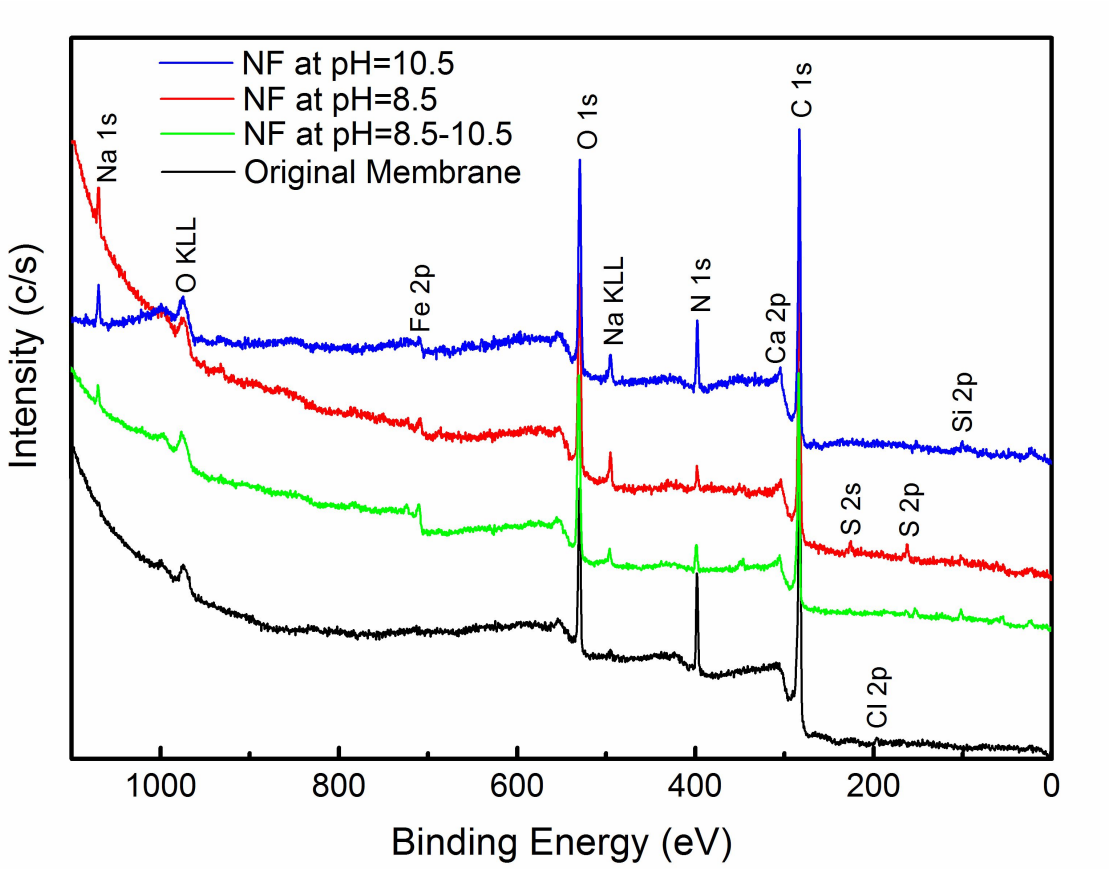

Figure 3.13: XPS survey spectra of NF90 membrane before and after filtration

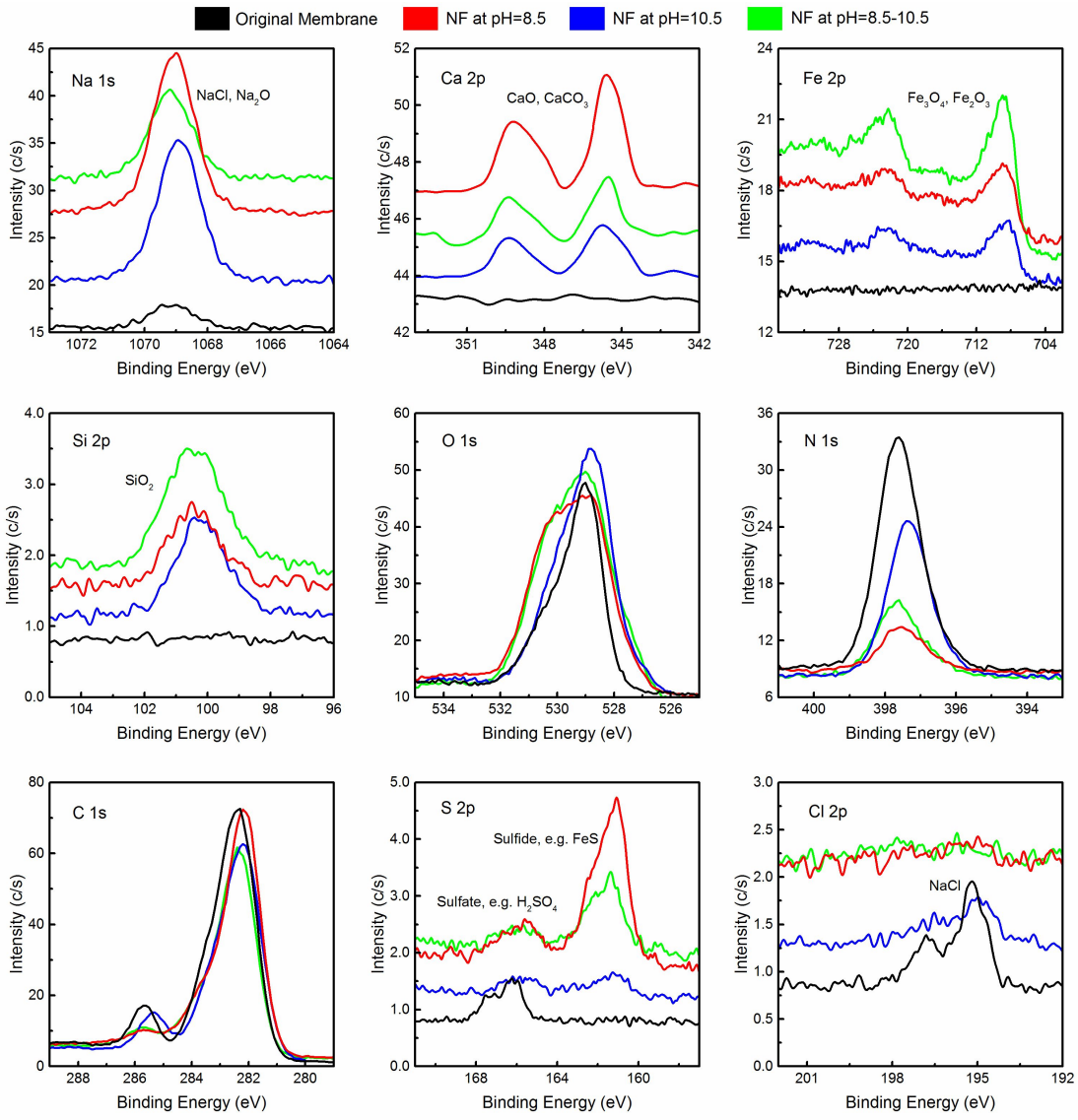

Figure 3.14: High resolution XPS spectra of NF90 membrane before and after filtration

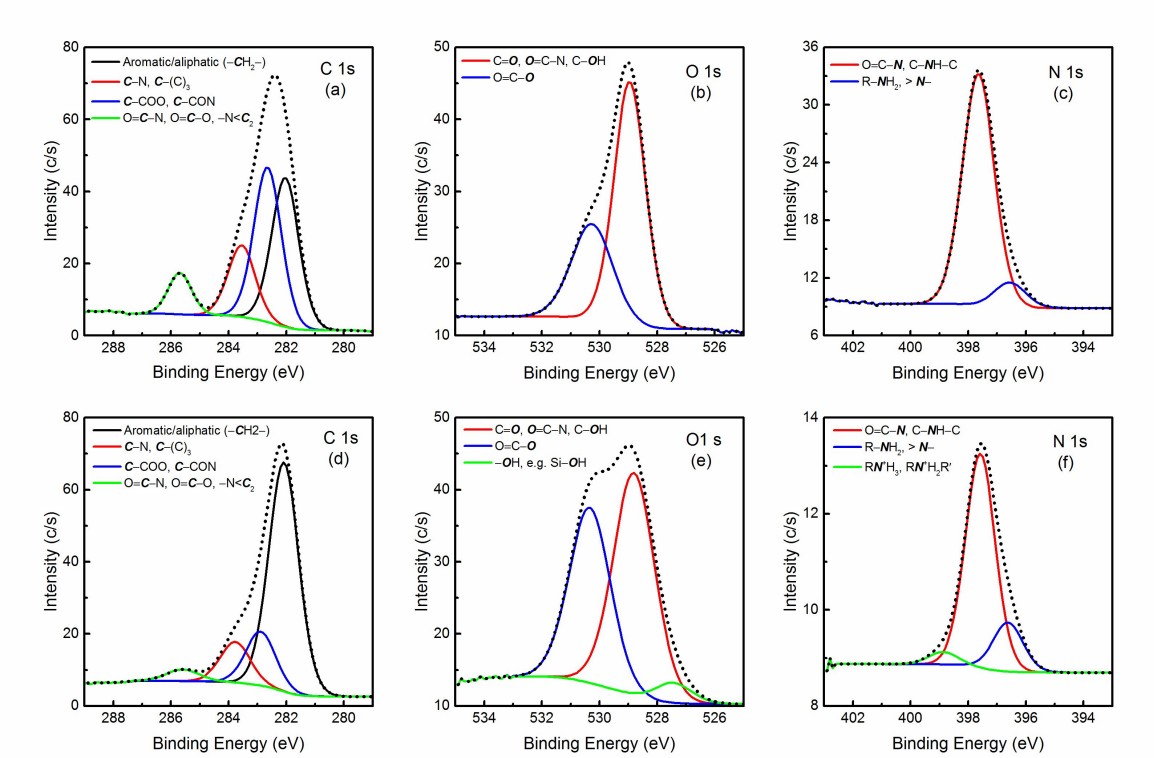

Figure 3.15: Detailed XPS deconvoluted C 1s, O 1s and N 1s scans of NF90 membrane before (a, b, c) and after filtration at pH=8.5 (d, e, f)

CHAPTER 4

CONCLUSIONS AND POSSIBLE FUTURE DIRECTIONS

4.1 Summary and Conclusions

In the first part of this thesis six types of polymeric thin film composite membranes including three NF membranes (NF270, NF290, and ESNA), two RO membranes (BW30 and ESPA) and one UF membrane were tested to remove DOM and TDS from SAGD WLS inlet water provided from a SAGD water treatment plant in Athabasca oil sands region of Alberta, Canada. Temperature of the feed was maintained at $50°C$ to have as much similar condition as real industrial produced water. The pressure for each membrane was set appropriately to get a constant initial permeation flux of 20 GFD. Constant initial permeation flux allowed us to rationalize different fouling behaviour of membranes by their different morphological and surface (hydrophilicity, roughness and zeta potential). The water flux of 20 GFD was reached at 30, 40, 80, 80, 120 and 120 psig trans-membrane pressure for UF, NF270, ESNA, NF90, ESPA and BW30 membranes. Performance of the membranes was invesitgated by measuring water permeation flux and TOC and TDS rejections, In order to further analyze the type of organic and inorganic materials in the permeate water, FEEMs and ICP-OES analyses were conducted. In addition, qualitative and quantitative analyses of fouling

layer deposited on the surface of each membrane was performed by A FESEM-EDX. Experiments for NF270, ESNA and ESPA were conducted at constant pH of the raw feed (pH=9), and pH for UF-TF, NF90 and BW30 was dynamic (9-7-10) to observe how water flux recovery and TDS and TOC rejections are affected by pH.

It was found that NF270 had a lower initial flux decline than ESPA and ESNA that was attributed to its smoother, more hydrophilic and more negatively charged surface in comparison with the two other membranes. These surface properties led to less fouling of membranes mainly by organic matter. Although ESNA membrane's surface was less negatively charged than ESPA, its initial flux decline was less than ESPA membrane which was attributed to its smoother surface.

TOC rejection for NF270, ESPA and ESNA increased by time which was justified by the hydrophobic interaction between organic material and the cake layer after fouling. The increase in TOC rejection was higher for NF270 due to its more originally hydrophilic surface. Unlike TOC, TDS rejection did not change too significantly for ESPA and ESNA, but decreased for NF270 because of cake enhanced concentration polarization. A slight increase in TDS rejection that happened for ESPA and ESNA confirmed that organic material in WLS inlet water were the major responsible material for fouling, since organic materials plugged membranes' hot spots and slowed down the transportation of salt.

For the pH varying experiments on UF, NF90 and BW30, pH of the feed which was 9 for raw feed decreased to 7 after 120 min , then increased to 10 at t=240 min. By decreasing pH from 9 to 7, flux decreased sharply for all three membranes. The reduction was more severe for salt rejecting NF90 and BW30 membranes. According to the FESEM images fouled material on the NF and RO membranes re-dissolved by increasing pH which resulted in flux recovery. The most significant flux recovery belonged to BW30 membrane which is denser, and the flux became even higher than the initial flux.

Increasing pH increased flux by two mechanisms: first by redissolving the fouled organic matter and second by changing the surface zeta potential of foulants and making them more negatively charged. The second one enhances membrane/foulant and foulant/floulant electrostatic repulsion, thus decrease fouling. Although TDS rejection increased with decreasing pH from 9 to 7 for NF90 and BW30 membranes due to formation of a compact cake-layer, it decreased for UF membrane which was irreversible by increasing pH. Decreasing pH increased TOC rejection for UF membrane because of pore constriction, but it slightly decreased TOC rejection for salt rejecting NF90 and BW30 by passage of small MWCO hydrophilic DOM.

According to the FEEMs results both hydrophobic and hydrophilic organic matter passed through NF270 and UF membranes, while for RO and NF90 almost all of the hydrophobic DOM deposited on the surface of the membranes. By deposition of hydrophobic DOM on the RO and NF90 membranes' surface, fouling became more severe at the initial stage of filtration because of hydrophobic interaction of organic matter with the cake-layer.

ICP-OES result showed that almost all divalent ions and iron were removed by NF90 and BW30, however they allowed 4% of silica to pass through. Salt rejecting NF90 and BW30 membranes also removed 93% and 97% of sodium and chloride respectively. 30%, 20% and 75% of Silica, sodium and calcium were removed by UF membrane respectively. According to the result, UF membrane is not capable of removing inogranic material, so it is not a good choice to filter WLS inlet water.

By considering the trade-Off relationship between energy consumption and product quality, the suitable membrane for WLS inlet water treatment was found to be NF90. It is worth nothing that although the applied pressure for NF270 membrane was only 10 psig more than that for UF, its TOC and TDS rejection were 20% and 40% more than UF. It mans that when a very high water quality is not needed for recycling to boilers NF270 is an outstanding candidate.

Flux decline was almost the same for NF90 and BW30 due to their similar surface properties. NF90 produced a high quality water close to the quality of RO (BW30) water by applying lower pressure (550 vs 825 KPa) which means less energy consumption. Since NF90 showed a better perforance in comparison with other membranes for treatment of WLS inlet water, it was selected for further studies in the second part of this thesis. A more detailed study was conducted on treatment of a model BFW which was prepared by diluting SAGD BBD water provided by a SAGD plant in northern Alberta. Four experiments were conducted by maintaining temperature, feed flow rate, and initial permeation flux at 50°C, $1.6\times10^{-5}m^3/s$ and $1.8\times10^{-5}m^3/m^2s$ and two pH values (8.5 and 10.5).

Since in BFW concentration of DOM (mostly hydrophobic acids) is much higher than silica and divalent ions (500mg/L vs $\sim$ 20 mg/L), the dominant fouling mechanism was expected to be DOM fouling. The sharp decline in flux at the beginning occured because of gel formation, pore blocking, and induced hydrophobic properties. Flux decline slowed down as filtration progressed due to the formation of more compact and thicker fouling layer which increased membrane resistance and consequently decreased permeation drag. High concentration of ions also intensified fouling by reducing charge of the membrane and macromolecules surface through double layer compression and charge screening that decreasesed electrostatic repulsion between membrane and DOM.

During the tests at constant pH 10.5, TOC rejection remained almost constant at about 98% , while TDS rejection increased from 80% to 95% within 6 hours run. This proved that the fouling of NF90 membrane was governed by plugging of hot spots by organic matter instead of cake enhance concentration polarization. Consistent TOC rejection at 98% attributed to the larger size of DOM compared to the dissolved solids in the water. In fact, NF90 rejected 98% of the DOM at a feed pH of 10.5, regardless of the fouling progress. At pH 8.5, permeation flux decreased about 7% at the first

two hours and then remained constant. TOC and TDS rejections remained constant at 98% for the whole experiment time. TDS rejection increased by decreasing pH to 8.5 because of co-precipitation of silica and organic matter on the surface of membrane and cake filtration. Increasing pH from 8.5 to 10.5 during the third experiment, improved water flux about 20% instantly. In experiment 4, first decreasing the pH from 10.5 to 8.5 decreased the water flux, then returning the pH back to 10.5 quickly returned the flux and rejection to previous trend. This behavior was attributed the rapid change in foulant/foulant and foulant/membrane interactions by changing the pH. The TDS rejection behavior was exactly opposite to water flux. It was increased by decreasing the pH but desecrated by increasing the pH, however the response to pH was very fast like water flux. Instantaneous change of flux and TDS rejection by injecting acid or alkaline into the feed water demonstrated the outstanding role of pH on fouling, especially in presence of both silica and organic matter.

EDX analysis of the fouling material on the surface of the membrane demonstrated that fouling layer contained silica and iron. According to XPS result inorganic material (mostly metal oxides) and organics (with carboxylic and amino acid as functional groups) were found in the deposited layer on the surface of membrane. FEEMs result showed that most of the materials that passed through the membrane were hydrophilic macromolecules. This study showed that NF90 has a high potential to be used as polishing step in SAGD produced water treatment to increase the quality of BFW.

The results of both studies can be interpreted to provide three possible ways to use NF90 membrane in SAGD produced water treatmen. Firstly membrane process can be used as a complete alternative for WLS-WAC process to remove TOC, TDS, divalent ions and silica. Secondly NF process can be used to purify the combination of BBD and make up water to decrease silica, DOM, TDS and divalent ions. The product can be get mixed with the product of conventional treating methods. Thirdly, membrane process can be used for purification of the output of current water treatment

processes which is the input of boiler (BFW). This helps to reduce fouling of steam generator's pipes and shut-down frequency of SAGD plant. Meanwhile, the conventional processes reduce the amount of silica and divalent ions to an acceptable range for membrane treatment. Applying conventional processes as pre-treatment prevents scaling of membranes and consequently increases the life time of membranes.

4.2 Possible Future Directions

In order to use NF and RO for treatment of certain waste water the fouling potential of that water must be measured first. Accommodating very harsh water into the membrane process may reduce the lifetime of membrane and is not practical in real application. A common way of finding the wastewater fouling potential is to measure its silt density index (SDI). The SDI is evaluated by measuring the rate of plugging of a 0.45 μm membrane at a constant trans-membrane pressure of 206.8 kPa (30 psi). The SDI provides the average water flux decline (%) per minute through the filter over a period of time such as 15 minutes. Typically, the SDI must be less than 5 to be suitable for a RO system. Hence, the future direction for this study could be providing more practical process and material suggestions for industry to use membranes. The following themes could be focused:

1. Selecting three major streams of SAGD produced water treatment plant, namely BBD, WLS inlet and BFW and measuring their SDI.

2. Performing a single stage NF or RO process for the waters having SDI less than 5 and suggesting the best membrane considering both product quality and energy efficiency.

3. For SDI >5 add make-up water to reduce it to less than 5 and find the volume of fresh water needed for membrane treatment. Use three SDI values 2, 3 and 5 (by adding various amount of fresh water) and find the fouling behaviour of membranes and suggest the best feed properties which may lead to a longer operation and less cost.

4. For SDI >5, conduct pre-treatment techniques like oxidation, adsorption and loose UF and MF membranes to reduce their SDI to the acceptable range and suggest the best hybrid process.

5. Using novel membrane process like forward osmosis (FO) for water treatment. The objective is to reduce energy consumption (FO is operated without applying pressure) and fouling of membranes by using FO process.

6. Performing simulation with common software (e.g. ROSA from Filmtec) and suggest the best process configuration (single or double stages) to have the maximum recovery (<80%) of water by using the selected membrane in previous stages.

BIBLIOGRAPHY

[1] Subhayan Guha Thakurta, Abhijit Maiti, David J. Pernitsky, and Subir Bhattacharjee. Dissolved organic matter in steam assisted gravity drainage boiler blow-down water. *Energy & Fuels*, 27(7):3883–3890, June 2013.

[2] S. Bhattacharjee. *Oil sands: A bridge between conventional petroleum and a sustainable energy future , in: S. Basu (Ed.), Towards Sustainable Clean Energy*. New York, 2011.

[3] Peggy J. Parks. *Water pollution / by Peggy J. Parks*. Farmington Hills, MI : KidHaven Press ; Detroit : Thomson/Gale, c2007, 2007.

[4] C. A. Brebbia and Paul C. Anagnostopoulos. *Water pollution V : modelling, measuring, and prediction / editors, C.A. Brebbia, P. Anagnostopoulos*. Southampton, UK ; Boston : WIT Press, c1999., 1999.

[5] E. W. Allen. Process water treatment in Canada's oil sands industry: II. A review of emerging technologies. *Journal of Environmental Engineering and Science*, 7(5):499–524, 2008.

[6] Rich Hill. Thermal in situ water conservation study, AI-EES and Jacobs Consultancy, Technical Report. Technical report, AI-EES and Jacobs Consultancy, 2012.

[7] W F Heins. Technical advancements in SAGD evaporative produced water treatment. *Journal of Canadian Petroleum Technology*, 48(11):27–32, 2009.

[8] R. Singh. *Hybrid Membrane Systems for Water Purification: Technology, Systems Design and Operations*. Elsevier Science, 2006.

[9] I. A. Al-Anezi I. S. Al-Mutaz. Silica removal during lime softening in water treatment plant. In *International Conf. on Water Resources & Arid Environment (2004)*, 2004.

[10] D. K. Pingale. Role of weak acid cation resin in water treatment. *CHEMICAL WEEKLY -BOMBAY-*, 50:201–208, 2005.

[11] E. T. Igunnu and G. Z. Chen. Produced water treatment technologies. *International Journal of Low-Carbon Technologies*, 0:1–21, July 2012.

[12] PrzemysÅaw Drzewicz, Atefeh Afzal, Mohamed Gamal El-Din, and Jonathan W Martin. Degradation of a model naphthenic acid, cyclohexanoic acid, by vacuum UV (172 nm) and UV (254 nm)/H2O2. *The Journal of Physical Chemistry. Ahemistry. A*, 114(45):12067–12074, November 2010.

[13] Ahmadun Fakhrul-Razi, Alireza Pendashteh, Luqman Chuah Abdullah, Dayang Radiah Awang Biak, Sayed Siavash Madaeni, and Zurina Zainal Abidin. Review of technologies for oil and gas produced water treatment. *Journal of hazardous materials*, 170(2-3):530–51, October 2009.

[14] B R Hansen and S R H Davies. Review of potential technologies for the removal of dissolved components from produced water. *Chemical Engineering Research and Design*, 72(A2):176–188, 1994.

[15] Christina C Small, Ania C Ulrich, and Zaher Hashisho. Adsorption of acid extractable oil sands tailings organics onto raw and activated oil sands coke. *Journal of Environmental Engineering*, 138:833–840, 2012.

[16] Christina C. Small, Zaher Hashisho, and Ania C. Ulrich. Preparation and characterization of activated carbon from oil sands coke. *Fuel*, 92(1):69–76, February 2012.

[17] Warren Zubot, Michael D MacKinnon, Pamela Chelme-Ayala, Daniel W Smith, and Mohamed Gamal El-Din. Petroleum coke adsorption as a water management option for oil sands process-affected water. *The Science of the Total Environment*, 427-428:364–372, June 2012.

[18] W F Mcternan, W E Blanton, G D Boardman, B T Nolan, and D J Kocornik. Polymer flotation and activated carbon adsorption treatment for in situ tar sand process water. *Environmental Progress*, 5(3):154–158, 1986.

[19] Mohamed Gamal El-Din, Hongjing Fu, Nan Wang, Pamela Chelme-Ayala, Leonidas Pérez-Estrada, PrzemysÅaw Drzewicz, Jonathan W Martin, Warren Zubot, and Daniel W Smith. Naphthenic acids speciation and removal during petroleum-coke adsorption and ozonation of oil sands process-affected water. *The Science of the Total Environment*, 409(23):5119–5125, November 2011.

[20] PrzemysÅaw Drzewicz, Leonidas Perez-Estrada, Alla Alpatova, Jonathan W Martin, and Mohamed Gamal El-Din. Impact of peroxydisulfate in the presence of zero valent iron on the oxidation of cyclohexanoic acid and naphthenic acids from oil sands process-affected water. *Environmental science & technology*, 46(16):8984–8991, August 2012.

[21] Yuhe He, Steve B Wiseman, Xiaowei Zhang, Markus Hecker, Paul D Jones, Mohamed Gamal El-Din, Jonathan W Martin, and John P Giesy. Ozonation attenuates the steroidogenic disruptive effects of sediment free oil sands process water in the H295R cell line. *Chemosphere*, 80(5):578–84, July 2010.

[22] Jonathan W Martin, Thaer Barri, Xiumei Han, Phillip M Fedorak, Mohamed Gamal El-Din, Leonidas Perez, Angela C Scott, and Jason Tiange Jiang. Ozonation of oil sands process-affected water accelerates microbial bioremediation. *Environmental Science & Technology*, 44(21):8350–8356, November 2010.

[23] Angela C Scott, Warren Zubot, Michael D MacKinnon, Daniel W Smith, and Phillip M Fedorak. Ozonation of oil sands process water removes naphthenic acids and toxicity. *Chemosphere*, 71(1):156–60, March 2008.

[24] Atefeh Afzal, PrzemysÅaw Drzewicz, Leónidas A Pérez-Estrada, Yuan Chen, Jonathan W Martin, and Mohamed Gamal El-Din. Effect of molecular structure on the relative reactivity of naphthenic acids in the UV/H2O2 advanced oxidation process. *Environmental Science & Technology*, 46(19):10727–10734, October 2012.

[25] Leónidas A Pérez-Estrada, Xiumei Han, PrzemysÅaw Drzewicz, Mohamed Gamal El-Din, Phillip M Fedorak, and Jonathan W Martin. Structure-reactivity of naphthenic acids in the ozonation process. *Environmental Science & Technology*, 45(17):7431–7437, September 2011.

[26] Zhixiong Cha, Cheng Fang Lin, Chia Jung Cheng, and P K Andy Hong. Removal of oil and oil sheen from produced water by pressure-assisted ozonation and sand filtration. *Chemosphere*, 78(5):583–90, January 2010.

[27] J C Anderson, S B Wiseman, N Wang, A Moustafa, L Perez-Estrada, M Gamal El-Din, J W Martin, K Liber, and J P Giesy. Effectiveness of ozonation treatment in eliminating toxicity of oil sands process-affected water to chironomus dilutus. *Environmental Science & Technology*, 46(1):486–93, January 2012.

[28] Erick Garcia-Garcia, Jun Qing Ge, Ayoola Oladiran, Benjamin Montgomery, Mohamed Gamal El-Din, Leonidas C Perez-Estrada, James L Stafford, Jonathan W Martin, and Miodrag Belosevic. Ozone treatment ameliorates oil sands process water toxicity to the mammalian immune system. *Water research*, 45(18):5849–5857, November 2011.

[29] Xiumei Han, Angela C Scott, Phillip M Fedorak, Mahmoud Bataineh, and Jonathan W Martin. Influence of molecular structure on the biodegradability of naphthenic acids. *Environmental science & technology*, 42(4):1290–5, February 2008.

[30] Geelsu Hwang, Tao Dong, Md Sahinoor Islam, Zhiya Sheng, Leónidas A Pérez-Estrada, Yang Liu, and Mohamed Gamal El-Din. The impacts of ozonation on oil sands process-affected water biodegradability and biofilm formation characteristics in bioreactors. *Bioresource technology*, 130:269–77, February 2013.

[31] Hamed Mahdavi, Ania C Ulrich, and Yang Liu. Metal removal from oil sands tailings pond water by indigenous micro-alga. *Chemosphere*, 89(3):350–4, September 2012.

[32] Hamed Mahdavi, Yang Liu, and Ania C Ulrich. Partitioning and bioaccumulation of metals from oil sands process affected water in indigenous Parachlorella kessleri. *Chemosphere*, 90(6):1893–9, February 2013.

[33] Tara J Penner and Julia M Foght. Mature fine tailings from oil sands processing harbour diverse methanogenic communities. *Cannadian Journal of Microbiology*, 56:459–470, 2010.

[34] E. Quagraine, H. Peterson, and J. Headley. In situ bioremediation of naphthenic acids contaminated tailing pond waters in the Athabasca oil sands regionDemonstrated field studies and plausible options: A review. *Journal of*

Environmental Science and Health, Part A: Toxic/Hazardous Substances & Environmental Engineering, 40(3):685–722, January 2005.

[35] Angela C Scott, Michael D MacKinnon, and Phillip M Fedorak. Naphthenic acids in athabasca oil sands tailings waters are less biodegradable than commercial naphthenic acids. *Environmental science & technology*, 39(21):8388–94, November 2005.

[36] Benjamin E Smith, C Anthony Lewis, Simon T Belt, Corinne Whitby, and Steven J Rowland. Effects of alkyl chain branching on the biotransformation of naphthenic acids. *Environmental Science & Technology*, 42(24):9323–9328, December 2008.

[37] Navdeep S Toor, Eric D Franz, Phillip M Fedorak, Michael D MacKinnon, and Karsten Liber. Degradation and aquatic toxicity of naphthenic acids in oil sands process-affected waters using simulated wetlands. *Chemosphere*, 90(2):449–58, January 2013.

[38] Eun-Sik Sik Kim, Yang Liu, and Mohamed Gamal El-Din. The effects of pretreatment on nanofiltration and reverse osmosis membrane filtration for desalination of oil sands process-affected water. *Separation and Purification Technology*, 81(3):418–428, October 2011.

[39] H. Peng, K. Volchek, M. MacKinnon, W.P. Wong, and C.E. Brown. Application on to nanofiltration to water management options for oil sands operation. *Desalination*, 170:137–150, 2004.

[40] Eun Sik Kim, Yang Liu, and Mohamed Gamal El-Din. Evaluation of membrane fouling for in-line filtration of oil sands process-affected water: the effects of pretreatment conditions. *Environmental Science & Technology*, 46(5):2877–2884, March 2012.

[41] Eun Sik Kim, Yang Liu, and Mohamed Gamal El-Din. An in-situ integrated system of carbon nanotubes nanocomposite membrane for oil sands process-affected water treatment. *Journal of Membrane Science*, 429:418–427, February 2013.

[42] Paul Swenson, Brenden Tanchuk, Elia Bastida, Weizhu An, and Steven M. Kuznicki. Water desalination and de-oiling with natural zeolite membranes Potential application for purification of SAGD process water. *Desalination*, 286:442–446, February 2012.

[43] A. Banerjee A.K. Mehrotra. Evaluation of reverse osmosis for the treatment of oil sands produced water. *Water Pollution Research Journal of Canada*, 21:141–152, 1986.

[44] Rafael Mujeriego and Takashi Asano. The role of advanced treatment in wastewater reclamation and reuse. volume 40, pages 1 – 9, Milan, Italy, 1999. Public health;Wastewater reuse;.

[45] R. Abdul-Rahman, H. Tsuno, and N. Zainol. Nitrogen nutrient removals from wastewater and river water. volume 45, pages 197 – 204, 2002. Sequencing batch reactors (SBT);.

[46] A. Wood. Constructed wetlands in water pollution control: Fundamentals to their understanding. *Water Science and Technology,*, 32:21–29, 1995.

[47] A.G. Werker, J.M. Dougherty, J.L. McHenry, and W.A. Van Loon. Review: Treatment variability for wetland wastewater treatment design in cold climates. *Ecological Engineering*, 19:1–11, 2002.

[48] Rana Kidak and Nilsun H. Ince. Ultrasonic destruction of phenol and substituted phenols: A review of current research. *Ultrasonics Sonochemistry*, 13:195 – 199, 2006.

[49] Detlef Bahnemann. Photocatalytic water treatment: Solar energy applications. *Solar Energy*, 77:445 – 459, 2004.

[50] Marcel Mulder. *Basic principles of membrane technology*. Kluwer Academic, Dordrecht, 2nd edition, 1997.

[51] T Bilstad, E Espedal, and Espedal E Bilstad T. Membrane separation of produced water. *Water Science and Technology*, 34(9):239–246, 1996.

[52] J C Campos, R M H Borges, A M Oliveira Filho, R Nobrega, G L Sant'Anna, and J Sant'Anna. Oilfield wastewater treatment by combined microfiltration and biological processes. *Water Research*, 36(1):95–104, January 2002.

[53] Jing Zhong, Xiaojuan Sun, and Cheli Wang. Treatment of oily wastewater produced from refinery processes using flocculation and ceramic membrane filtration. *Separation and Purification Technology*, 32(1-3):93–98, July 2003.

[54] Eric M. V. Hoek, Albert S. Kim, and Menachem Elimelech. Influence of crossflow membrane filter geometry and shear rate on colloidal fouling in reverse osmosis and nanofiltration separations. *Environmental Engineering Science*, 19(6):357–372, November 2002.

[55] E. Kissa. *Dispersions: Characterization, Testing, and Measurement*. Taylor & Francis, 1999.

[56] Menachem Elimelech, William H Chen, and John J Waypa. Measuring the zeta (electrokinetic) potential of reverse osmosis membranes by a streaming potential analyzer. *Desalination*, 95:269–286, 1994.

[57] H Jacobasch and J Schurz. Characterization of polymer surfaces by means of electrokinetic measurements. *Progress in Colloid & Polymer Science*, 77:40–48, 1988.

[58] H.J. Jacobasch, G. Baubock, and J. Schurz. Problems and results of zeta-potential measurements on fibers. *Colloid and Polymer Science*, 263:3–24, 1985.

[59] Stanley Hartland. *Surface and interfacial tension [electronic resource] : measurement, theory, and applications.* New York ; Basel : Marcel Dekker, c2004., 2004.

[60] A Zaidi, K Simms, and S Kak. The use of micro/ultrafiltration for the removal of oil and suspended solids from oilfield brines. *Water Science and Technology*, 25(10):163–176, 1992.

[61] I W Cumming, R G Holdich, and I D Smith. The rejection of oil using an asymmetric metal microfilter to separate an oil in water dispersion. *Water Research*, 33(17):3587–3594, December 1999.

[62] Elham Gorouhi, Mohtada Sadrzadeh, and Toraj Mohammadi. Microfiltration of oily wastewater using PP hydrophobic membrane. *Desalination*, 200(1-3):319–321, November 2006.

[63] T Leiknes and M J Semmens. Membrane filtration for preferential removal of emulsified oil from water. *Water Science & Technology*, 41(10-11):101–108, 2000.

[64] T C Arnot, R W Field, and A B Koltuniewicz. Cross-flow and dead-end microfiltration of oily-water emulsions Part II . Mechanisms and modelling of flux decline. *Journal of Membrane Science*, 169:1–15, 2000.

[65] D Bhattacharyya, A B Jumawan, R B Grieves, and L R Harris. Ultrafiltration characteristics of oil-detergent-water systems: Membrane fouling mechanisms. *Separation Science and Technology*, 14(6):529–549, August 1979.

[66] Soobok Lee, Yves Aurelle, and Henry Roques. Concentration polarization, membrane fouling and cleaning in ultrafiltration of soluble oil. *Journal of Membrane Science*, 19(1):23–38, 1984.

[67] Charles A. Dyke and Craig R. Bartels. Removal of organics from offshore produced waters using nanofiltration membrane technology. *Environmental Progress*, 9(3):183–186, August 1990.

[68] F T Tao, S Curtice, R D Hobbs, J L Sides, J D Wieser, C A Dyke, D Tuohey, and P F Pilger. Reverse osmosis process successfully converts oil field brine into freshwater. *The Oil and Gas Journal*, 38:88–91, 1993.

[69] Glenn F Doran, Kimberly L Williams, Joseph A Drago, Sunny S Huang, and Lawrence Y C Leong. Pilot study results to convert oil field produced water to drinking water or reuse quality. In *SPE Annaual Technical Conference and Exhibition*, pages 403–417, New Orleans, 1998. Society of Petroleum Engineers, Inc.

[70] M D MacKinnon and H Boerger. Description of two treatment methods for detoxifying oil sands tailings pond water. *Water Pollution Research Journal of Canada*, 21(4):496–512, 1986.

[71] Jacob Masliyah, Zhiang Joe Zhou, Zhenghe Xu, Jan Czarnecki, and Hassan Hamza. Understanding water-based bitumen extraction from Athabasca oil sands. *The Canadian Journal of Chemical Engineering*, 82:628–654, 2004.

[72] Joyce S Clemente and Phillip M Fedorak. A review of the occurrence, analyses, toxicity, and biodegradation of naphthenic acids. *Chemosphere*, 60(5):585–600, July 2005.

[73] Qilin Li and Menachem Elimelech. Organic fouling and chemical cleaning of nanofiltration membranes: measurements and mechanisms. *Environmental science & technology*, 38(17):4683–93, September 2004.

[74] Qilin Li and Menachem Elimelech. Synergistic effects in combined fouling of a loose nanofiltration membrane by colloidal materials and natural organic matter. *Journal of Membrane Science*, 278(1-2):72–82, July 2006.

[75] Elizabeth Arkhangelsky, Filicia Wicaksana, Chuyang Tang, Abdulrahman a Al-Rabiah, Saeed M Al-Zahrani, and Rong Wang. Combined organic-inorganic fouling of forward osmosis hollow fiber membranes. *Water Research*, 46(19):6329–38, December 2012.

[76] Christopher Bellona, Jörg E Drewes, Pei Xu, and Gary Amy. Factors affecting the rejection of organic solutes during NF/RO treatment–a literature review. *Water research*, 38(12):2795–809, July 2004.

[77] Christopher Bellona, Melissa Marts, and Jeorg E. Drewes. The effect of organic membrane fouling on the properties and rejection characteristics of nanofiltration membranes. *Separation and Purification Technology*, 74(1):44–54, July 2010.

[78] By Anne Braghetta, Francis A Digiano, and William P Ball. Nanofiltration of natural organic matter: pH and ionic strength effects. *Journal of Environmental Engineering*, 123:628–641, 1997.

[79] Kimberly L. Jones and Charles R. OMelia. Protein and humic acid adsorption onto hydrophilic membrane surfaces: effects of pH and ionic strength. *Journal of Membrane Science*, 165(1):31–46, January 2000.

[80] MaÅgorzata Kabsch-Korbutowicz, Katarzyna Majewska-Nowak, and Tomasz Winnicki. Analysis of membrane fouling in the treatment of water solutions

containing humic acids and mineral salts. *Desalination*, 126(1-3):179–185, November 1999.

[81] G.F. Doran, K.L. Williams, J.A. Drago, S.S. Huang, and L.Y.C. Leong. Pilot study results to convert oil field produced water to drinking water or reuse quality, in: SPE Annaual Technical Conference and Exhibition. *Society of Petroleum Engineers, Inc.*, pages 403–417, 1998.

[82] Li Liangxiong, T.M. M Whitworth, and Robert Lee. Separation of inorganic solutes from oil-field produced water using a compacted bentonite membrane. *Journal of Membrane Science*, 217(1-2):215–225, June 2003.

[83] Mehmet Cakmakce, Necati Kayaalp, and Ismail Koyuncu. Desalination of produced water from oil production fields by membrane processes. *Desalination*, 222(1-3):176–186, March 2008.

[84] Cynthia Murray-Gulde, John E Heatley, Tanju Karanfil, John H Rodgers, and James E Myers. Performance of a hybrid reverse osmosis-constructed wetland treatment system for brackish oil field produced water. *Water Research*, 37(3):705–13, February 2003.

[85] S. Mondal and S. Ranil Wickramasinghe. Produced water treatment by nanofiltration and reverse osmosis membranes. *Journal of Membrane Science*, 322(1):162–170, September 2008.

[86] Pei Xu, Jörg E. Drewes, and Dean Heil. Beneficial use of co-produced water through membrane treatment: technical-economic assessment. *Desalination*, 225(1-3):139–155, May 2008.

[87] David W Jennings and Arif Shaikh. Heat-exchanger deposition in an inverted steam-assisted Gravity drainage operation . Part 1 . inorganic and organic analyses of deposit samples. *Energy & Fuels*, 21(1):176–184, 2007.

[88] Sanyi Wang, Eric Axcell, Ron Bosch, and Virgil Little. Effects of chemical application on antifouling in steam-assisted gravity drainage operations. *Energy & Fuels*, 19(4):1425–1429, July 2005.

[89] J Zhong, X Sun, and C Wang. Treatment of oily wastewater produced from refinery processes using flocculation and ceramic membrane filtration. *Separation and Purification Technology*, 32(1-3):93–98, 2003.

[90] Andrea Iris Schäfer. *Natural organics removal using membranes*. Phd thesis, The University of New South Wales, 1999.

[91] S M Santos and M R Weisner. Ultrafiltration of water generated in oil and gas production. *Water Environment*, 69:1120–1127, 1997.

[92] Seungkwan Hong and Menachem Elimelech. Chemical and physical aspects of natural organic matter (NOM) fouling of nanofiltration membranes. *Journal of Membrane Science*, 132(2):159–181, September 1997.

[93] Hideo Kawaguchi, Zhengguo Li, Yoshihiro Masuda, Kozo Sato, and Hiroyuki Nakagawa. Dissolved organic compounds in reused process water for steam-assisted gravity drainage oil sands extraction. *Water research*, 46(17):5566–74, November 2012.

[94] Matthew a. Petersen and Hans Grade. Analysis of Steam Assisted Gravity Drainage Produced Water using Two-Dimensional Gas Chromatography with Time-of-Flight Mass Spectrometry. *Industrial & Engineering Chemistry Research*, 50(21):12217–12224, November 2011.

[95] QL Li and M Elimelech. Organic fouling and chemical cleaning of nanofiltration membranes: Measurements and mechanisms. *ENVIRONMENTAL SCIENCE & TECHNOLOGY*, 38:4683 – 4693, 2004.

[96] By Anne Braghetta, Francis A Digiano, and William P Ball. NOM accumulation at NF membrane surface: Imact of chemistry and shear. *Journal of Environmental Engineering*, 124:1087–1098, 1998.

[97] C Jucker and M M Clark. Adsorption of aqautic humic substances on hydrophobic ultrafiltration membranes. *Journal of Membrane Science*, 97:37–52, 1994.

[98] Cecilia M. C. Law, Xiao-Yan Li, and Qilin Li. The combined colloid-organic fouling on nanofiltration membrane for wastewater treatment and reuse. *Separation Science and Technology*, 45(7):935–940, April 2010.

[99] Zhi Wang, Yuanyuan Zhao, Jixiao Wang, and Shichang Wang. Studies on nanofiltration membrane fouling in the treatment of water solutions containing humic acids. *Desalination*, 178(1-3):171–178, July 2005.

[100] Wei Yuan and Andrew L. Zydney. Effects of solution environment on humic acid fouling during microfiltration. *Desalination*, 122(1):63–76, May 1999.

[101] A I Schäfer, A G Fane, and T D Waite. Nanofiltration of natural organic matter: Removal, fouling and the influence of multivalent ions. *Desalination*, 118:109–122, 1998.

[102] H Dach. *Comparison des operations de nanofiltration et d osmose inverse pour le dessalement selectif des eaux saumatres: De l echelle du laboratoire au pilote industriel*. PhD thesis, UNIVERSIT DANGERS, 2008.

[103] Mara Jose Lopez-Munoz, Arcadio Sotto, Jesus M. Arsuaga, and Bart Van der Bruggen. Influence of membrane, solute and solution properties on the retention of phenolic compounds in aqueous solution by nanofiltration membranes. *Separation and Purification Technology*, 66(1):194–201, April 2009.

[104] A R S Teixeira, J L C Santos, and J G Crespo. Sustainable membrane-based process for valorisation of cork boiling wastewaters. *Separation and Purification Technology*, 66(1):35–44, April 2009.

[105] Yi-Li Lin, Pen-Chi Chiang, and E-E Chang. Removal of small trihalomethane precursors from aqueous solution by nanofiltration. *Journal of Hazardous Materials*, 146:20–29, 2007.

[106] Anna M Comerton, Robert C Andrews, David M Bagley, and Chunyan Hao. The rejection of endocrine disrupting and pharmaceutically active compounds by NF and RO membranes as a function of compound and water matrix properties. *Journal of Membrane Science*, 313:323–335, 2008.

[107] K V Plakas, A J Karabelas, T Wintgens, and T Melin. A study of selected herbicides retention by nanofiltration membranesThe role of organic fouling. *Journal of Membrane Science*, 284:291–300, November 2006.

[108] Ebrahim Negaresh, Alice Antony, Mojgan Bassandeh, Desmond E Richardson, and Greg Leslie. Selective separation of contaminants from paper mill effluent using nanofiltration. *Chemical Engineering Research and Design*, 90:576–583, April 2012.

[109] C Bellona and J E Drewes. The role of membrane surface charge and solute physico-chemical properties in the rejection of organic acids by NF membranes. *Journal of Membrane Science*, 249(1-2):227–234, 2005.

[110] H.M. Krieg, S.J. Modise, K. Keizer, and H.W.J.P. Neomagus. Salt rejection in nanofiltration for single and binary salt mixtures in view of sulphate removal. *Desalination*, 171(2):205–215, January 2005.

[111] A Alturki, N Tadkaew, J.a. McDonald, S J Khan, W E Price, and L D Nghiem. Combining MBR and NF/RO membrane filtration for the removal of trace or-

ganics in indirect potable water reuse applications. *Journal of Membrane Science*, 365:206–215, December 2010.

[112] A Somrani, A H Hamzaoui, and M Pontie. Study on lithium separation from salt lake brines by nanofiltration (NF) and low pressure reverse osmosis (LPRO). *Desalination*, 317:184–192, May 2013.

[113] Y Wang and C Y Tang. Protein fouling of nanofiltration, reverse osmosis, and ultrafiltration membranesThe role of hydrodynamic conditions, solution chemistry, and membrane properties. *Journal of Membrane Science*, 376:275–282, July 2011.

[114] Pei Xu, Jörg E. Drewes, Tae-Uk Kim, Christopher Bellona, and Gary Amy. Effect of membrane fouling on transport of organic contaminants in NF/RO membrane applications. *Journal of Membrane Science*, 279(1-2):165–175, August 2006.

[115] Dipankar Nanda, Kuo-Lun Tung, Chi-Chung Hsiung, Ching-Jung Chuang, Ruoh-Chyu Ruaan, Yan-Che Chiang, Chih-Shen Chen, and Tien-Hwa Wu. Effect of solution chemistry on water softening using charged nanofiltration membranes. *Desalination*, 234:344–353, December 2008.

[116] K Kimura, G Amy, J E Drewes, T Heberer, T U Kim, and Y Watanabe. Rejection of organic micropollutants (disinfection by-products, endocrine disrupting compounds, and pharmaceutically active compounds) by NF/RO membranes. *Journal of Membrane Science*, 227:113–121, December 2003.

[117] Chalor Jarusutthirak, Gary Amyb, and Jean-philippe Crou. Fouling characteristics of wastewater effluent organic matter (EfOM) isolates on NF and UF membranes. *Desalination*, 145:247–255, 2002.

[118] W Peng, I Escobar, and D White. Effects of water chemistries and properties of membrane on the performance and foulinga model development study. *Journal of Membrane Science*, 238:33–46, July 2004.

[119] M. Pontié, H. Dach, J. Leparc, M. Hafsi, and A Lhassani. Novel approach combining physico-chemical characterizations and mass transfer modelling of nanofiltration and low pressure reverse osmosis membranes for brackish water desalination intensification. *Desalination*, 221(1-3):174–191, March 2008.

[120] A Subramani and E Hoek. Direct observation of initial microbial deposition onto reverse osmosis and nanofiltration membranes. *Journal of Membrane Science*, 319:111–125, July 2008.

[121] Kha L. Tu, Allan R. Chivas, and Long D. Nghiem. Effects of membrane fouling and scaling on boron rejection by nanofiltration and reverse osmosis membranes. *Desalination*, 279(1-3):269–277, September 2011.

[122] H Kelewou, A Lhassani, M Merzouki, P Drogui, and B Sellamuthu. Salts retention by nanofiltration membranes: Physicochemical and hydrodynamic approaches and modeling. *Desalination*, 277:106–112, August 2011.

[123] K Boussu, Y Zhang, J Cocquyt, P Van der Meeren, A Volodin, C Van Haesendonck, J A Martens, and B Van der Bruggen. Characterization of polymeric nanofiltration membranes for systematic analysis of membrane performance. *Journal of Membrane Science*, 278(1-2):418–427, July 2006.

[124] J J Lee. *Removal of microcystin-LR from drinking water using adsorption and membrane processes, PhD Thesis*. Phd thesis, PhD Thesis, Ohio State University, 2009.

[125] Yeomin Yoon, Paul Westerhoff, Jaekyung Yoon, and Shane A Snyder. Removal of 17B estradiol and fluoranthene by nanofiltration and ultrafiltration. *Journal of Environmental Engineering*, 130:1460–1467, 2004.

[126] X Ren, C Zhao, S Du, T Wang, Z Luan, J Wang, and D Hou. Fabrication of asymmetric poly (m-phenylene isophthalamide) nanofiltration membrane for chromium(VI) removal. *Journal of Environmental Sciences*, 22(9):1335–1341, 2010.

[127] David Norberg, Seungkwan Hong, James Taylor, and Yu Zhao. Surface characterization and performance evaluation of commercial fouling resistant low-pressure RO membranes. *Desalination*, 202:45–52, 2007.

[128] P Xu and J E Drewes. Viability of nanofiltration and ultra-low pressure reverse osmosis membranes for multi-beneficial use of methane produced water. *Separation and Purification Technology*, 52:67–76, November 2006.

[129] Yongki Shim, Hong-Joo Lee, Sangyoup Lee, Seung-Hyeon Moon, and Jaeweon Cho. Effects of natural organic matter and ionic species on membrane surface charge. *Environmental science technology*, 36:3864–3871, 2002.

[130] O C Nieto. *Quantitative characterization of physico-chemical properties of the active layers of reverse osmosis and nanofiltration membranes, and their relation to membrane performance*. PhD thesis, PhD Thesis, University of Illinois at urbana-champaign, 2010.

[131] K P Ishida, R Bold, and D W Phipps Jr. Identification and evaluation of unique chemicals for optimum membrane compatibility and improved cleaning efficiency. Technical Report April, Orange County Water District, Final Report, Orange County Water District, Fountain Valley, CA, 2005.

[132] Roy Bernstein, Sofia Belfer, and Viatcheslav Freger. Bacterial attachment to RO membranes surface-modified by concentration-polarization-enhanced graft polymerization. *Environmental science & technology*, 45:5973–5980, July 2011.

[133] F Fadhillah, S M J Zaidi, Z Khan, M M Khaled, F Rahman, and P T Hammond. Development of polyelectrolyte multilayer thin film composite membrane for water desalination application. *Desalination*, 318:19–24, June 2013.

[134] Chuyang Y Tang, Young-Nam Kwon, and James O Leckie. Effect of membrane chemistry and coating layer on physiochemical properties of thin film composite polyamide RO and NF membranes. *Desalination*, 242:168–182, June 2009.

[135] M Hesampoura, J Tanninen, S Reinikainen, S Platt, and M Nyström. Nanofiltration of single and mixed salt solutions: Analysis of results using principal component analysis (PCA). *chemical engineering research and design*, 88:1569–1579, 2010.

[136] J. Tanninen, M Manttari, and M Nystrom. Effect of salt mixture concentration on fractionation with NF membranes. *Journal of Membrane Science*, 283:57–64, 2006.

[137] Andrea J C Semião and Andrea I Schäfer. Removal of adsorbing estrogenic micropollutants by nanofiltration membranes. Part AExperimental evidence. *Journal of Membrane Science*, 431:244–256, March 2013.

[138] A Simon, L Nghiem, P Le-Clech, S J Khan, and J E Drewes. Effects of membrane degradation on the removal of pharmaceutically active compounds (PhACs) by NF/RO filtration processes. *Journal of Membrane Science*, 340:16–25, September 2009.

[139] Laia Llenas, Xavier Martínez-Lladó, Andriy Yaroshchuk, Miquel Rovira, and Joan de Pablo. Nanofiltration as pretreatment for scale prevention in seawater reverse osmosis desalination. *Desalination and Water Treatment*, 36(1-3):310–318, December 2011.

[140] S Alzahrani, A Mohammad, N Hilal, P Abdullah, and O Jaafar. Identification of foulants, fouling mechanisms and cleaning efficiency for NF and RO treatment of produced water. *Separation and Purification Technology*, 118:324–341, October 2013.

[141] N Park, B Kwon, I S Kim, and J Cho. Biofouling potential of various NF membranes with respect to bacteria and their soluble microbial products (SMP): characterizations, ux decline, and transport parameters. *Journal of Membrane Science*, 258:43–54, 2005.

[142] Yi Mo, J Chen, W Xue, and X Huang. Chemical cleaning of nanofiltration membrane filtrating the effluent from a membrane bioreactor. *Separation and Purification Technology*, 75:407–414, November 2010.

[143] V G J Rodgers and R E Sparks. Effect of transmembrane pressure pulsing on concentration polarization. *Journal of Membrane Science*, 68(1-2):149–168, April 1992.

[144] Long D. Nghiem and Simon Hawkes. Effects of membrane fouling on the nanofiltration of trace organic contaminants. *Desalination*, 236(1-3):273–281, January 2009.

[145] *Role of Weak Acid Cation Resin in Water Treatment.*

[146] Darrell A Patterson, Lay Yen Lau, Chayaporn Roengpithya, Emma J. Gibbins, and Andrew G. Livingston. Membrane selectivity in the organic solvent nanofiltration of trialkylamine bases. *Desalination*, 218:248–256, January 2008.

[147] Eric M Vrijenhoek, Seungkwan Hong, and Menachem Elimelech. Influence of membrane surface properties on initial rate of colloidal fouling of reverse osmosis and nanofiltration membranes. *Journal of Membrane Science*, 188(1):115–128, 2001.

[148] B B Gupta, P Blanpain, and M Y Jaffrm. Permeate flux enhancement by pressure and flow pulsations in microfiltration with mineral membranes. *Journal of Membrane Science*, 70:257–266, 1992.

[149] K Abel. Influence of oscillatory flows on protein ultrafiltration. *Journal of Membrane Science*, 133(1):39–55, September 1997.

[150] N D Nikolov, V Mavrov, and J D Nikolova. Ultrafiltration in a tubular membrane under simultaneous action of pulsating pressures in permeate and feed solution. *Journal of Membrane Science*, 83:167–172, 1993.

[151] R J Wakeman and C J Williams. Additional techniques to improve microfiltration. *Separation and Purification Technology*, 26(1):3–18, January 2002.

[152] O Gundogdu, M A Koenders, R J Wakeman, and P Wu. Permeation through a bed on a vibrating medium: theory and experimental results. *Chemical Engineering Science*, 58(9):1703–1713, May 2003.

[153] S Muthukumaran, S Kentish, M Ashokkumar, and G Stevens. Mechanisms for the ultrasonic enhancement of dairy whey ultrafiltration. *Journal of Membrane Science*, 258(1-2):106–114, August 2005.

[154] Marcos R Guilherme, Gilsinei M Campese, Eduardo Radovanovic, Adley F Rubira, Elias B Tambourgi, and Edvani C Muniz. Thermo-responsive sandwiched-like membranes of IPN-PNIPAAm/PAAm hydrogels. *Journal of Membrane Science*, 275(1-2):187–194, April 2006.

[155] Chuyang Y. Tang, Young-Nam Kwon, and James O. Leckie. Fouling of reverse osmosis and nanofiltration membranes by humic acidEffects of solution composition and hydrodynamic conditions. *Journal of Membrane Science*, 290(1-2):86–94, March 2007.

[156] Chuyang Y Tang, Young-Nam Kwon, and James O Leckie. Characterization of humic acid fouled reverse osmosis and nanofiltration membranes by transmission electron microscopy and streaming potential measurements. *Environmental Science & Technology*, 41(3):942–949, February 2007.

[157] Yi-Ning Wang and Chuyang Y Tang. Nanofiltration membrane fouling by oppositely charged macromolecules: investigation on flux behavior, foulant mass deposition, and solute rejection. *Environmental Science & Technology*, 45(20):8941–7, October 2011.

[158] D Violleau, H Essis-tome, H Habarou, J P Croud, and M Pontid. Fouling studies of a polyamide nanofiltration membrane by selected natural organic matter : an analytical approach. *Desalination*, 173:223–238, 2005.

[159] Jaeweon Cho, Gary Amy, and John Pellegrino. Membrane filtration of natural organic matter: comparison of flux decline, NOM rejection, and foulants during filtration with three UF membranes. *Desalination*, 127(3):283–298, February 2000.

[160] A E Childress and M Elimelech. Effect of solution chemistry on the surface charge of polymeric reverse osmosis and nanofiltration membranes. *Journal of Membrane Science*, 119(2):253–268, 1996.

[161] R D Cohen and R F Probstein. Colloidal fouling of reverse osmosis membranes. *Journal of Colloid and Interface Science*, 114(1):194–207, 1986.

[162] Menachem Elimelech, Xiaohua Zhu, Amy E. Childress, and Seungkwan Hong. Role of membrane surface morphology in colloidal fouling of cellulose acetate and composite aromatic polyamide reverse osmosis membranes. *Journal of Membrane Science*, 127(1):101–109, 1997.

[163] Sangyoup Lee, Jaeweon Cho, and Menachem Elimelech. Influence of colloidal fouling and feed water recovery on salt rejection of RO and NF membranes. *Desalination*, 160:1–12, 2004.

[164] Long D. Nghiem and Poppy J. Coleman. NF/RO filtration of the hydrophobic ionogenic compound triclosan: Transport mechanisms and the influence of membrane fouling. *Separation and Purification Technology*, 62(3):709–716, September 2008.

[165] Arza Seidel and Menachem Elimelech. Coupling between chemical and physical interactions in natural organic matter (NOM) fouling of nanofiltration membranes : implications for fouling control. *Journal of Membrane Science*, 203:245–255, 2002.

[166] W E I Yuan and Andrew L Zydney. Humic acid fouling during ultrafiltration. *Environmental Science & Technology*, 34(23):5043–5050, 2000.

[167] Lianfa Song and Menachem Elimelech. Particle deposition onto a permeable surface in laminar flow. *Journal of Colloid and Interface Science*, 173:165–180, 1995.

[168] C Combe, E Molis, P Lucas, R Riley, and M M Clark. The effect of CA membrane properties on adsorptive fouling by humic acid. *Journal of Membrane Science*, 154(1):73–87, March 1999.

[169] E. M V Hoek and M. Elimelech. Cake-enhanced concentration polarization : A new fouling mechanism for salt-rejecting membranes. *Environmental Science and Technology*, 37(24):5581–5588, 2003.

[170] Moshe Herzberg, Seoktae Kang, and Menachem Elimelech. Role of extracellular polymeric substances (EPS) in biofouling of reverse osmosis membranes. *Environmental Science & Technology*, 43(12):4393–4398, June 2009.

[171] Abhijit Maiti, Mohtada Sadrezadeh, Subhayan Guha Thakurta, David J. Pernitsky, Subir Bhattacharjee, and Mohtada Sadrzadeh. Characterization of boiler blowdown water from steam-assisted gravity drainage and silicaorganic coprecipitation during acidification and ultrafiltration. *Energy & Fuels*, 26(9):5604–5612, September 2012.

[172] Hasan Guleryuz, Ingeborg Kaus, Claudine Filiàtre, Tor Grande, and Mari-Ann Einarsrud. Deposition of silica thin films formed by solgel method. *Journal of Sol-Gel Science and Technology*, 54(2):249–257, March 2010.

[173] K Rezwan, a R Studart, J Vörös, and L J Gauckler. Change of zeta potential of biocompatible colloidal oxide particles upon adsorption of bovine serum albumin and lysozyme. *The Journal of Physical Chemistry. B*, 109(30):14469–14474, August 2005.

[174] Margarida Ribau Teixeira and Maria Jo Rosa. pH adjustment for seasonal control of UF fouling by natural waters. *Desalination*, 151:165–175, 2002.

[175] Douglas B Burns and Andrew L Zydney. Buffer effects on the zeta potential of ultrafiltration membranes. *Journal of Membrane Science*, 172(September 1999):39–48, 2000.

[176] Menachem Elimelech and Amy E. Childress. Zeta potential of reverse osmosis membranes: Implications for membrane performance. Technical Report December, University of California, Los Angeles, 1996.

[177] D Elzo, I Huisman, E Middelink, and V Gekas. Charge effects on inorganic membrane performance in a cross-flow microfiltration process. *Colloids and Surfaces A: Physicochemical and Engineering Aspects*, 138:145–159, 1998.

[178] F.L. Hua, Y.F. Tsang, Y.J. Wang, S.Y. Chan, H. Chua, and S.N. Sin. Performance study of ceramic microfiltration membrane for oily wastewater treatment. *Chemical Engineering Journal*, 128(2-3):169–175, April 2007.

[179] Alberto Lobo, Ángel Cambiella, José Manuel Benito, Carmen Pazos, and José Coca. Ultrafiltration of oil-in-water emulsions with ceramic membranes: Influence of pH and crossflow velocity. *Journal of Membrane Science*, 278(1-2):328–334, July 2006.

[180] Wen Chen, Paul Westerhoff, Jerry A Leenheer, and Karl Booksh. Fluorescence excitation-emission matrix regional integration to quantify spectra for dissolved organic matter. *Environmental Science & Technology*, 37(24):5701–5710, December 2003.

[181] Y Bessiere, B Jefferson, E Goslan, and P Bacchin. Effect of hydrophilic/hydrophobic fractions of natural organic matter on irreversible fouling of membranes. *Desalination*, 249(1):182–187, November 2009.

[182] B A Farnand and T A Krug. Oil removal from oilfield produced water by cross flow ultrafiltration. *Journal of Canadian Petroleum Technology*, 28(6):18–24, 2000.

[183] Ron S Faibish and Yoram Cohen. Fouling and rejection behavior of ceramic and polymer-modified ceramic membranes for ultrafiltration of oil-in-water emul-

sions and microemulsions. *Colloids and Surfaces A: Physicochemical and Engineering Aspects*, 191(1-2):27–40, October 2001.

[184] Q Li and M Elimelech. Natural organic matter fouling and chemical cleaning of nanofiltration membranes. *Water Science and Technology: Water Supply*, 4(5-6):245–251, 2004.

[185] T Rizwan and S Bhattacharjee. Initial deposition of colloidal particles on a rough nanofiltration membrane. *Canadian Journal of Chemical Engineering*, 85(5):570–579, 2007.

[186] Md. Abdullah-Al Mamun. *Colloidal fouling of salt rejecting nanofiltration membranes: Transient electrokinetic model and experimental study*. Msc thesis, University of Alberta, 2012.

[187] Nicole C Mueller, Bart van der Bruggen, Volkmar Keuter, Patricia Luis, Thomas Melin, Wouter Pronk, Robert Reisewitz, David Rickerby, Gilbert M Rios, Wilco Wennekes, and Bernd Nowack. Nanofiltration and nanostructured membranes–should they be considered nanotechnology or not? *Journal of Hazardous Materials*, 211-212:275–280, April 2012.

[188] L D Nghiem and S Hawkes. Effects of membrane fouling on the nanofiltration of pharmaceutically active compounds (PhACs): Mechanisms and role of membrane pore size. *Separation and Purifcation Technology*, 57:176–184, 2007.

[189] James L Weishaar, George R Aiken, Brian a Bergamaschi, Miranda S Fram, Roger Fujii, and Kenneth Mopper. Evaluation of specific ultraviolet absorbance as an indicator of the chemical composition and reactivity of dissolved organic carbon. *Environmental Science & Technology*, 37(20):4702–4708, October 2003.

[190] Hiroshi Yamamura, Kenji Okimoto, Katsuki Kimura, and Yoshimasa Watanabe. Influence of calcium on the evolution of irreversible fouling in microfiltration/ultrafiltration membranes. *Journal of Water Supply: Research and TechnologyAQUA*, 56(67):425–434, 2007.

[191] Sangyoup Lee, Jaeweon Cho, and Menachem Elimelech. Combined influence of natural organic matter (NOM) and colloidal particles on nanofiltration membrane fouling. *Journal of Membrane Science*, 262(1-2):27–41, October 2005.

[192] C Tang, Y Kwon, and J Leckie. Probing the nano- and micro-scales of reverse osmosis membranesA comprehensive characterization of physiochemical properties of uncoated and coated membranes by XPS, TEM, ATR-FTIR, and streaming potential measurements. *Journal of Membrane Science*, 287(1):146–156, January 2007.

[193] M J Ariza, J Benavente, E Rodríguez-Castellón, and L Palacio. Effect of hydration of polyamide membranes on the surface electrokinetic parameters: surface characterization by x-ray photoelectronic spectroscopy and atomic force microscopy. *Journal of Colloid and Interface Science*, 247(1):149–58, March 2002.

[194] Ashish Kulkarni, Debabrata Mukherjee, and William N. Gill. Flux enhancement by hydrophilization of thin film composite reverse osmosis membranes. *Journal of Membrane Science*, 114(1):39–50, May 1996.